Bettina Kothbauer

# Random and site-directed mutagenesis of *Gt*HNL

## Improvement of *Gt*HNL with respect to enzyme activity and pH stability

Supervisor:
Schwab, Helmut, Univ.-Prof. Dipl.-Ing. Dr.techn.

Co-Supervisors:
Wiedner, Romana, Dipl.-Ing. Dr.
Steiner, Kerstin, Dipl.-Ing. Dr.nat.techn.

# List of Contents

# 1 Acknowledgement

# 2 Abstract

Hydroxynitrile lyases (HNL) were first discovered in plants. Recently, they could also be detected in bacteria. HNLs catalyse the reversible cleavage of cyanohydrins, which are important building blocks for pharmaceuticals and agrochemicals. The aim of this thesis was the improvement of an HNL from *Granulicella tundricola* (*Gt*HNL) with respect to enzyme activity and pH stability using site – directed and random mutagenesis. One variant (a triple mutant) could be generated that showed improved properties in cleaving (*R*) – mandelonitrile with 281 U/mg, and converted benzaldehyde to (*R*) - mandelontirile completely within two hours with an enantiomeric excess (*ee*) of 100%.

# 3 Introduction

## 3.1 Cyanogenesis in nature

### 3.1.1 Cyanogenesis in plants

Hydroxynitrile lyases (HNL) catalyse the reversible cleavage of cyanohydrins, also termed cyanogenesis, releasing prussic acid (HCN) and the respective ketone or aldehyde (Figure 1). Cyanohydrins are also degraded spontaneously (base catalysed) at higher pH (1) (2) (3).
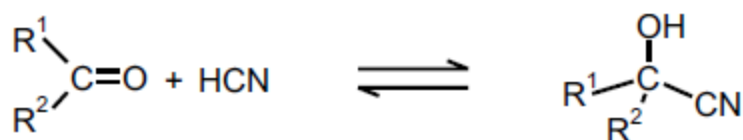


Figure 1: Cleavage and formation of cyanohydrins (4).

HCN is highly toxic as it causes inhibition of the mitochondrial respiration pathway by inhibiting cytochrome c oxidase and other metal dependent enzymes (5) (6). Therefore, cyanogenesis is used by plants as a defence mechanism against herbivores and microorganism and is induced when the tissue gets damaged (7). Cyanogenesis in plants is mostly a two step process where a sugar moiety is cleaved from cyanogenic glycosides by one or more $\beta$ – glycosidases and $\alpha$ – hydroxynitrile is produced. Then the $\alpha$ – hydroxynitrile gets cleaved by the activity of an $\alpha$ – hydroxynitrilelyase to the respective keto-compound and HCN (8). Besides using the cleavage of cyanogenic glucosides and the release of HCN as defence mechanism, plants can use them also as nitrogen source. Therefore HCN gets refixed with L – cysteine by $\beta$ – cyanoalanine synthetase resulting in $\beta$ – cyanoalanine. $\beta$ – cyanoalanine hydrolase hydrolyses $\beta$ – cyanoalanine to L – asparagine (9). Cyanogenic glucosides in plants are metabolised from L – amino acids by cytochrome P450 and glucosyl transferase (compare Figure 2) (8).
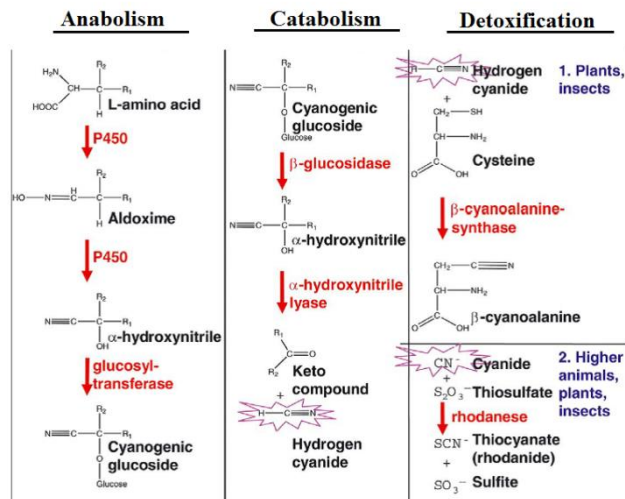
**Figure 2: Biochemical role of cyanogenic glucosides and HCN in plants (8).**

### 3.1.2 Bacterial cyanogenesis

Cyanogenesis can not only be found in plants but also in several microorganisms although the cleavage of cyanohydrins in bacteria follows a completely different metabolic pathway. Cyanogenesis in bacteria is tightly regulated resulting in very low local concentrations (1 mM) of HCN that might have no harmful effects on organisms (6). However, it has been reported that *Pseudomonas aeruginosa*, isolated from burn wound infections, is able to produce HCN but the effect of HCN on the patient was not clear at this moment (10). High levels of cyanide were also detected in the sputum of cystic fibrosis patients that were infected with *Pseudomonas aeruginosa* (11). Bacterial cyanogenesis was first described by Emerson and Clawson and Young in 1913 in a *Bacillus* strain (12) but can also be found in several other bacteria e.g. *Chromobacterium violaceum*, *Pseudomonas fluorescens* or *Rhizobium leguminosarum* (6) (13).

It is suggested that bacteria use HCN as a nitrogen source for growth and that it is produced by oxidative decarboxylation of glycine or other amino acids with $CO_2$ as by-product. Cyanide is a secondary metabolite and is formed at the end of the growth phase. In *Chromobacterium violaceum*, HCN derives from the methylene carbon of glycine while $CO_2$ is formed from the carboxyl group of glycine. In *P. aeruginosa*, threonine instead of glycine can function as precursor for cyanide as well, although it is less effective (14) (15) (16). In both species a HCN synthase seems to be the enzyme responsible for cyanogenesis. In vitro, the enzyme is coupled to the membrane and is sensible to $O_2$ exposure (6).

This thesis focuses on the reversible cyanogenesis by bacterial hydroxyl nitrile lyases because of their great importance in organic synthesis as they can form C-C bonds enantioselectively (17). HNL activity in bacteria was detected so far in *Xylella fastidiosa* (18), *Pseudomonas mephitica, Burkholderia phytofirmans* (19) and *Granulicella tundricola* (20)*.*

## 3.2 Hydroxynitrile lyases in industry

In industrial scale, biocatalysts are used for converting natural substrates into natural products using natural reactions and pathways (traditional biocatalysis). Traditional biocatalysis is used in the food industry to produce e.g. bread, cheese, wine or beer or in the synthesis of natural antibiotics. Broad – substate – range biocatalysis converts synthetic products (non-natural) into other chemical intermediates using natural reactions and pathways. This type of biocatalysis is often needed in pharmaceutical industry to produce drugs and non-natural antibiotics. Enzymes in multistep biocatalysis are used for the conversion of natural products into fuels and other non – natural products by non-natural reactions and pathways (21).

Figure 3 shows some examples for the application of cyanohydrins in agro – and pharmaceutical industry (22). One of the earliest reports of the application of enzymes for synthesising cyanohydrins was the synthesis of mandelonitrile from benzaldehyde using a crude enzyme preparation from almonds reported by Rosenthaler (23). (*R*) as well as (*S*)-selective HNLs are known and applied in cyanohydrin synthesis. E.g.: the (*R*)-selective HNL originating from *Prunus amygdalus* and the (*S*)-selective HNL which was isolated from *Hevea brasiliensis* (22). In order to keep the chemical background reaction low and to obtain no racemic products, the synthesis reaction should be carried out in organic solvents, at low temperature and at low pH (24) (25). Moreover it is recommended to use two-phase systems for the production of cyanohydrins to assure optimum enzyme performance in the buffered aqueous phase and to gain high yields of product by offering an organic phase as reservoir of substrate and product (26).
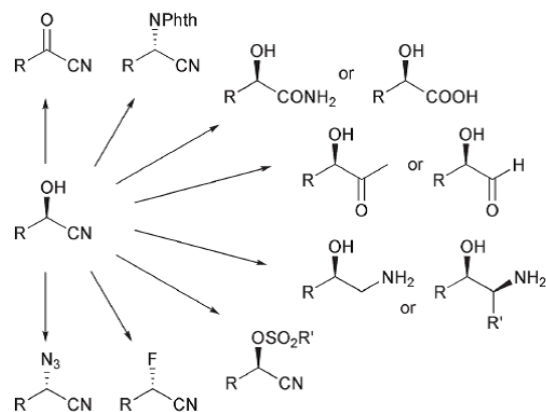
Figure 3: Cyanohydrins as precursors for a variety of pharmaceutical products (27).

In this thesis, the cleavage and formation of (*R*) – mandelonitrile is used as standard reaction in order to identify variants of *Gt*HNL that show improved properties concerning pH stability and catalytic activity. (*R*) – and (*S*) – mandelonitrile are formed in industrial scale from benzaldehyde and HCN using recombinant (*R*) – HNL originating from *Prunus amygdalus* or (*S*) – HNL isolated from *Hevea brasiliensis.* Subsequently, both cyanohydrins are converted to mandelic acids by acidic hydrolysis which are applied in cosmetic industries (28), for racemate resolution by the formation of diastereomeric salts (22) and is a precursor for antibiotics like cephalosporins (29).

## 3.3  Classification of HNLs

Lyases are devided into carbon – carbon, carbon – oxygen, carbon – nitrogen, carbon – sulphur, carbon – halide, phosphorous – oxygen and other lyases. HNLs belong to carbon – carbon lyases (30). Moreover, HNLs can be classified into at least five different types of proteins with oxynitrilase activity. HNLs belonging to the first class are flavine adenine dinucleotide (FAD) dependent with (*R*) – mandelonitrile as their natural substrate. They can be isolated from *Rosaceae* and show similarities to oxidoreductases. HNLs of the second class exhibit α/β – hydrolase fold (e. g. HNL from *Hevea brasiliensis, Manihot esculenta, Baliospermum montanum*). HNL isolated from *Sorghum bicolor* represents the third class and has sequence similarities to carboxypeptidases. The fourth class comprises those HNLs, which have homologies to alcohol dehydrogenases, and need zinc as cofactor (HNL from *Linum usitatissimum*) (31) (32). Most recently three HNLs from endophytic bacteria were described that belong to the cupin superfamily of proteins and respresent the fifth class of HNL (20).

## 3.4 Hydroxynitrily lyase activity of *Granulicella tundricola* (*Gt*HNL)

Recently, HNL activity could be detected in an acidobacterium called *Granulicella tundricola* (*Gt*HNL) (20). The sequence of *Gt*HNL is highly similar to two previously described cupins with HNL activity that were isolated from bacterial endophytes called *Pseudomonas mephitica* and *Burkholderia phytofirmans* (19). Cupins are proteins that are structurally highly conserved but show high diversity in functionalities that are often still unexplained so far. They can be found in Archaea, Bacteria and Eukaryota (33). As cupins also show low sequence identities among homologues, it is recommended to do structure – based analysis, especially concerning the generation of evolutionary models (34).

The cupin superfamily is named on the basis of the latin term for a small barrel 'cupa'. It was discovered when similarities between the wheat protein germin and spherulin, a protein related to stress, were found (35). Proteins that belong to the cupin superfamily exhibit two conserved motifs that contain histidine (motif 1: G-(X)5-H-X-H-(X) 3,4-E-(X)6-G; motif 2: G-(X)5-P-X-G-(X)2-H-(X)3-N), each belonging to two β – strands that are separated by a less conserved region being part of another two β – strands with an intervening variable loop. The two motifs also include the residues for the binding of metals, which is also characteristic for many proteins of the cupin superfamily (36). Proteins belonging to the cupin superfamily often show enzymatic activities (dioxygenases, decarboxylases, hydrolases, isomerases, epimerases) but also exhibit non – enzymatic functions as e.g. transcription factors or seed storage proteins (34). Cupins can be classified into different subgroups based upon whether the proteins exhibit a single cupin domain (monocupins) or whether they have two (bicupin) or more cupin domains (multicupin). Most of the monocupins are enzymes, but also microbial transcription factors were found that include a cupin domain. Proteins that belong to the monocupins are dioxygenases, germin and germin – like proteins (GLPs), auxine binding protein which is known to be involved in plant growth, phosphomannose isomerase and nuclear proteins. dioxygenases can also be found in the class of bicupins next to oxalate decarboxylase which is manganese – dependent and catalyzes the formation of formate and $CO_2$ from oxalate. Also seed storage globulins can found among bicupins (36).

HNL from *Granulicella tundricola* is manganese dependent as it was reported by Hajnal et al.. Two histidine and one glutamine residue in Motif 1 and one histidine residue located in Motif 2 act as ligands for the binding of the manganese ion in the active site (20)(Figure 4).
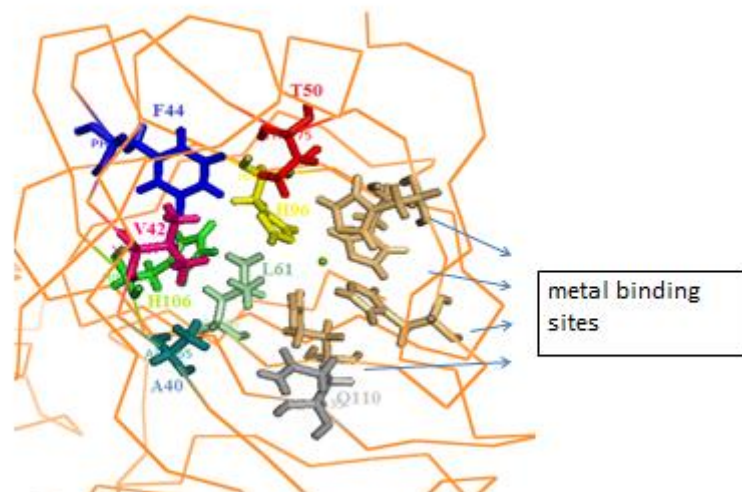
**Figure 4: Active site and metal binding residues of *Gt*HNL. Active site amino acids: A40 (light blue), H106 (green), V42 (purple), F44 (dark blue), L61 (metallic green), H96 (yellow), T50 (red), Q110 (grey). Metal binding residues are coloured in gold.**

*Gt*HNL forms a homotetramer, a dimer of two tetramers is shown in Figure 5. One monomer is composed of eleven β- strands. Metal binding residues are H53, H55, Q59 and H94. Putative active site positions are A40, V42, F44, T50, L61, H96, H106 and Q110 (20).
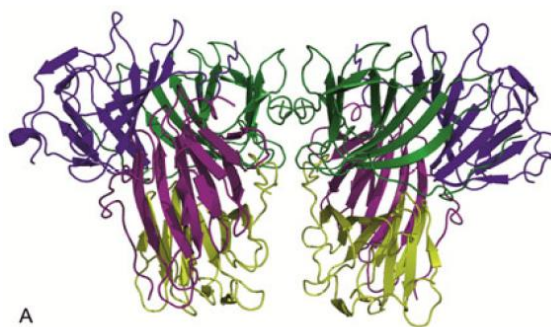


**Figure 5: Structure of two homotetramers of *Gt*HNL (20).**

In this diploma thesis designed evolution was used to generate mutagenesis libraries of *Gt*HNL to search for improved variants in respect to enzyme activity and stability at low pH. Stability at low pH is of great importance in order to suppress the spontaneous unselective addition of HCN to aldehydes/ketones (22). Putative active – site positions were exchanged by site – directed mutagenesis. Random mutagenesis by error prone PCR was used to introduce mutations randomly. Metal binding positions were protected from mutations otherwise the enantioselectivity would

become worse as it was tested by Hajnal et al. In this study of Hajnal et al. *Gt*HNL had converted 80% benzaldehyde to (*R*) – mandelonitrile after 6 h with an *ee* of 90% (20).

## 3.5 Designed Evolution Methods

Natural evolution introduces mutations to enable organisms the adaption to environmental conditions. In nature, improved variants might be generated mainly to provide advantageous properties in order to withstand selection pressure. For example, organisms living in deep – sea hydrothermal vents are adapted to high temperatures and high pressure whereas organisms that were found in hot springs show high tolerance to high temperature and acidity. Consequently, enzymes originating from organisms living in hot springs might be more stable in lower pH than organisms isolated from hydrothermal vents in the sea. It has to be mentioned that not all differences in enzyme properties can be attributed to adaptive mechanisms as silent mutations, which have no effect on the fitness of the organism, are also occurring constantly (37).

In enzyme engineering, the process of natural evolution is too slow for developing enzymes with improved or new properties for the application in industry. Hence, enzyme engineering has turned out to be an efficient method to introduce mutations that might improve enzymes in respect to stability, catalytic activity or enantioselectivity (38) (39). Enzyme engineering is also used to broaden the substrate range of enzymes in order to enable the conversion of more bulky substrates into important industrial products. E.g.: The synthesis of enantiopure alcohols for drugs which are lowering cholesterol in the body using a recombinant carbonyl-reductase, the production of intermediates for herbicides which is catalysed by an HNL and a nitrile-hydratase-catalysed production of acrylamide for polymers (21).

Proteins can be engineered either using rational design (site-directed mutagenesis) or directed evolution (random mutagenesis). Directed evolution can be realized by random recombination of related sequences (e.g. gene shuffling) or by introducing mutations in a random way (e.g. error prone PCR). Using rational design affords the knowledge of the enzyme structure and relationships between sequence, structure and function whereas random approaches need only the availability of the gene coding for the enzyme. High – throughput screening methods are required to identify improved variants within the random libraries (40) (Compare Figure 6). Generally, it is not possible to create and screen random libraries that are perfectly representative and include every possible variant. E.g.: To assure that every possible variant in a random library of a theoretical protein consisting of only ten amino acids is represented once, demands an impossibly high number of $6*10^{12}$ clones that have to be generated and screened for desired properties. The number of clones

that are necessary to get a library that is representative for the respective protein can be calculated with the following equation (41):

$$19^M * \frac{N!}{(N-M)! * M!} = number\ of\ possible\ variants$$

M … number of amino acids changed simultaneously

N … sequence length

Compared to the directed evolution approach, mutagenesis by rational design has the advantage that significantly smaller number of clones leads to "smarter" libraries that are more reliable and might reveal improved variants with higher probability in shorter time and less effort, especially in respect to screening the libraries (42).

Besides the enormous high numbers of clones needed for representative libraries, random mutagenesis has to cope with some further problems. On the one hand there is the problem of mutational bias of DNA polymerases, on the other hand the mutation frequencies are mostly too low that mutations are introduced right next to each other. A third challenge is the organisation of the genetic code itself and the fact that some amino acids are encoded by up to six codons, whereas other amino acids (e.g. Trp and Met) are only encoded by one single triplet (43). Due to these facts, random mutagenesis using error prone PCR has some disadvantages and drawbacks that can lead to libraries where only 20% of all possible variants are represented within the library and are not accessible (44). Another random method, called sequence saturation mutagenesis (SeSaM) is reported to overcome the limitations caused by biased polymerases. This method involves a PCR with biotinylated primer and thio-analogues of dNTPs, which get incorporated in a random way. Next step is the cleavage of phosphothioate bonds with iodine resulting in DNA fragments of different sizes. Then the DNA fragments are treated with terminal transferase, which adds universal bases (deoxyinosine). In the next step, the DNA fragments are extended by PCR to the full-length gene and the universal bases are replaced with standard nucleotides. Besides the advantage of avoiding biased polymerases, SeSaM also enables the saturation of every single nucleotide position, especially when they are located right next to each other (45).

A great advantage of directed evolution is that variants can be generated that include mutations that were not expected to be beneficial. E.g. amino acids that are involved in stability are often located distantly from the active site and might only get identified by introducing mutations randomly (46).
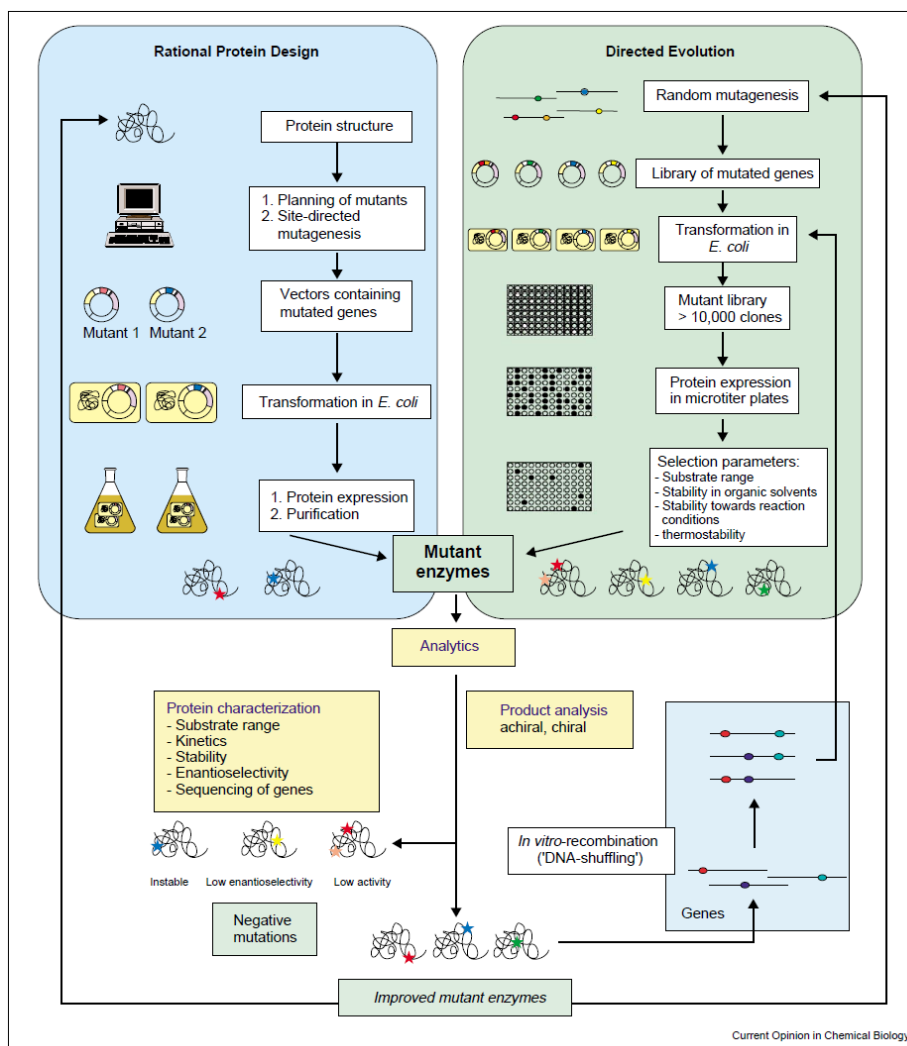
**Figure 6: Comparison of rational design and random mutagenesis (40).**

Semi-rational design is an approach, which combines random and rational mutagenesis, and is the key to generate "smarter" libraries. It is based on the knowledge of biochemical and/or structural information and enables the introduction of random mutations at interesting sites of the gene. Combinatorial active site saturation testing (CASTing) is an example for a semi-rational approach and uses e.g. structural information of the protein for the identification of amino acids in interesting regions that subsequently get mutated in a random way (e.g. site-saturation mutagenesis). In contrast to single site-specific mutagenesis, CASTing allows the determination of synergistic effects of neighbouring residues (46). In comparison to site-specific mutagenesis, the semi-rational approaches increase the size of the libraries extremely but computational methods are in development that create and screen virtual libraries and can identify unfavourable mutations (42).

As mentioned above, industry is very interested in the usage of HNLs for the synthesis of cyanohydrins. Using biphasic systems is beneficial for synthesizing cyanohydrins as carbonyl

compounds are mostly poorly soluble in water and the organic phase permits higher substrate concentrations and makes product recovery easier. Although stirring causes shear stress to the enzymes, it is essential to assure optimal contact between the aqueous and organic phases as the HNLs develop their enzyme activity at the solvent/water interface. In order to suppress the spontaneous unselective addition of HCN to the aldehydes or ketones, it is important that the reaction is carried out at low pH and low temperature (22) (47). Therefore, the generation of enzymes that can stand these harsh reaction conditions is of great importance.

In this thesis, site – directed as well random mutagenesis approaches were used to generate enzymes with improved properties regarding pH stability and enzyme activity. Cyanogenesis of variants in mutant libraries was tested using a colony – based filter assay (48).

### 3.5.1   Site-directed mutagenesis of *Gt*HNL

Site-directed mutagenesis of *Gt*HNL needed structural information that was provided by Hajnal et al. In this approach, rational design was combined with site-saturation mutagenesis by exchanging amino acids at putative active site positions (site-saturation mutagenesis) using NNK codons. At position N any nucleotide can be introduced, whereas at position K only T and G can be introduced. The application of NNK codon degeneracy is a conventional way to perform saturation mutagenesis that involves 32 codons which encode for the 20 proteinogenic amino acids. If only one NNK codon is introduced in the sequence in order to exchange one amino acid at least 94 transformants are required to ensure 95% coverage of all possible variants (49) (39) (50). In the case that some transformants are wildtype colonies, 250 clones were screened in this thesis. Forward and reverse primers including NNK codons were first extended in two separate modified QuikChange® PCRs. Generally, QuikChange® mutagenesis is used to introduce mutations at specifc sites of the gene and uses DNA polymerase with proof reading activity for extension of the primers. The PCR products are treated with *DpnI* that recognises dam methylation sites and digests the wildtype DNA. This step assures that only mutagenic DNA gets transformed in *E. coli* or other types of cells.

Some mutations like F44A, L61A and Q110A tested by Hajnal et al. didn't show any effect in the efficiency of cleaving (*R*)-mandelonitrile. Metal binding sites H53, H55, Q59, H94 were exchanged to alanine and were tested in cleavage and synthesis reaction. Q59 was also exchanged to glutamate, but as it was expected, none of the variants were more efficient in synthesizing or cleaving (*R*)-mandelonitrile than the wildtype *Gt*HNL, three of the four alanine variants lost cyanogenesis and synthesis activity completely. Mutant H94A was still active in cleavage reaction, but showed a dramatic loss in its capability to synthesize (*R*)-mandelonitrile. This experiment has proven that H53,

H55, Q59 and H94 are essential for the activity of *Gt*HNL.T50A showed a comparable conversion and *ee* to the wildtype whereas H96A completely had lost its cyanogenesis activity. H96R resulted in insoluble protein and H96K was inactive as well. All variants of H96 were inactive in mandelonitrile synthesis. H106A and H106K were inactive in both directions. H106D showed WT activity in filter assay, but had only a conversion of 26% with a low *ee* (20). Thus, it was concluded that the metal binding site as well as the additional histidine residues in the active site are important for the activity.

### 3.5.2 Directed evolution of *Gt*HNL

Random mutagenesis, coupled with a high – throughput screening method is very useful, when the enzyme properties are not well understood yet but also if variants should be generated with improved properties which might be influenced from amino acids distant from the active site (e. g. stability mutants). *Taq* DNA polymerase is the most suitable polymerase for error prone PCR as it has no proof – reading activity and its fidelity is very low. The error – rate of *Taq* DNA polymerase can be increased by adding high $MgCl_2$ concentrations and $MnCl_2$ to the PCR mixture. Unequal concentrations of dNTPs and increased extension times can also have effects on the fidelity of *Taq* DNA polymerase (51).

In this thesis, *Gt*HNL was devided into three fragments by primer design to protect the metal binding sites from mutations, as they are essential for proper enzyme activity and selectivity. Moreover, the gene was divided into three fragments in order to reduce the size of the random library. *Gt*HNL is build-up of 132 amino acids, in order to generate a proper random library of the whole gene, $2*10^{40}$ clones would be necessary. Dividing the gene for mutagenesis into three fragments, reduces the number of clones for each library to $3*10^{32}$ (fragment 1), $4.3*10^{30}$ (fragment 2), $6.2*10^{29}$ (fragment 3) which indeed are also not feasible in practice but makes the libraries a little bit "smarter" at least.

# 4 Materials and Methods

## 4.1 Growth media and solutions

### 4.1.1 Growth media

LB – medium Lennox (Carl Roth GmbH + Co. KG; Art.Nr.: X964.3):

    10 g/L tryptone

    5 g/L yeast extract

    5 g/L sodium chloride (NaCl)

    pH 7.0 +/- 0.2

    20 g/L medium

LB – agar Lennox (Carl Roth GmbH + Co. KG; Art.Nr.: X965.3):

    10 g/L tryptone

    5 g/L yeast extract

    5 g/L sodium chloride (NaCl)

    15 g/L agar - agar

    pH 7.0 +/- 0.2

    35 g/L agar

2xYT medium (Carl Roth GmbH + Co. KG; Art. Nr.: X966.3):

    16 g/L tryptone

    10 g/L yeast extract

    5 g/L sodium chloride (NaCl)

    pH 7.0 +/- 0.2

    31 g/L medium

SOC medium

    20 g/L bacto tryptone (Becton, Dickinson and Company; Art. Nr.: 211820)

    0.58 g/L NaCl (Carl Roth GmbH + Co. KG; Art. Nr.: 3957.1; CAS: 7647-14-5)

    5 g/L bacto yeast extract (Becton, Dickinson and Company; Art. Nr.: 212720; CAS: 8013-01-2)

2 g/L $MgCl_2$ (pro analysis; Art. Nr.: 5833; CAS: 7786-30-3)

0.18 g/L KCl (Carl Roth GmbH + Co. KG; Art. Nr.: 6781.1; CAS: 7447-40-7)

2.46 g/L $MgSO_4$ (Carl Roth GmbH + Co. KG; Art. Nr.: T888.1; CAS: 10034-99-8)

3.46 g/L glucose (Carl Roth GmbH + Co. KG; Art. Nr.: 6887.1; CAS: 14431-43-7)

### 4.1.2   Solutions

<u>0.1 M citrate phosphate buffer, pH 3.0, pH 3.5, pH 4.0, pH 4.5, pH 5.0, pH 5.5</u>

Solution A        0.1 M citric acid monohydrate ($C_6H_8O_7.H_2O$) (Carl Roth GmbH + Co. KG; Art. Nr.: 3958.1; CAS: 13-139-0135-0)

Solution B        0.1 M dipotassium hydrogen phosphate ($K_2HPO_4.3H_2O$) (Carl Roth GmbH + Co. KG; Art. Nr.: P749.2; CAS: 13-139-0174-9)

Both solutions were mixed to obtain a buffer solution with desired pH which was checked with a pH electrode.

<u>Solution for the detection filters:</u>

Solution A        Copper (II) ethylacetoacetate 1% (w/v) (ABCR GmbH & Co. KG; Art. Nr.: 93-2920)

0.25 g dissolved in 25 mL chloroform

Solution B        N,N,N',N' – Tetramethyl-4,4'- methylenedianiline (Fluka Analytical; Art. Nr.: 87800)

0.25 g dissolved in 25 mL chloroform (Carl Roth GmbH, CAS 67-66-3)

Solution B was slowly added to solution A. The resulting mixture was used to prepare the HCN sensitive detection filters.

<u>20 mM (*R*) – mandelonitrile (Alfa Aesar GmbH & Co KG; Art. Nr.: H56658; CAS: 10020-96-9):</u>

2.4 µL (*R*) – mandelonitrile per ml 0.1 M citrate phosphate Buffer, pH 3.5

<u>Glycerol (Carl Roth GmbH ; Art. Nr.: 7530.4; CAS: 56-81-5)</u>

Respective amount of glycerol was mixed with deionised $H_2O$ to gain a solution of desired concentration (10%, 30%, 50%).

## 0.1 M sodium phosphate Buffer, pH 7.2

Solution A    0.1 M sodium dihydrogen phosphate (NaH$_2$PO$_4$.2H$_2$O) (Carl Roth GmbH + Co. KG; Art.Nr.: T879.2; CAS: 7558-80-7)

Solution B    0.1 M disodiumhydrogen phosphate (Na$_2$HPO$_4$) (Carl Roth GmbH + Co. KG; Art. Nr.: T876.2; CAS: 7558-79-4)

Both solutions were mixed to obtain a buffer solution with pH 7.2.

## 0.1 M MES oxalate buffer, pH 5.5

Solution A    0.1 M oxalic acid dihydrate (Sigma Aldrich; CAS: 6153-56-6)

Solution B    0.1 M MES (Carl Roth GmbH; CAS: 4432-31-9)

0.1 M oxalic acid dihydrate and 0.1 M MES were dissolved in 50 mL deionised water, the pH was adjusted with 2 M NaOH and the solution filled up to 100 mL with deionised water.

## 1 M HEPES buffer (Carl Roth GmbH; Art.Nr.: 9105.4; CAS: 7365-45-9)

238 g were dissolved in 1 L deionised H$_2$O.

## 20 x MES buffer (NuPAGE life technologies; Art. Nr.: NP0002)

The concentrate was diluted with deionised water in a 1:20 ratio.

## 1 M sodium acetate buffer pH 4.0

1 M sodium acetate was adjusted with 1 M acetic acid to pH 4.0.

## QFF buffer A pH 6.7

50 mM BisTris (Carl Roth GmbH + Co. KG; Art. Nr.: 9140.3; CAS: 6976-37-0)

30 mM NaCl (Carl Roth GmbH + Co. KG; Art. Nr.: 3957.1; CAS: 7647-14-5)

HCl was used to obtain a buffer solution of pH 6.7. Solution was filled up to 1 L with deionised water.

## QFF buffer B pH 6.7

50 mM BisTris (Carl Roth GmbH + Co. KG; Art. Nr.: 9140.3; CAS: 6976-37-0)

1 M NaCl (Carl Roth GmbH + Co. KG; Art. Nr.: 3957.1; CAS: 7647-14-5)

HCl was used to obtain a buffer solution of pH 6.7. Solution was filled up to 1 L with deionised water.

SEC buffer pH 7.0

50 mM Sodiumdihydrogenphosphate Dihydrate ($NaH_2PO_4.2H_2O$) (Carl Roth GmbH + Co. KG; Art. Nr.: T879.2; CAS: 7558-80-7)

100 mM NaCl (Carl Roth GmbH + Co. KG; Art. Nr.: 3957.1; CAS: 7647-14-5)

NaOH was used to obtain a buffer solution of pH 7.0. Solution was filled up with water to 1 L.

All buffers for protein purification were sterile filtered through a 0.2 µm filter (sartorius stedim biotech ).

Coomassie G250 staining solution

2.5 g Brilliant Blue were dissolved in 75 mL acetic acid, 200 mL ethanol were added and the mixture was filled up to 1 L with deionised water.

SDS – PA Gel Destaining solution

75 mL acetic acid and 200 mL ethanol were filled up with water to 1 L.

### 4.1.3 Stock – Solutions

Ampicillin [100 mg/mL] (Carl Roth GmbH + Co. KG; Art. Nr.: K029.2; CAS: 69-52-3)

2 g Ampicilline sodium salt dissolved in 20 mL deionised $H_2O$ and sterile filtered with a 0.2 µm syringe filter.

Kanamycin [40 mg/mL] (Carl Roth GmbH + Co. KG; Art. Nr.: T832.2; CAS: 25389-94-0)

800 mg Kanamycin sulphate dissolved in 20 mL deionised $H_2O$ and sterile filtered with a 0.2 µm syringe filter.

0.1 M Manganese (II) chloride tetrahydrate ( Sigma Aldrich; Art. Nr.: 203734-5G; CAS: 13446-34-9)

198 mg $MnCl_2.4H_2O$ dissolved in 10 mL deionised $H_2O$.

1 M IPTG (Biosynth; Art. Nr.: I-8000; CAS: 367-93-1)

4.76 g IPTG dissolved in 20 mL deionised $H_2O$.

Twenty µL of 100 mM stocks of dATP, dCTP, dGTP, dTTP were mixed with 120 µL of $H_2O$ to a volume of 200 µL in total.

## 4.2 Plasmids and Strains

pMS470Δ8 (Figure 7) was used for library preparations in *E. coli* Top10F'. It is a high copy number plasmid and, was first described by Balzer et al. 1992 (52)**.** It carries an ampicillin resistance gene.

In pET vectors, target genes are cloned under control of strong bacteriophage T7 transcription and translation signals. Expression is induced by T7 RNA polymerase in the host cell (*E. coli* BL21(DE3) Gold)) (Novagen). It is inducible with IPTG and carries a kanamycin resistance gene. pET26b(+) (Figure 8) was used for expression.
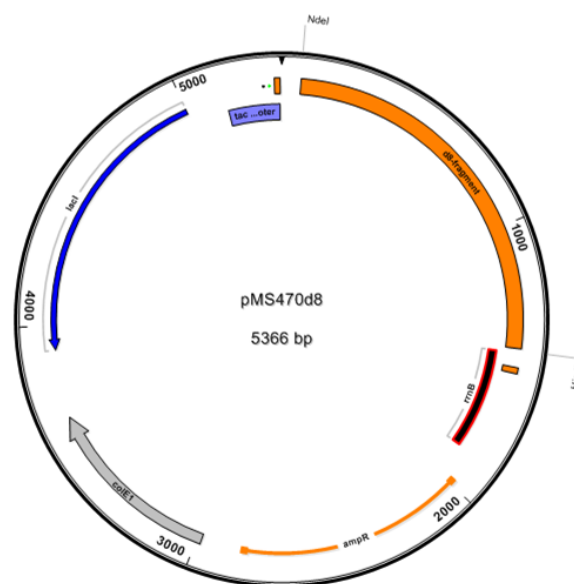


**Figure 7: pMS470Δ8 vector including tac promoter and terminator, *Nde*I and *Hind*III restriction sites, lacI coding sequence, Δ8 fragment, colE1 origin and ampicillin resistance gene.**
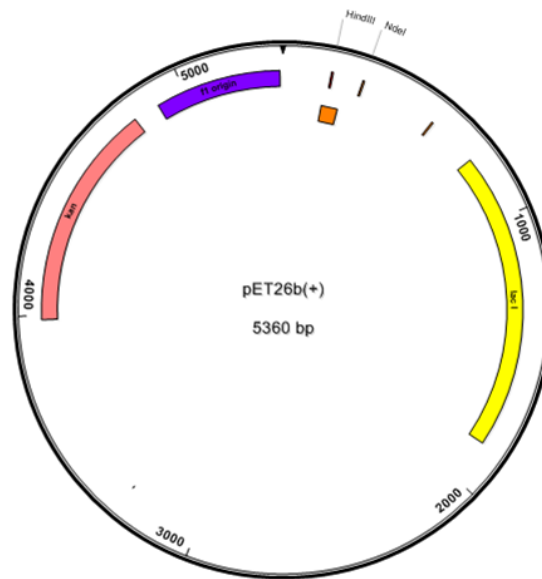
**Figure 8: pET26b(+) vector including T7 promoter and terminator, multiple cloning site (MCS), lacI coding sequence, pBR322 origin, kanamycin resistance and f1 origin.**

*Escherichia coli* Top10F' was used for standard cloning work and library preparation. Genotype: F'{*lac*Iq*Tn*10(TetR)} *mcr*A Δ(*mrr-hsd*RMS-*mcr*BC) Φ80*lacZ*ΔM15 Δ*lac*X74 *rec*A1 *ara*D139 Δ(*ara-leu*)7697 *gal*U *gal*K *rps*L *end*A1 *nup*G. In addition to the ordinary *E. coli* TOP10 strain, this strain includes a F' episome which carries the tetracycline resistance gene and enables the isolation of single – stranded DNA from vectors that have a f1 origin of replication (Lifetechnologies).

*E. coli* BL21 (DE3) Gold was used as strain for protein expression. Genotype: F$^-$ ompT hsdS($r_B^-m_B^-$) dcm$^+$ Tet$^r$ gal λ(DE3) endA Hte. This strain is a derivative of *E. coli* B and is a protein expression strain that lacks two proteases, which might degrade proteins during purification. The Dcm methylase, which naturally is not present in *E. coli* B is inserted. *E. coli* BL21 (DE3) Gold is resistant to tetracycline and has an increased transformation efficiency compared to ordinary *E. coli* BL21 cells (genomics agilent).

## 4.3   Site – directed mutagenesis

In order to introduce all natural amino acids at putative active site positions of *Gt*HNL (shown in yellow in Figure 9), degenerated oligonucleotides containing the NNK codon at targeted positions were used. N represents all four bases whereas K stands for C and G.

```
atggagattaagcgggttgggtcgcaggcttcgggcaaggggccggcggattggtttacgggtacggt
gaggatcgatccgctgtttcaggctcccgatccggcgctggtggcgggtgcgagtgtgacgtttgagc
cggggggctcggacggcgtggcatacgcatccgctggggcagactttgatcgtgactgctggatgtgga
tgggcgcagcgggagggtggggctgtggaggagatccatccgggggatgtggtgtggttttcgccggg
ggagaagcattggcatggggctgcgccgaccacggccatgacgcatcttgcgatccaggaacggctgg
atggcaaggcggtagattggatggagcatgtgacggacgagcagtatcggcggtaa
```

**Figure 9: DNA - sequence of *Gt*HNL. Codons which belong to amino acids in the active site are shown in yellow, triplets which encode for metal – binding amino acids are coloured in red.**

### 4.3.1 Primer design

Degenerated primers contained the NNK triplet at targeted positions. The NNK codon should be located in the middle of the primer flanked with 10 to 15 bases of the original sequence. List of primer sequences can be looked up in Table 1. Primers were ordered from IDT – Integrated DNA Technologies.

**Table 1: Primers used for site – directed mutagenesis. *Gt*HNL is designated as Cu9.**

| Primer name | Primer sequence | Mean Tm (°C) | Length (bp) |
|---|---|---|---|
| Cu9A40Xfw | 5'- ACTGGTTGCCGGTNNKAGCGTTACCTTTGAAC -3' | 65.4 | 32 |
| Cu9A40Xrv | 5'- GTTCAAAGGTAACGCTMNNACCGGCAACCAGT -3' | 65.4 | 32 |
| Cu9V42Xfw | 5'- CCGGTGCAAGCNNKACCTTTGAACCGG -3' | 66.2 | 27 |
| Cu9V42Xrv | 5'- CCGGTTCAAAGGTMNNGCTTGCACCGG -3' | 66.2 | 27 |
| Cu9F44Xfw | 5'- CGGTGCAAGCGTTACCNNKGAACCGGGTG -3' | 68.5 | 29 |
| Cu9F44Xrv | 5'- CACCCGGTTCMNNGGTAACGCTTGCACCG -3' | 68.5 | 29 |
| Cu9T50Xfw | 5'- CGGGTGCACGTNNKGCATGGCATACC -3' | 66.7 | 26 |
| Cu9T50Xrv | 5'- GGTATGCCATGCMNNACGTGCACCCG -3' | 66.7 | 26 |
| Cu9L61Xfw | 5'- CGCTGGGTCAGACCNNKATTGTTACCGCAG -3' | 65.9 | 30 |
| Cu9L61Xrv | 5'- CTGCGGTAACAATMNNGGTCTGACCCAGCG -3' | 65.9 | 30 |
| Cu9H96Xfw | 5'- GGTGAAAAACATTGGNNKGGTGCAGCAC -3' | 63.4 | 28 |
| Cu9H96Xrv | 5'- GTGCTGCACCMNNCCAATGTTTTTCACC -3' | 63.4 | 28 |
| Cu9H106Xfw | 5'- CACCGCAATGACCNNKCTGGCAATTCAG -3' | 64.4 | 28 |
| Cu9H106Xrv | 5'- CTGAATTGCCAGMNNGGTCATTGCGGTG -3' | 64.4 | 28 |
| Cu9Q110Xfw | 5'- CATCTGGCAATTNNKGAACGTCTGGAC -3' | 60.6 | 27 |
| Cu9Q110Xrv | 5'- GTCCAGACGTTCMNNAATTGCCAGATG -3' | 60.6 | 27 |

## 4.3.2 Generation of site – saturation libraries by a modified QuikChange method

In order to generate site – saturation libraries at positions A40, V42, F44, T50, L61, H96, H106 and Q110, respective forward and reverse primers were extended first in two separate reactions with pMS470Δ8_*Gt*HNL as template. Afterwards 25 µL of each PCR product were mixed for a slow re-annealing. The components for the PCR mixture are listed in Table 2.

**Table 2: PCR components for the extension of primers used for site-directed mutagenesis**

| | |
|---|---|
| Template  pMS470Δ8_*Gt*HNL 100 ng/µL | 2 µL |
| Fw or rv. Primer A40X | 1.5 µL |
| dNTPs (10 mM) | 1 µL |
| *Pfu* Buffer 10x | 5 µL |
| *Pfu* DNAPolymerase | 1 µL |
| H$_2$O | 39.5 µL |
| Total volume | 50 µL |

Following PCR program was applied using Thermal Cycler 2720 from Applied Biosystems.

| | | |
|---|---|---|
| 95°C | 2 min | |
| 95°C | 1 min | |
| 60°C/58°C | 1 min | 30 cycles |
| 72°C | 15 min | |
| 72°C | 10 min | |
| 4°C | ∞ | |

Single-stranded PCR products were re-annealed by using following program:

| | |
|---|---|
| 95°C | 5 min |
| 90°C | 1 min |
| 80°C | 1 min |
| 70°C | 0.5 min |
| 60°C | 0.5 min |
| 50°C | 0.5 min |
| 40°C | 0.5 min |
| 37°C | holding |

### 4.3.3 Transformation in electrocompetent *E. coli* Top10F' cells

Eight µL of the PCR products were digested with *Dpn*I (Fermentas) in Tango Buffer (Fermentas) for two hours at 37°C and were desalted on de-salting filters (Millipore) for 30 minutes. *Dpn*I digests the template DNA because it is able to recognise its dam methylation sites. This step assures that no wildtype plasmids get transformed in the *E. coli* cells.  Five µL of the de – salted products and 70 µL of electrocompetent *E. coli* Top 10F' cells were used for transformation. The cells were re-generated in 700 µL SOC medium for 50 minutes at 37°C and 750 rpm (Eppendorf Thermomixer Comfort). Thirty µL were plated on LB-Amp plates and incubated at 37°C over night.

## 4.4 Random mutagenesis of *Gt*HNL

### 4.4.1 Primer Design

In order to avoid mutations at metal binding sites (shown in red in Figure 10), three random mutagenesis libraries were constructed. The *Gt*HNL gene was divided into three fragments, with a length of 204 bp, 142 bp and 153 bp. The fragments were mutated by error prone PCR by different strategies and subsequently used as megaprimers for the amplification of the whole plasmid pMS470Δ8_*Gt*HNL.The primers for the generation of mutagenic megaprimers are shown in Table 3, primer binding sites are shown in Figure 10. Primers were ordered from IDT – Integrated DNA Technologies.
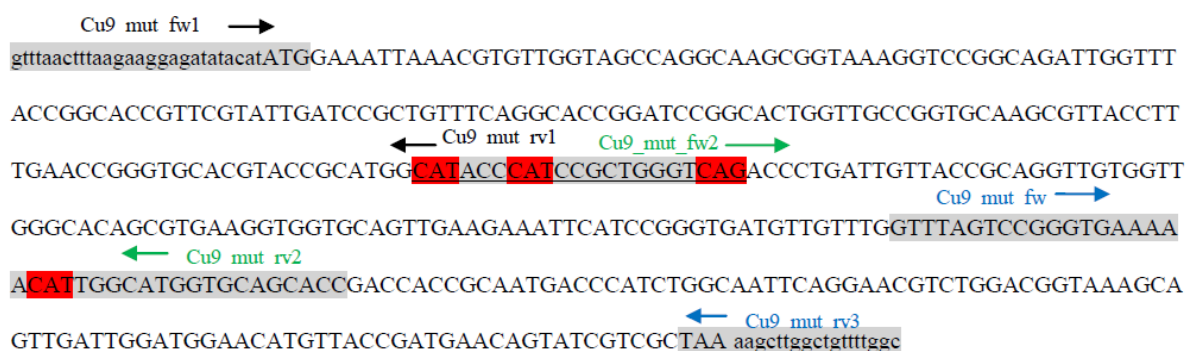


**Figure 10: DNA-sequence of *Gt*HNL. Triplets which encode for metal – binding amino acids are coloured in red. Primer binding sites are indicated with a grey background. *Gt*HNL is designated as Cu9.**

| Primer name | Primer sequence | Mean Tm (°C) | Length (bp) |
|---|---|---|---|
| Cu9_mut_fw1 | 5'- GTTTAACTTTAAGAAGGAGATATACATATG -3' | 50.6 | 30 |
| Cu9_mut_rv1 | 5'- CTGACCCAGCGGATGGGTATG -3' | 59.9 | 21 |
| Cu9_mut_fw2 | 5'- CATACCCATCCGCTGGGTCAG -3' | 59.9 | 21 |
| Cu9_mut_rv2 | 5'- GGTGCTGCACCATGCCAATG -3' | 60.1 | 20 |
| Cu9_mut_fw3 | 5'- GTTTAGTCCGGGTGAAAAACAT -3' | 53.5 | 22 |
| Cu9_mut_rv3 | 5'- GCCAAAACAGCCAAGCTTTTA -3' | 54.6 | 21 |

### 4.4.2 Generation of mutagenic megaprimers by error prone PCR by the addition of MnCl$_2$ and increased concentration of MgCl$_2$

Mutagenic megaprimers were created in a PCR poisoned by MnCl$_2$ (Sigma Aldrich) (0.4 mM) and increased concentration of MgCl$_2$ (7 mM, Fermentas). *Dream Taq DNA – Polymerase* (Fermentas) was used for elongation. The components in the PCR set - up can be looked up in Table 4.

Table 4: List of PCR components for the generation of mutagenic megaprimers.

| | |
|---|---|
| Template  pMS470Δ8_*Gt*HNL (1 ng/µL) | 1 µL |
| forward primer (10 pmol/µL) | 2 µL |
| reverse primer (10 pmol/µL) | 2 µL |
| dNTPs (10 mM stock) | 1 µL |
| *Dream Taq* Buffer 10 x (Fermentas) | 5 µL |
| MgCl$_2$ (25 mM stock) | 10 µL |
| MnCl$_2$ (10 mM stock) | 2 µL |
| *Dream Taq Polymerase* (Fermentas) | 0.5 µL |
| H$_2$O | 26.5 µL |
| Total volume | 50 µL |

PCR program for the generation of mutagenic megaprimers:

95°C    2 min

95°C    30 sec ⎤
55°C    30 sec ⎬ 35 cycles
72°C    20 sec ⎦

72°C    10 min

4°C      ∞

### 4.4.3 Generation of mutagenic megaprimers by GeneMorphII Mutagenesis Kit (Mutazyme II; Agilent Technologies)

Mutazyme II is a mix of two error – prone *DNA polymerases*, *Mutazyme I DNA Polymerase* and a novel *Taq DNA – Polymerase* mutant that has an increased error – rate than the wildtype. Mutazyme II avoids mutation bias and should lead to equivalent mutation rates at A's and T's vs. G's and C's. The PCR components for the generation of the megaprimers can be looked up in Table 5.

Table 5: Components for the generation of megaprimers carrying random mutations.

| | |
|---|---|
| Template  pMS470Δ8_*Gt*HNL (1 ng/µL) | 1 µL |
| forward primer (10 pmol/µL) | 2 µL |
| reverse primer (10 pmol/µL) | 2 µL |
| dNTPs (40 mM stock) | 1 µL |
| Mutazyme II reaction buffer 10 x | 5 µL |
| Mutazyme II *DNA Polymerases* | 1 µL |
| $H_2O$ | 38 µL |
| Total volume | 50 µL |

PCR program for the generation of mutagenic megaprimers by Mutazyme II:

95°C     2 min
95°C     30 sec
55°C     30 sec     } 35 cycles
72°C     1 min
72°C     10 min
4°C      ∞

### 4.4.4 Gel purification and extension of the megaprimers

The PCR products of the error prone PCR and the Mutazyme PCR were loaded on a preparative gel (1% agarose). The gel was run at 90 V for 1.5 h. Bands of correct size were cut out and DNA was purified with Wizard® SV Gel Clean – Up System. The DNA was eluted in 50 µL nuclease – free water.

The purified PCR products were used as megaprimers in another PCR with pMS470Δ8_*Gt*HNL as the template. The PCR components for the extension of the megaprimers can be looked up in Table 6.

**Table 6: Components of the megaprimer PCR.**

| | |
|---|---|
| Template pMS470Δ8_*Gt*HNL (1 ng/µL) | 1 µL |
| megaprimer | 15 µL |
| dNTPs (10 mM stock) | 1 µL |
| *Pfu* Buffer 10x (Promega) | 5 µL |
| *Pfu* Polymerase (Promega) | 1 µL |
| H$_2$O | 27 µL |
| Total volume | 50 µL |

Following PCR program was used for megaprimer extension:

95°C    2 min

95°C    1 min

60°C    30 sec    30 cycles

72°C    10 min

4°C    ∞

### 4.4.5    Transformation in electrocompetent *E. coli* cells

The PCR products were cleaned up with Wizard® SV PCR Clean – Up System as it is described in 4.5. DNA was eluted in 30 µL of nuclease – free water. Afterwards two µL *DpnI* (Fermentas), 5 µL Tango Buffer 10x (Fermentas) and 13 µL H$_2$O were added to the purified DNA to get rid of wildtype plasmids. The *DpnI* digest was carried out at 37°C for one hour. Prior to transformation, the DNA was de-salted with Wizard® SV PCR Clean – Up System. Five µL of the DNA were transformed in 70 µL of electrocompetent *E. coli* Top10F' cells. The cells were regenerated in 700 µL of SOC – medium at 37°C and 750 rpm for one hour. Hundred as well as 200 µL of each transformation (fragment 1, 2, 3, each mutated either by standard error prone PCR or with MutazymeII) were plated on 250 mL LB – Amp Bioassay Trays with sterile glass beats and grown at 37°C over night.

## 4.5    DNA purification with Wizard® SV Gel and PCR Clean – Up System

### 4.5.1    Gel slice preparation

Following gel electrophoresis, DNA bands of correct sizes were excised and placed in a 1.5 mL reaction tube. Five hundred µL Membrane Binding Solution were added to the gel slices and

incubated at 60°C and 1100 rpm on the thermo mixer until they were completely dissolved. SV Minicolumns were inserted into the Collection Tubes and dissolved gel mixtures were transferred to the Minicolumn assemblies.

### 4.5.2  PCR product preparation

An equal volume (50 µL) of Membrane Binding Solution was added to the PCR products and mixtures were transferred to the Minicolumn assemblies.

### 4.5.3  Binding, Washing and Elution of DNA

After one minute of incubation at room temperature, the assemblies were centrifuged in an eppendorf centrifuge 5415R/5424 at maximum speed for one minute. The flow-throughs were discarded and Minicolumns were reinserted into the Collection Tubes. DNA was washed two times with 700 µL and 500 µL Membrane Wash Solution by centrifugation at maximum speed for one minute. Flow-throughs were discarded and Minicolumn assemblies were centrifuged once again for two minutes at maximum speed to allow evaporation of any residual ethanol of the Membrane Wash Solution. Minicolumns were transferred to clean 1.5 mL reaction tubes. Thirty µL nuclease – free water were put on the center of the Minicolumns and incubated for two minutes at room temperature. DNA was eluted by centrifugation at maximum speed for one minute.

## 4.6  Preparation of electrocompetent *E. coli* cells

Two flasks containing 50 mL 2xTY media were inoculated with a single colony of *E.coli* Top10F'/BL21 (DE3) Gold and grown overnight at 37°C at 150 rpm (Certomat® BS-1, Sartorius). Six main culture flasks were inoculated with the pre – culture to an $OD_{600}$ of 0.1 and grown at 37°C until the $OD_{600}$ reached ~ 1 (Eppendorf Biophotometer plus). After incubation on ice for one hour, the cultures were harvested for 10 minutes at 3000 g and 4°C (Beckman centrifuge, rotor JA – 10). The cells were washed one time with 1 mM Hepes buffer, pH 7 (10 min at 4000 g and 4°C)  and one time (after resuspension of the pellets in a small volume of Hepes buffer) with 10% glycerol (15 min at 5000 g and 4°C). The pellets were re-suspended in three mL 10% glycerol and 160 µL aliquots were transferred in 1.5 mL reaction tubes. Then the cells were stored at -70°C. One sample was thawed and used in a test – transformation with pUC19 (0.00001 µg/µL). Twenty µL, 50 µL and 100 µL were plated out on a LB agar plate containing 100 µg/mL ampicillin and grown overnight at 37°C. Colonies were counted and the transformation rate (cfu/µg) was calculated.

## 4.7 Cultivation in Microtiterplates

### 4.7.1 Site-directed library

For each site-saturation library, three 96-well plates were filled with 100 µL LB medium (supplemented with ampicillin) per well and inoculated with single colonies picked from of the transformation plate using sterile toothpicks. *E. coli* Top10F' harbouring pMS470Δ8_*Gt*HNL was used as positive control and the same strain harbouring the empty plasmid pMS470Δ8 was used as negative control. The plates were incubated at 37°C over night in a box filled with some water in order to prevent evaporation of the liquid in the wells of the plates.

### 4.7.2 Random library

384-well microtiter plates were filled with 55 µL of 2xTY medium (supplemented with ampicillin) per well using the MicroFill Microplate Dispenser (BioTek). Prior to use the dispenser was purged consecutively with water, 80 % ethanol and medium. Transformants from each library (error prone PCR and Mutazyme libraries of fragments 1, 2 and 3) were transferred in twenty 384-well plates with the help of the QPix picking robot (Genetix) (total of 120 plates). Additionally, *E. coli* TOP10F' harbouring pMS470Δ8_*Gt*HNL and empty pMS470Δ8 were included on each plate as positive and negative control, respectively. The 384-well plates were incubated at 37°C over night in a box filled with some water in order to prevent evaporation of the medium.

## 4.8 Colony – based HNL – Activity Assay

### 4.8.1 Preparation of the detection filter

For the preparation of the HCN sensitive detection filters, Whatman filters (Whatman International Ltd.) were soaked with a solution containing 1 % Copper (II) ethylacetoacetate and 1 % N,N,N',N' – Tetramethyl-4,4'- methylenedianiline dissolved in chloroform. After drying, the filters can be stored protected from light at 4°C.

### 4.8.2    Site – directed library

The variants cultivated in 96-well plates were stamped with a 96-pin stamp on Biodyne® Nylon membranes (Pall Corporation) and transferred on rectangular LB-Amp plates. The plates were incubated over night at 37°C. The nylon membranes with the grown colonies were put on LB induction plates including 0.1 mM IPTG and 0.1 mM MnCl$_2$. Induction was carried out for 24 hours at 20 to 25°C. The membranes with the induced transformants were pre-equilibrated in 0.1 M citrate phosphate buffer, pH 3.5 for 15 minutes. They were transferred up side down on filters soaked with substrate solution (20 mM (*R*)-mandelonitrile in 0.1 M citrate phosphate buffer, pH 3.5) and covered with a net to separate it from HCN sensitive detection paper, which was placed on the top of the assembly. Timer was started and the set up was weighed with the cover of a microtiter plate to keep the filter in uniform proximity to the colonies. Times until the first signals arose were recorded and pictures were taken.

The clones which showed the strongest and/or fastest signals were chosen for re – screening. Plasmids were isolated and finally sent for sequencing (LGC Genomics).

### 4.8.3    Random library

*Gt*HNL random mutants were cultivated in 384-well microtiter plates and stamped on Biodyne® Nylon membranes using a 384-pin stamp. The membranes were transferred on LB-Amp agar plates and incubated over night at 37°C. Next day, the nylon membranes carrying the colonies were put on LB induction plates and treated as described above. To screen for *Gt*HNL variants with improved stability at pH 3.5, the colonies were treated with freeze and thaw cycles (three times for 10 minutes freezing and 15 minutes thawing) prior to equilibration in 0.1 M citrate phosphate buffer, pH 3.5. Further procedure was the same as with the site-directed libraries.

## 4.9    DNA isolation by GeneJET Plasmid Miniprep Kit

GeneJET Plasmid Miniprep Kit from Thermo Scientific was used for DNA isolation. Cell material was re-suspended by vortexing in 250 µL of Resuspension Buffer, 250 µL of Lysis Buffer was added and samples were inverted three to four times. 350 µL of Neutralization Buffer was added and samples were inverted three to four times. The samples were centrifuged for five minutes at and supernatant was transferred to the mini columns. After a centrifugation step of one minute the columns were

washed two times with 500 µL of Washing Solution. To assure that ethanol gets removed completely, the samples were centrifuged for another two minutes before they were eluted in 50 µL of $H_2O$.

# 4.10 Cloning into pET26b(+)

## 4.10.1 Cloning using restriction enzymes and T4 DNA – Ligase

For expression of *Gt*HNL variants, the mutated genes were sub-cloned from pMS470Δ8 to pET26b(+) expression vector. *Gt*HNL with site-directed mutations, *Gt*HNL including mutations in fragment 1 as well as the pET26b(+) vector were cut with *Nde*I (Fermentas) and *Hind*III (Fermentas) at 37°C over night. The restriction set – ups are shown in Table 7.

Table 7: Cutting set – up with *Nde*I and *Hind*III of insert and vector pET26b(+).

| Insert | Vector |
|---|---|
| 10 µL insert (isolated plasmid) | 2 µg DNA |
| 1 µL *Nde*I (Fermentas) | 1 µL *Nde*I (Fermentas) |
| 1 µL *Hind*III (Fermentas) | 1 µL *Hind*III (Fermentas) |
| 3 µL Buffer R 10x (Fermentas) | 5 µL Buffer R 10x (Fermentas) |
| 15 µL $H_2O$ | x µL $H_2O$ |
| 30 µL total | 50 µL total |

Inserts and vector were cleaned up via preparative gel electrophoresis and with Wizard® SV Gel Clean – Up System. DNA was eluted in 30 µL $H_2O$ and concentration of vector and inserts was determined with NanoDrop 2000 (Thermo Scientific). The ligation was done by *T4 DNA – Ligase* (Promega) at 16°C overnight. Usually, a vector – insert ratio of 1:3 was applied, considering the size of insert (406 bp) and vector (5350 bp). Fifty ng of vector were used, hence 11 ng of insert were added to the ligation mixture. This was calculated with the equation below. The ligation set-up can be looked up in Table 8.

$$ng\ (insert) = \frac{3}{1} * ng(vector) * \frac{bp\ (insert)}{bp\ (vector)}$$

| |
|---|
| 50 ng vector |
| 11 ng insert |
| 1 µL T4 DNA – Ligase (Promega) |
| 1 µL Ligase Buffer 10x (Promega) |
| x µL H$_2$O |
| 10 µL total |

Ligation mixture was de-salted for 45 minutes on de-salting filters (MF$^{TM}$ – Membrane Filters, Millipore) and 7 µL were used for the transformation in 70 µL electrocompetent *E. coli* BL21 (DE3) cells. Hundred µL of the transformation mixture as well the remaining transformation mixture were plated on LB-Kan plates.

## 4.10.2 Cloning using the Gibson Assembly Protocol

### 4.10.2.1 *Insert Amplification*

*Gt*HNL harbouring mutations in fragment 2 and 3 was cloned pursuing Gibson Assembly protocol by New England BioLabs. This protocol uses an exonuclease, which creates single – stranded 3' overhangs, a *DNA Polymerase* and a *DNA Ligase*. For Gibson Assembly new primers had to be designed because the inserts get amplified for the assembly, these are listed below, *Gt*HNL is designated as Cupin9:

**synCupin9 (pET26)_for:**
5' – AATAATTTTGTTTAACTTTAAGAAGGAGATATACATATGGAAATTAAACGTGTTGGTAGC – 3'

**synCupin9 (pET26)_rev:**
5'-GGTGGTGGTGGTGGTGCTCGAGTGCGGCCGCAAGCTTTTAGCGACGATACTGTTCATCG – 3'

List of PCR components for the amplification of *Gt*HNL having mutations in fragment 2 and 3 can be looked up in Table 9. PCR program is shown below.

| | |
|---|---|
| Template  Template  pMS470Δ8_mutated *Gt*HNL (isolated plasmid appr. 1 ng/µL) | 1 µL |
| forward primer (10 pmol/µL) | 1 µL |
| reverse primer (10 pmol/µL) | 1 µL |
| dNTPs (10 mM stock) | 1 µL |
| *Phusion* DNA Polymerase (Fermentas) | 1 µL |
| *Phusion* Buffer HF 5x (Fermentas) | 10 µL |
| $H_2O$ | 35 µL |
| Total volume | 50 µL |

PCR program for the amplification of mutated *Gt*HNL for Gibson cloning:

98°C     2 min

95°C     0.5 min ⎫

55°C     0.5 min ⎬  30 cycles

72°C     0.5 min ⎭

72°C     7 min

4°C      ∞

The PCR products as well as a pET26b(+) vector cut with *Nde*I and *Hind*III were loaded on a preparative gel. Bands of the size of 500 bp were cut out, cleaned up with Wizard® SV Gel Clean – Up System and eluted in 30 µL $H_2O$. Concentration of vector and inserts were determined by NanoDrop 2000.

#### 4.10.2.2 *Preparation of reaction buffer and the assembly master mix*

Six mL of 5x ISO reaction buffer were prepared by mixing following components in a 15 mL tube. The components are summarized in Table 10.

Table 10: List of components for the preparation of reaction buffer for Gibson Assembly.

| component | stock solution | volume/amount |
|---|---|---|
| 25% (w/v) PEG-8000 | PEG-8000 | 1.5 g |
| 500 mM Tris/Cl pH 7.5 | 1 M Tris/Cl pH 7.5 | 3000 µL |
| 50 mM $MgCl_2$ | 2 M $MgCl_2$ | 150 µL |
| 50 mM DTT | 1 M DTT | 300 µL |

| 1 mM dATP | 100 mM dATP | 60 µL |
|---|---|---|
| 1 mM dCTP | 100 mM dCTP | 60 µL |
| 1 mM dGTP | 100 mM dGTP | 60 µL |
| 1 mM dTTP | 100 mM dTTP | 60 µL |
| 5 mM NAD | 100 mM NAD | 300 µL |
| - | sterile ddH$_2$O | up to 6000 µL |
| total volume | - | 6000 µL |

1.2 mL of assembly master mix were prepared by combining components which are listed in Table 11.

Table 11: List of components for the preparation of the assembly master mix.

| component | volume to add |
|---|---|
| 5 x ISO reaction buffer | 320 µL |
| *T5* exonuclease, 10 U/µL | 0.64 µL |
| *Phusion* DNA Polymerase, 2 U/µL | 20 µL |
| *Taq* DNA ligase, 40 U/µL | 160 µL |
| sterile ddH$_2$O | 699.36 µL |
| Total volume | 1200 µL |

### 4.10.2.3 *Gibson Assembly*

Thirty ng of insert and 322 ng of vector were added to 15 µL of the Gibson Assembly Mastermix. The insert to vector ratio was equimolar and total volume of DNA added to the mastermix was never more than ten µL. The assembly mix was incubated for one h at 50°C. Five µL of the mix were directly transformed in 70 µL *E. coli* BL21 (DE3) Gold cells. Concentrated cells were plated on LB-Kan plates and grown overnight at 37°C.

### 4.10.3 Colony PCR

To check if the cells harbour the vector with the desired inserts, a colony PCR was made with four colonies of each sample. Therefore, colonies from the transformation plates were picked with a toothpick and streaked out on a LB-Kan agar masterplate. The same toothpick was used for adding some cell material (= template) into the colony PCR mix. Primer sequences are listed in Table 12. The components for the colony PCR are summarized in Table 13 and the PCR program can be looked up beneath.

| Primer name | Primer sequence | Mean Tm (°C) | Length (bp) |
|---|---|---|---|
| T7_prom | 5'- TAATACGACTCACTATAGG -3' | 44.5 | 19 |
| T7_term | 5'- GCTAGTTATTGCTCAGCGG -3' | 53.4 | 19 |

**Table 13: Colony PCR set up to check if mutated *Gt*HNL is inserted in pET26b(+).**

| | |
|---|---|
| T7term primer (10 pmol/µL) | 0.5 µL |
| T7prom primer (10 pmol/µL) | 0.5 µL |
| dNTPs (10 mM stock) | 0.5 µL |
| *Dream Taq* DNA Polymerase (Fermentas) | 0.2 µL |
| *Dream Taq* Buffer 10x (Fermentas) | 2.5 µL |
| H$_2$O | 20 µL |
| Total volume | 25 µL |

Colony PCR program:

95°C    10 min

95°C    0.5 min ⎫

53°C    0.5 min ⎬ 25 cycles

72°C    1 min ⎭

72°C    7 min

4°C    ∞

PCR products (about 600 bp in the case of successful cloning) were loaded on a control gel to check if the vector carries the desired insert. Positive clones were streaked out to get single colonies.

## 4.11 Cultivation and cell disruption by sonication

The hits of the mutant library screening were cultivated in shake flasks. Single colonies were used to inoculate 100 mL LB-medium (supplemented with kanamycin) in 300 mL shaking flasks and were grown at 37°C and 150 rpm over night. Main culture flasks including 330 mL LB medium (supplemented with kanamycin) were inoculated with 3.3 mL of the pre – cultures and grown at 37°C

and 120 rpm to an OD$_{600}$ of about 0.8. For induction of protein expression 0.1 mM IPTG was added. At the same time MnCl$_2$ (final concentration 0.1 mM) was added and the cells were further incubated at 25°C and 120 rpm for about 20 hours. Glycerol stocks were made of the pre – cultures by adding one mL of the cultures to 450 µL 50 % glycerol in LB. After 20 hours of expression, the cells were harvested for 20 minutes at 4500 rpm and 4°C (Beckman centrifuge, rotor JA – 10). For disruption of cells by sonication, the pellets were dissolved in 25 mL of 10 mM sodium phosphate buffer, pH 7.2. Branson Sonifier 250 was used for sonication. Duty Cycles were set to 80, Output Control 8 and sonication was carried out for six minutes under permanent cooling on an ice-water bath. After disruption lysates were kept on ice. The broken cells were centrifuged at 20 000 rpm and 4°C for one hour. The supernatants were poured in 50 mL tubes on ice. 17.5 to 20 mL were concentrated to about 50 mg/mL using Viva Spin Columns (cut-off 10.000 MWC, Sartorius Stedium Biotech S.A.) by centrifugation (Eppendorf centrifuge 810 R) at 4000 rpm for one to four hours at 4°C.

## 4.12 Estimation of protein concentration by Bradford

Biorad Protein Assay, which is based on the method of Bradford, was used for estimation of total protein content in lysates. The binding of Coomassie Brilliant Blue G – 250 to proteins leads to a shift in the absorption maximum of the dye from 465 nm to 595 nm. The protein concentration can be estimated by monitoring the increase in absorption at 595 nm (53).

For estimation of the protein concentration a calibration curve was established with a BSA (bovine serum albumin) standard. Therefore, a 2 mg/mL BSA stock solution was diluted with water to obtain the following standard concentrations: 0.125 mg/mL, 0.250 mg/mL, 0.500 mg/mL, 0.750 mg/mL, 1 mg/mL. The dilutions for the generation of the calibration curve are listed in Table 14. Calibration curve is shown in Figure 11.

Table 14: Concentrations of BSA used for establishing the calibration curve.

| Conc. [mg/mL] | BSA stock [µL] | H$_2$O [µL] |
|---|---|---|
| 1 | 50 | 50 |
| 0.75 | 37.5 | 62.5 |
| 0.5 | 25 | 75 |
| 0.25 | 12.5 | 87.5 |
| 0.125 | 6.25 | 93.75 |
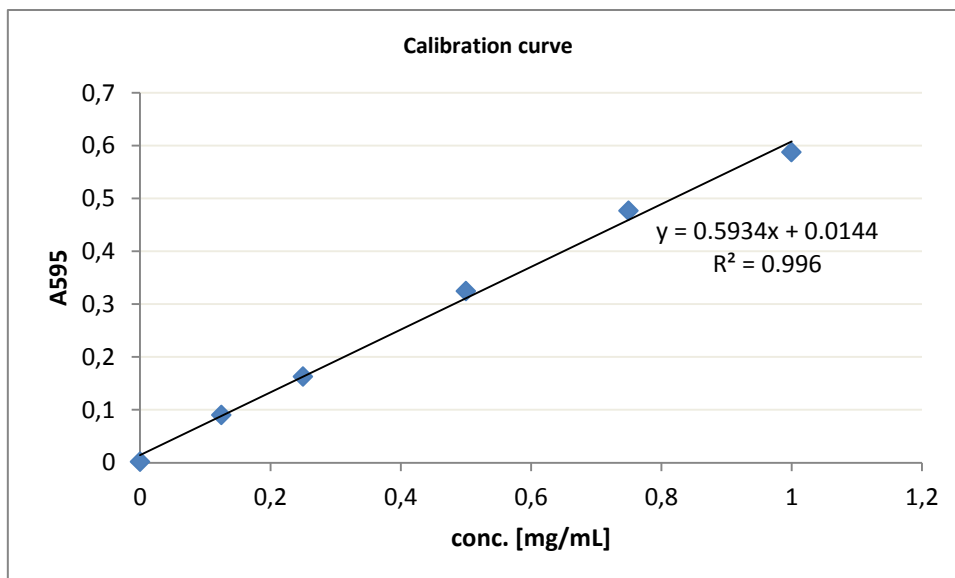
**Figure 11: Calibration curve for the estimation of protein concentrations by Bradford. Correlation coefficient $R^2$ is 0.996.**

The concentrated Bradford solution (Biorad) was diluted 1:5 with water (Fresenius). 990 µL of the Bradford solution was mixed with ten µL of the standard dilutions or ten µL of (diluted) lysates and incubated for 10 minutes at room temperature.

The samples were measured in duplicate at 595 nm (Agilent Technologies – Cary Series UV-Vis Spectrophotometer).

## 4.13 Protein analysis by SDS – PAGE

Expression levels and localisation of the desired proteins were determined by SDS-polyacrylamide gel electrophoresis of lysates and pellets. Precast BisTris Gels from NuPage (10- or 15-well) were used. Usually, approximately ten µg of protein were loaded on the gel. Small aliquotes of the pellets (~ 50 µg) were dissolved in 6 M urea (tenfold volume) at 1050 rpm and 37°C on the thermomixer. Samples were prepared as shown in Table 15.

**Table 15: Preparation of samples for SDS Page .**

| Sample | Lysate (approximately 10 µg) or pellet (0.5 µL) |
|---|---|
| Sample Buffer (Nupage) | 2 µL |
| $H_2O$ | Up to 8 µL total volume |

The samples were incubated at 95°C for ten minutes. Three µl of Page Ruler prestained protein ladder (Fermentas) (Figure 12) were used as protein ladder and eight µl of samples were loaded on the gel. The chamber was filled with 1x MES buffer and the gel was run at 200 V, 120 mA, 25.0 W for 35 minutes (Invitrogen life technologies; XCell Surelock, PowerEase 500). It was stained with Coomassie G250 and destained with destaining solution.
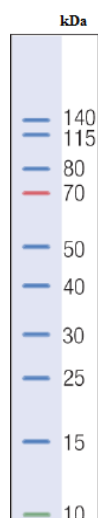
**Figure 12: Page Ruler prestained protein ladder using precast Bis-Tris Gel (4-12%) and MES buffer as running buffer (Fermentas).**

## 4.14 HNL activity assay in microtiterplates

Concentrated cell lysates were used for the activity assay. Hundred µL of 0.1 M MES oxalate buffer, pH 5.6; 0.1 M citrate phosphate buffer, pH 5.6 or 0.1 M citrate phosphate buffer, pH 3.5 were put in 96-well plates and mixed with 50 µL of lysates. The reaction was started with 10 µL of substrate (20 mM (*R*)-mandelonitrile). A detection filter was put on the top of the microtiter plate and the time of signal arising was noted.

## 4.15 Cyanohydrin Synthesis with HCN in organic solvent and quantification of (*R,S*)-mandelonitrile by HPLC

Activities of the mutants were tested in the synthesis reaction (54) and the products were analysed by HPLC. For cyanohydrins synthesis, fresh benzaldehyde (Sigma Aldrich, Art.Nr.: 418099, CAS 100-

52-7) was distilled freshly by Kugelrohr distillation to eliminate benzoic acid which might be an inhibitor for the enzyme and arises due to benzaldehyde oxidation. Benzoic acid evaporates at 250°C whereas benzaldehyde has its boiling point at 178°C at normal pressure. A manometer was used to control the pressure of 52 mbar during distillation. At this pressure 70°C would be adequate for benzaldehyde evaporation but because of a temperature gradient in the oven of the Kugelrohr distiller, the temperature was set to 150 °C. The collection bulb has to be cooled with acetone from time to time. Finally, freshly distilled benzaldehyde was overlayed with argon to avoid oxidation to benzoic acid. The purity of benzaldehyde (0.5 mM in HPLC eluent) was analysed by HPLC. Eluent was 96:04 heptan : isopropanol 0.1% TFA (trifluoro acetic acid). TFA is useful to get better peak shapes. The parameters of the HPLC were as follows: 0.9 ml/min flow; MWD detector; Daicel ODH column, Chiralcel (250 mm long, 4.6 mm internal diameter, 5 µm diameter particle size). The samples were measured at 210 nm (cyanohydrins), 280 nm (benzaldehyde) and 254 nm (aromatic components). Data were evaluated with Agilent ChemStation. Conversions and $ee$ – values were calculated with following equations:

$$100 * \left( 1 - \frac{\frac{benzaldehyde}{internal\ standard}}{\frac{benzaldehyde}{internal\ standard}at\ time\ 0} \right) = \text{conversion } [\%]$$

$$100 * \frac{A-B}{A+B} = ee\ [\%]$$

A .. R – enantiomer

B .. S - enantiomer

### 4.15.1 Synthesis of HCN in MTBE

During HCN synthesis the presence of a HCN detector is necessary. 4.9 g (0.1 mol) of NaCN (Sigma Aldrich; 97%; CAS: 143-33-9) were dissolved in 10 mL of water. After the NaCN was fully dissolved, 25 mL of MTBE was added and the mixture was cooled on ice with stirring. Ten ml of 30% aqueous HCl were slowly added to the mixture. The generated HCN was extracted simultaneously into the MTBE, and NaCl as a side – product of the ion – exchange reaction precipitates at 0°C in the aqueous phase.

After the complete amount of HCl has been added, the solution was left to equilibrate at room temperature for 30 minutes. The phases were separated in a separatory funnel and seven mL of MTBE were added twice to the organic phase and stirred. The remaining water was separated. The HCN – MTBE solution was stored in a darkened bottle over one ml of 1 M sodium acetate buffer, pH 4.5.

### 4.15.2 Reaction mixture

The benzaldehyde (0.5 M final concentration) as well as the internal standard (1,3,5-triisopropyl benzene, Art.Nr.: 161004, CAS: 717-74-8) and the HCN in MTBE were mixed stirred until the components were visually fully dissolved (list of components can be looked up in Table 16). Benzaldehyde and internal standard were pre-dissolved in the HCN in MTBE solution and a sample was withdrawn before starting the reactions. This value was taken as the initial value for substrate and internal standard. 450 µL of concentrated lysates were mixed with 50 µL of 1 M sodium acetate buffer, pH 4.0. One mL of the stock solution was added and mixed at 5°C. Samples were taken after 1, 2, 4, 8 and 24 hours. Ten µL of the samples were mixed with 990 µL of eluent and analysed by HPLC. A single run was set to 40 minutes.

Table 16: Components of the stock solution for reaction mixture.

| MTBE - HCN | 27.9 mL |
|---|---|
| Benzaldehyde | 1.5 mL |
| Triisopropylbenzene | 600 µL |

### 4.15.3 Elimination of HCN

5 N NaOH and $H_2O_2$ were used for the destruction of HCN. With the addition of NaOH HCN is converted to cyanide which gets not absorbed that easy through the skin than HCN.  Cyanide gets oxidized to cyanate and finally to anoxic carbonate by the addition of $H_2O_2$. The destruction of HCN was done on ice because the production of heat.

## 4.16 Combination of beneficial mutations

Mutants which either showed better conversion and *ee*-values in cyanohydrin synthesis or stronger signals in the HNL activity filter assay were combined and analysed in the cyanohydrin synthesis reaction.

### 4.16.1 Beneficial site – directed mutations

For the combination of site – directed mutations, new primers were designed which carry the codon for the beneficial amino – acid instead of the NNK triplet. Plasmid pET26b(+)_*Gt*HNL_Q110H was used as template for PCR. In the case of A40H + V42T and A40R + V42T combinations, primers were designed which include both mutations. All primers are listed in Table 17 and were ordered from IDT.

Table 17: Primer to generate A40HV42T and A40RV42T combinations. *Gt*HNL is designated as Cu9.

| Primer name | Primer sequence | Mean Tm (°C) | Length (bp) |
|---|---|---|---|
| Cu9A40HV42T_fw | 5'-ACTGGTTGCCGGTCATAGCACTACCTTTGAACCGGG-3' | 68.5 | 36 |
| Cu9A40HV42T_rv | 5'- CCCGGTTCAAAGGTAGTGCTATGACCGGCAACCAGT -3' | 68.5 | 36 |
| Cu9A40RV42T_fw | 5'-ACTGGTTGCCGGTAGGAGCACTACCTTTGAACCGGG-3' | 69.5 | 36 |
| Cu9A40RV42T_rv | 5'- CCCGGTTCAAAGGTAGTGCTCCTACCGGCAACCAGT -3' | 69.5 | 36 |

In the case of V42TQ110H, A40R_C5Q110H, H106YQ110H and H106NQ110H, mutagenesis was done like it is described in 4.3.2 with pET26b(+)_*Gt*HNL_Q110H as template. PCR products were digested with *DpnI* and transformed in electrocompetent *E. coli* BL21(DE3) Gold like it is described in 4.3.3. Transformants were streaked out for plasmid isolation and 20 µL were sent to sequencing.

A40HV42TQ110H was combined by a single-primer PCR amplifying the whole plasmid carrying Q110H mutation in *Gt*HNL. List of components can be looked up in Table 18, the PCR program is listed below.

Table 18: Components in PCR mixture for the combination of A40HV42TQ110H. *Gt*HNL is designated as Cu9 in the rv primer.

| | |
|---|---|
| Template pET26b(+)_*Gt*HNL_Q110H | 1 µL |
| Cu9A40HV42T_rv (5pmol/µL) | 10 µL |
| dNTPs (2 mM) | 5 µL |

| | |
|---|---|
| *Pfu* Buffer HF 10x (Promega) | 5 µL |
| DMSO (Fermentas) | 1.5 µL |
| *Pfu* DNAPolymerase (Promega) | 1 µL |
| H$_2$O | 26.5 µL |
| Total volume | 50 µL |

PCR program to generate the triple mutant A40HV42TQ110H:

95°C    5 min
95°C    30 sec ⎫
60°C    30 sec ⎬ 27 cycles
68°C    14.5 min ⎭
68°C    7 min
4°C     ∞

PCR products were treated with *DpnI* and transformed into *E. coli* BL21 (DE3) Gold as it is described in 4.3.3. Transformants were streaked out for plasmid isolation and 20 µL plasmid DNA were sent to sequencing.

### 4.16.2 Beneficial random mutations

Advantageous mutations discovered in the screening of random libraries were combined in another PCR. No beneficial mutations were found in fragment 2 whereas one mutant carrying mutations in fragment 1 (= Mn_C9) exhibited improved activity (or stability). The mutations found in clone Mn_C9 were combined with different mutations located in fragment 3 (Mn_A5, Mn_A6, Mn_C4). Primer T7_prom and Cu9_mut_rv1 were used to generate a megaprimer of mutagenic fragment 1 carrying the specific mutations. This megaprimer was used to amplify plasmid pET26b(+) carrying either *Gt*HNL Mn_A5, Mn_A6 or Mn_C4 mutations. List of PCR components can be looked up in Table 19. The PCR program is listed beneath.

**Table 19: PCR mixture to generate combinations of random mutations. *Gt*HNL is designated as Cu9 in the rv primer.**

| | |
|---|---|
| Template  pET26b(+)_*Gt*HNL _Mn_C9  appr. 1 ng/µL | 1 µL |
| Primer T7_prom (10 pmol/µL) | 2 µL |
| Primer Cu9_mut_rv1 (10 pmol/µL) | 2 µL |

| dNTPs (10 mM) | 1 µL |
|---|---|
| *Pfu* Buffer 10x (Promega) | 5 µL |
| *Pfu* DNAPolymerase (Promega) | 0.5 µL |
| H$_2$O | 38.5 µL |
| Total volume | 50 µL |

PCR program to combine random mutations:

| | | |
|---|---|---|
| 95°C | 2 min | |
| 95°C | 30 sec | |
| 55°C | 30 sec | 30 cycles |
| 72°C | 1 min | |
| 72°C | 10 min | |
| 4°C | ∞ | |

PCR products were loaded on a preparative gel, purified with Wizard® SV Gel Clean – Up System and eluted in 50 µL H$_2$O.

The PCR products were used as megaprimers in another PCR like it is described in 4.4.4. pET_*Gt*HNL_Mn_A5, Mn_A6, Mn_C4 were used as templates. PCR products were treated and transformed like it is described in 4.4.5. Transformants were streaked out for plasmid isolation, plasmid DNA was extracted and 20 µL of each were sent to sequencing.

### 4.16.3 Combination of site – directed and random mutations

To combine advantageous mutations of fragment 1, fragment 3 as well as mutations in the active site, primer A40HV42T was used in a single – primer PCR where plasmid harbouring mutations in fragment 1 ( = Mn_C9) and 3 ( = Mn_A6) was used as template. In this PCR only one primer has to be added to the PCR and the whole plasmid gets amplified like it is described in 4.16.1.

## 4.17 Protein Purification

### 4.17.1 Cultivation and Expression

Clones Mn_A3 and triple mutant T were cultivated in flasks. Glycerol stocks were used to inoculate 100 ml LB–medium (supplemented with kanamycin) in 300 mL flasks (three flasks for each clone). Cultivation, expression as well as harvesting and cell disruption was done as it is described in 4.11. Instead of 10 mM sodium phosphate buffer, pH 7.2, ten mL of buffer A for QFF was used for resuspension of the cell pellets. Cells were pooled before disruption (30 mL Mn_A3, 30 mL T in total). During purification samples were kept on ice constantly.

### 4.17.2  Anion exchange chromatography

Ion exchange chromatography is based on the electrostatic and reversible interaction of charged molecules to oppositely charged groups attached to an insoluble matrix. The pH value at which molecules have no net charge is called isoelectric point (pI). Exposure to pH below the pI leads to positively charged molecules and it binds to cation exchanger, whereas pH higher than the pI leads to a negative net charge and the molecule binds to anion exchanger (55). For the purification of *Gt*HNL variants, three Q Sepharose Fast Flow (QFF) columns in series (anion exchanger, 5 ml, GE Healthcare) were used with a bead structure of 6 % highly cross – linked agarose and a bead size of 45 – 165 μm and the charged group: - $N+(CH_3)_3$. *Gt*HNL variants T and Mn_A3 have both a pI of 5.74 (ProtParam), so buffer A and B for the purification with QFF were set to pH 6.7. The samples (appr. 30 mL) were loaded onto the column with a flow of 2 mL/min. To wash the proteins from the columns with buffer A or buffer B, the flow was set to 4 mL/min. First fractions (10 mL) were eluted with 100% A, one ml fractions were eluted with 10% B and last fractions (10 mL) were eluted with 100% B. Absorption at 280 nm was monitored.

Selected fractions were loaded on SDS – gels to be able to decide which fractions include purified Mn_A3 and T and can be pooled. 6.5 μL of fraction was mixed with 2.5 μL loading dye (NuPage) and one μL reducing agent (NuPage). Five μL were put on the gel. Two μL of cleared lysate were mixed with 4.5 μL $H_2O$, 2.5 μL loading dye and one μL reducing agent. Five μL were loaded on the gel. SDS – PAGE was carried out at the same conditions as described in 4.13. Fractions including the protein were pooled and the protein concentration was determined using NanoDrop 2000 (A280 E1% = 24.20 (Mn_A3) and 24.15 (T), calculated with ProtParam). The sample was concentrated using in Viva Spin 20 Columns (10.000 MWC) to approximately 30 mg/mL.

### 4.17.3  Size exclusion chromatography

Size exclusion chromatography (SEC) is based on size separation of molecules with respect to the pore size of the matrix on the column (56). Superdex 75 Hi Load 16/600 column (125 mL, GE Healthcare) was used for further purification of Mn_A3 and T. It is recommended that a maximum

volume of five mL is loaded on the column with 0.5 mL/min. Proteins were eluted with SEC buffer with 0.8 mL/min. Selected fractions were analysed with SDS – PAGE like it is described in 4.17.2. Selected fractions were pooled and concentrated using Viva Spin 20 Columns (10.000 MWC) to 16 mg/mL (five mL in total).

## 4.18 pH – stability test

Lysates and purified proteins were tested for stability in 0.1 M citrate phosphate buffer pH 3.0, 3.5, 4.0, 4.5, 5.0, 5.5 and in 0.1 M MES oxalate buffer, pH 5.6. Fifty μl of lysate or purified protein were incubated in 100 μL of respective buffers for 30 minutes and centrifuged for ten minutes at 12000 rpm. The residual amount of proteins in the supernatants was controlled on a SDS – polyacrylamide gel like it is described in 4.13.

## 4.19  Activity assay in quartz cuvettes with purified protein

HNL specific activity of purified proteins of Mn_A3 and triplemutant T towards (*R*)-mandelonitrile was determined by following the formation of benzaldehyde in 0.1 M citrate phosphate buffer, pH 5.5 and 4.5 as well as in 0.1 M MES oxalate buffer, pH 5.6. In order to check the activity in citrate phosphate buffer, (*R*)–mandelonitrile was dissolved by vortexing in 30 mM citrate phosphate buffer, pH 3.5. For the estimation of enzyme activity in MES oxalate buffer, (*R*)–mandelonitrile was dissolved in 1 mM or 3 mM oxalic acid. Benzaldehyde formation was determined using 2.5 mM (12.5 mM stock, 1 mM oxalic acid) and 18 mM (90 mM stock, 3 mM oxalic acid) substrate solution and measured in quartz cuvettes at 280 nm and 25°C over ten minutes. Mn_A3 was also tested using 5 mM and 10 mM substrate solutions. Chemical background (= blank; buffer mixed with substrate solution) and samples were measured simultaneously and in duplicates. Eight hundred μL buffer were mixed with 200 μL substrate solution (90 mM, 50 mM, 25 mM or 12.5 mM or 90 mM stocks). Activities were monitored with different amounts of proteins. Set ups of the reaction solutions can be looked up in Table 20 and Table 21. Substrate solutions were kept on ice.

**Table 20: Different amounts of proteins (Mn_A3, T) that were tested in the quartz cuvette assay in in citrate phosphate buffer, pH 5.5 and pH 4.5 using different substrate concentrations.**

| citrate phosphate buffer pH 5.5 | | | citrate phosphate buffer pH 4.5 | | |
|---|---|---|---|---|---|
| Sample | substrate conc. [mM] | amount [μg] | Sample | substrate conc. [mM] | amount [μg] |
| Mn_A3 | 18 | 50 | Mn_A3 | 18 | 50 |

| Sample | substrate conc. [mM] | amount [µg] | Sample | substrate conc. [mM] | amount [µg] |
|---|---|---|---|---|---|
| Mn_A3 | 18 | 16 | Mn_A3 | 5 | 160 |
| Mn_A3 | 2.5 | 320 | Mn_A3 | 2.5 | 800 |
| Mn_A3 | 2.5 | 160 | Mn_A3 | 2.5 | 32 |
| T | 18 | 6.4 | T | 2.5 | 16 |
| T | 18 | 3.2 | T | 2.5 | 32 |
| T | 18 | 2 | T | 2.5 | 160 |
| T | 18 | 1.6 | | | |
| T | 18 | 0.8 | | | |
| T | 18 | 0.4 | | | |
| T | 2.5 | 8 | | | |
| T | 2.5 | 4 | | | |
| T | 2.5 | 2 | | | |

Table 21: Different amounts of proteins (Mn_A3, T) that were tested in the quartz cuvette assay in MES oxalate buffer, pH 5.6 using different substrate concentrations.

| Sample | substrate conc. [mM] | amount [µg] |
|---|---|---|
| Mn_A3 | 18 | 50 |
| Mn_A3 | 10 | 160 |
| Mn_A3 | 5 | 160 |
| Mn_A3 | 5 | 80 |
| T | 18 | 6.4 |
| T | 18 | 3.2 |
| T | 18 | 1.6 |
| T | 18 | 0.6 |

Reaction solutions were disposed of as described in 4.15.3.

Enzyme activity was calculated with the following equation:

$$activity\ [U/mL] = \frac{V}{\varepsilon * d * v}\ \Delta A/\min * D$$

V … total volume in the quartz cuvette = 1 mL

ε … extinction coefficient of benzaldehyde at 280 nm = 1.376 l/(mmol*cm)

d … diameter of quartz cuvette = 1 cm

v … enzyme volume in the cuvette

D … dilution factor

# 5 Results

## 5.1 Evaluation of mutant libraries

### 5.1.1 Evaluation of site – directed libraries

In order to check the efficiency of the site-saturation mutagenesis prior to screening, five colonies of each library were picked for plasmid isolation and sequencing of the insert. Exchange of nucleotides and amino acids in different variants of the libraries are shown Table 22. Four of five clones originating from the A40 library included the wildtype *Gt*HNL sequence, all clones from the F44 library that were sent to sequencing were identified as wildtype *Gt*HNLs. Mutagenesis of the V42, T50, L61, H96, H106 and Q110 libraries seemed to worked out more successful as the number of wildtype sequences among the sequenced clones was lower.

Table 22: Sequencing results of randomly picked variants from site – saturation libraries.

| Clone | nucleotide exchange | amino acid exchange | Clone | nucleotide exchange | amino acid exchange |
|---|---|---|---|---|---|
| A40X.1 | Wildtype | - | H96X.1 | C286G | H96V |
| A40X.2 | G118T | A40F | | A287T | |
| | C119T | | H96X.2 | A287T | H96L |
| | A120T | | H96X.3 | C286T | H96F |
| A40X.3 | Wildtype | - | | A287T | |
| A40X.4 | Wildtype | - | H96X.4 | C286G | H96V |
| A40X.5 | Wildtype | - | | A287T | |
| F44X.1 | Wildtype | - | H96X.5 | C286T | H96Stop |
| F44X.2 | Wildtype | - | | T288G | |
| F44X.3 | Wildtype | - | H106X.1 | x | - |
| F44X.4 | Wildtype | - | H106X.2 | C316G | H106A |
| F44X.5 | Wildtype | - | | A317C | |
| T50X.1 | x | - | | T318G | |
| T50X.2 | A148G | T50A- | H106X.3 | Wildtype | - |
| | C150G | | H106X.4 | A317G | H106R |
| T50X.3 | A148G | T50A- | | T318G | |
| | C150G | | H106X.5 | C316G | H106A |
| L61X.1 | C181A | L61N- | | A317C | |
| | T182A | | | T318G | |
| | G183T | | Q110X.1 | C328G | Q110G |
| L61X.2 | C181A | L61S | | A329G | |
| | T182G | | | G330T | |
| | G183T | | Q110X.2 | G330T | Q110H |
| L61X.3 | G183T | L61L | Q110X.3 | A329C | Q110P |
| L61X.4 | x | - | Q110X.4 | x | - |

| L61X.5 | C181T | L61L | Q110X.5 | C328T | Q110F |
|---|---|---|---|---|---|
| V42X.1 | G124C | V42P | | A329T | |
| | T125C | | | G330T | |
| V42X.2 | x | - | | | |
| V42X.3 | Wildtype | - | | | |
| V42X.4 | T125G | V42G | | | |
| V42X.5 | Wildtype | - | | | |

## 5.1.2 Evaluation of random libraries

In order to check the mutation rates using 0.4 mM MnCl$_2$ for mutagenesis, plasmids of six (fragment 1) or two colonies (fragments 2 and 3) were isolated and sent to sequencing. Sequencing results and mutation rates are summarized in Table 23. The mutation rate of fragment 1 was 2.4 % and the mutation rate of fragment 2 was 2.9 %. Most mutations were located in fragment 3 with a mutation rate of 3.2 %.

Table 23: Sequencing results and mutation rates of fragment 1, 2 and 3 of *Gt*HNL. 0.4 mM MnCl$_2$ was used for mutagenesis.

| fragment | nucleotide exchange | amino acid exchange | mutation rate |
|---|---|---|---|
| 1.1 | T15C | - | |
| | G81A | - | |
| | G91A | - | |
| | G112T | - | |
| 1.2 | G23A | S8N | |
| | C33T | - | |
| | G34A | G12S | |
| 1.3 | T17A | V6D | |
| | C137T | P46L | |
| | G146A | R49H | |
| 1.4 | T2C | M1T | 2.4% |
| | A50G | D17G | |
| | A64G | T22A | |
| | A153G | - | |
| 1.5 | T52C | W18R | |
| | T68C | V23A | |
| | T75C | - | |
| | T126A | - | |
| | G140C | G47A | |
| | A144G | - | |
| 1.6 | A37G | L13E | |
| | T86C | F29S | |
| | A153G | - | |
| 2.1 | A212T | Q71L | 2.9% |

| | | | |
|---|---|---|---|
| 2.2 | C179G | T60S | |
| | T185C | I62T | |
| | T216A | - | |
| | A228G | - | |
| | G271T | G91C | |
| 3.1 | G322A | A108T | |
| | A383G | Q128R | |
| 3.2 | A309T | - | 3.2% |
| | C315A | - | |
| | T378A | D126E | |
| | A383G | Q128R | |
| | C388G | R129G | |

In order to get an overview of the number of mutations generated by the Mutazyme II Kit, plasmids of four colonies the fragment 1 library were isolated and sent to sequencing. Sequencing results and mutation rate (0.8 %) are summarized in Table 24.

Table 24: Sequencing results and mutation rates in fragment 1 of *Gt*HNL. GeneMorphII Mutagenesis Kit was used for mutagenesis.

| sample | nucleotide exchange | amino acid exchange | mutation rate |
|---|---|---|---|
| M1.1 | A64T | T22S | 0.8% |
| | T130C | F44C | |
| M1.2 | G146A | R49H | |
| M1.3 | G122A | S41N | |
| M1.4 | T141A | | |

Furthermore, test-screenings using 20 mM (*R*)-mandelonitrile were made in order to estimate the number of inactive clones within the libraries. The percentages of inactive clones are listed in Table 25. In contrast to the $MnCl_2$ fragment 2 library with only 25 % inactive clones, the Mutazyme II library of fragment 2 showed a high number of inactive clones (57 %).

Table 25: Amount of inactive clones within the libraries.

| | $MnCl_2$ | Mutazyme II |
|---|---|---|
| fragment 1 library | 34% | 43% |
| fragment 2 library | 25% | 57% |
| fragment 3 library | 49% | 30% |

## 5.2 Screening and re-screening of mutant libraries with the colony-based HNL-Activity Assay

### 5.2.1 Screening of site-directed libraries

About 270 clones from each site-directed library were screened for improved activity towards 20 mM (*R*)-mandelonitrile. Hits of the primary screenings were collected for re-screening. One of the screening filters of the A40 library is shown in Figure 13. The first signal appeared after 40 seconds (variant C3), whereas the signal of the wildtype appeared after one minute. Best variants were collected for a re-screening, as it is shown in Figure 14. In the re-screening signals of variants A2 (21 sec), C3 (41 sec) and C5 (52 sec) arose first, the wildtype signal appeared after five minutes and showed only a faint signal.
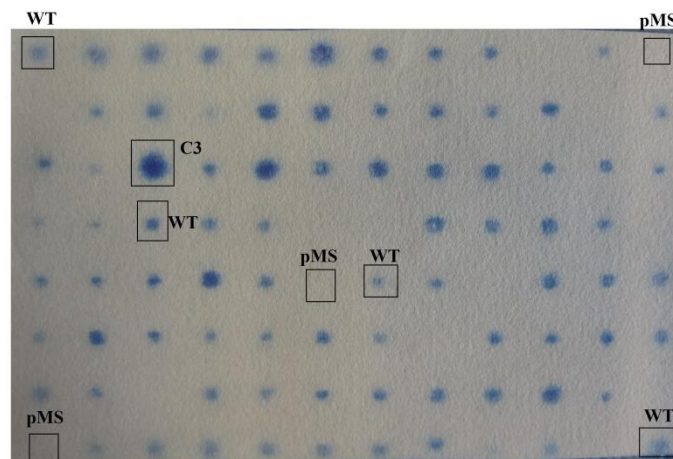


**Figure 13: Screening filter of A40 library in *E. coli* Top10F' after 10 minutes of reaction. Colonies were screened with 20 mM (*R*)-mandelonitrile WT indicates the wildtype, pMS indicates pMS470Δ8 (negative control). Mutant C3 signal appeared after 40 seconds, wildtype signal appeared after one minute.**
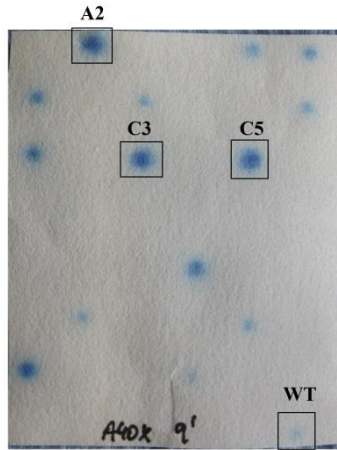
Figure 14: Re–screening filter of A40 library after nine minutes of reaction. Variant A2 appeared after 21 sec., C3 after 41 sec. and mutant C5 after 52 sec.. WT signal appeared after five min.

Variant D6, shown on the screening filter and the re-screening filter in Figure 15 and Figure 16, originates from the Q110 library and appeared after 59 sec in the primary screening, whereas the wildtype signal appeared after 1.10 minutes. In the re-screening D6 (30 sec) as well the wildtype signals (52sec) arose faster than in the primary screening.
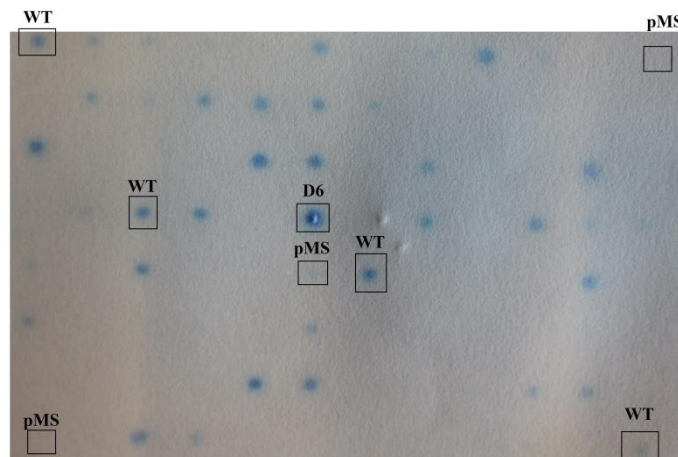


Figure 15: Screening filter of Q110 library in *E. coli* Top10F' after six minutes of reaction. Colonies were screened with 20 mM (*R*)-mandelonitrile WT indicates the wildtype, pMS indicates pMS470Δ8 (negative control). D6 appeard after 59 seconds, WT appeared after 1.10 min.
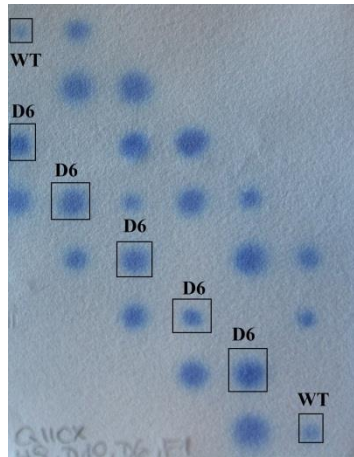
**Figure 16: Re – screening filter hits originating from the Q110 libraries. D6 appeared after 30 seconds while the wildtype signal (WT) appeared after 52 seconds.**

One improved variant was found in the V42 library, shown in Figure 17. Compared to the wildtype and the other clones on the filter, mutant A5 showed the strongest signal in the primary screening of V42 library.
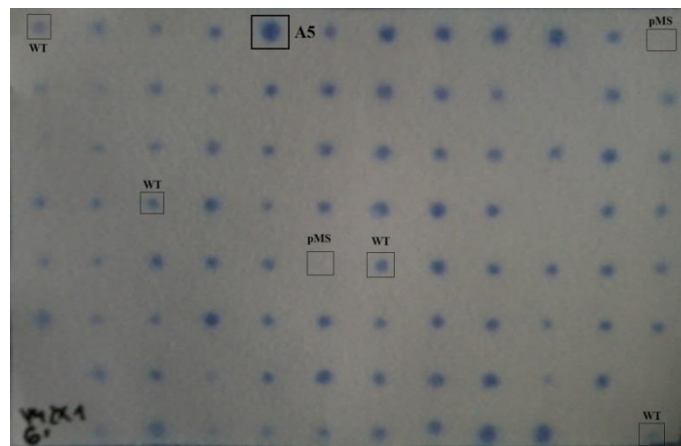


**Figure 17: Screening filter of V42 library in *E. coli* Top10F' after six minutes of reaction. Colonies were screened with 20 mM (*R*)-mandelonitrile WT indicates the wildtype, pMS indicates pMS470Δ8 (negative control). Hit A5 showed the strongest signal on the filter whereas the wildtype signal was very weak.**

Another example of a primary screening filter is shown in Figure 18. The filter belongs to the H106 library and shows two variants that were more efficient in cleaving (*R*)-mandelonitrile (B5 and D8). Signals of both variants came up after 1.20 minutes, while the wildtype signal appeared after four minutes.
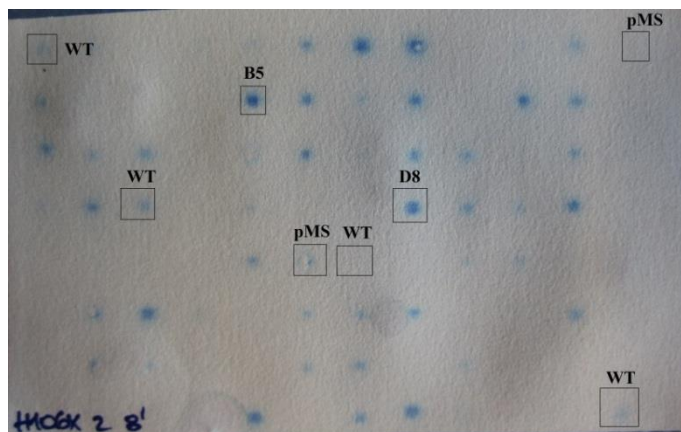


**Figure 18: Screening filter of H106 library in *E. coli* Top10F' after eight minutes of reaction. Colonies were screened with 20 mM (*R*)-mandelonitrile WT indicates the wildtype, pMS indicates pMS470Δ8 (negative control). Hits B5 and D8 appeared after 1.20 min, WT signal appeared after 4.0 min.**

Hits from the primary screenings of site-directed libraries, except those originating from the A40 and Q110 libraries which were re-screened separately, were re-screened together. This re-screening filter is shown in Figure 19. Variant A5 (V42 library), B5 and D8 (H106 library) showed again stronger and faster signals than the wildtype signals.
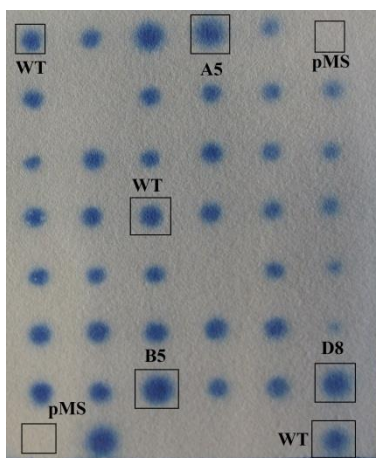


**Figure 19: Re – Screening filter site – directed libraries. A5 appeared after 40 sec, B5 after 46 sec, D8 after 50 sec and wildtype signal arose after one min.**

The exchange of some of the targeted amino acids led to libraries containing high numbers of variants which have lost cyanogenesis activity. Compared to the A40 library, with 16% inactive clones, the exchange of glutamine at position 110 revealed a library with 67% inactive clones. This is summarized in Table 26.

Table 26: Percentages of inactive clones within site–directed libraries.

| library | inactive clones (%) |
|---------|---------------------|
| A40 | 16 |
| V42 | 7 |
| F44 | 11 |
| T50 | 62 |
| L61 | 38 |
| H96 | 46 |
| H106 | 54 |
| Q110 | 67 |

### 5.2.1.1 *Sequencing of Hits*

After re-screening, plasmids were isolated from the selected clones and sent to sequencing. Sequencing results are summarized in Table 27.

Table 27: Sequencing results of hits from the site – directed libraries. *compared to the sequencing results in 5.1.1, most of the clones within this library probably are wildtype, which is the reason that no improved variants were found.

| Library | Hits | nucleotide exchange | amino acid exchange | |
|---------|------|---------------------|---------------------|---|
| A40X | A2 | G118A | A40R | 21 sec (WT 5 min) |
| | | C119G | | |
| | | A120G | | |
| | C3 | G118C | A40H | 41 sec (WT 5 min) |
| | | C119A | | |
| | | A120T | | |
| | C5 | G118C | A40R | |
| | | C119G | | 52 sec (WT 5 min) |
| | | A120G | | |
| V42X | A5 | C124A | V42T | 40 sec (WT 1 min) |
| | | T125C | | |
| F44X | no hits* | - | - | |
| L61X | no hits | - | - | |
| T50X | no hits | - | - | |
| L61X | no hits | - | - | |
| H96X | no hits | - | - | |

| H106X | D8 | C316A | H106N | 50 sec ( WT 1 min) |
|---|---|---|---|---|
| | B5 | C316T | H106Y | 46 sec (WT 1 min) |
| Q110X | D6 | G330T | Q110H | 30 sec (WT 52 sec) |

One clone originating from the Q110 library that showed no signal in the screening was sent to sequencing. The results showed that the exchange from aspartate to tyrosine at position 340 leads to the loss of cyanogenesis activity. Most of the other clones that were not active anymore and that were also sent to sequencing exhibited a lot of insertions or deletions within the *Gt*HNL sequence.

### 5.2.2    Screening of random libraries

Random libraries were screened for variants with improved stability under acidic pH (3.5). About 5100 colonies of the Mutazyme library of fragment 1 and 3640 colonies of the $MnCl_2$ library of fragment 1, 3280 colonies of the Mutazyme library fragment 2 and 1100 colonies of the $MnCl_2$ library of fragment 2 and 3640 colonies of the Mutazyme library and $MnCl_2$ library of fragment 3 were screened towards 20 mM (*R*)-mandelonitrile after disruption of cells by repeated cycles of freezing and thawing. Twenty-eight hits were found in the Mutazyme and 37 hits were found in the $MnCl_2$ library of fragment 1. First hits of the Mutazyme library came up after 3.19 minutes whereas wildtype signals came up after 4.18 minutes. First hits of the $MnCl_2$ library showed signals after 50 seconds (G13, 7), whereas first wildtype signals came up after 1.30 minutes. No hits in the Mutazyme library and seven colonies in the $MnCl_2$ library of fragment 2 seemed to have improved cyanogenesis activity. Best variants in the $MnCl_2$ library came up after 1.30 minutes; wildtype signal appeared after two minutes. The Mutazyme library of fragment 3 revealed 16 improved variants, the $MnCl_2$ library of fragment 3 revealed 22 hits. Best hits in the Mutazyme library came up after 40 seconds while first wildtype signals appeared after one minute. First signals of variants in the $MnCl_2$ library appeared after 39 seconds, while first wildtype signals came up after 1.30 minutes. The whole reaction was stopped between five and ten minutes. No background signals of colonies harbouring pMS470Δ8 or pET26b(+) were detected. Numbers of screened clones, numbers of hits and times until first signals came up are summarized in Table 28. One example of a primary screening filter of the $MnCl_2$ library of fragment 1 is shown in Figure 20. One hit was found on this filter, Mn_A3, which appeared after 1.20 minutes and was ten seconds faster than the wildtype signal.

| library | total number of screened colonies | Number of Hits | Time of first signals of variants | Time of first wildtype signals |
|---|---|---|---|---|
| fragment 1 Mutazyme | 5100 | 28 | 3.19 min | 4.18 min |
| fragment 1 MnCl₂ | 3640 | 37 | 50 sec | 1.30 min |
| fragment 2 Mutazyme | 3280 | no hits | 1 min | 53 sec |
| fragment 2 MnCl₂ | 1100 | 7 | 1.30 min | 2 min |
| fragment 3 Mutazyme | 3640 | 16 | 40 sec | 1 min |
| fragment 3 MnCl₂ | 3640 | 22 | 39 sec | 1.30 min |
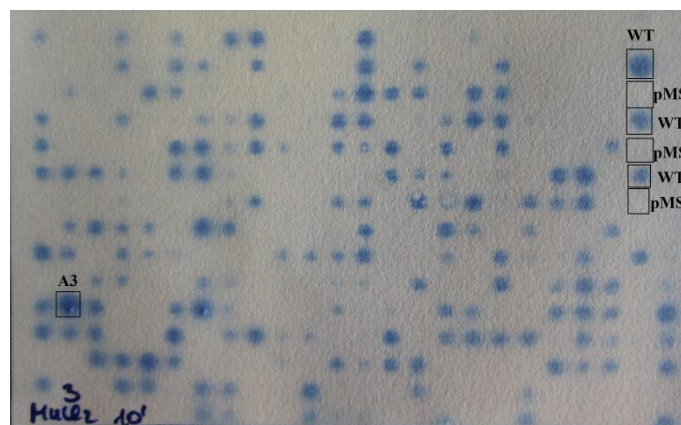


**Figure 20: Primary screening filter of the MnCl₂ library of fragment 1 showing hit Mn_A3 which appeared after 1.20 min. The wildtype (WT) signal came up after 1.30 min. The whole reaction was stopped after ten minutes and 20 mM (*R*)-mandelonitrile were used for screening.**

Hits were collected for re-screening in pMS470Δ8 in *E.coli* Top10F'. Figure 21 shows the re-screening filter of the hits originating from the MnCl₂ library of fragment 1. It was screened towards 20 mM (*R*)-mandelonitrile and reaction was stopped in this case after eleven minutes. Mn_A3 appeared after

1.01 minutes, wildtype (WT) appeared after 2.50 minutes in the re-screening. Figure 22 shows the re-screening filter of the Mutazyme II library of fragment 1 with the hit MZ_C5, which appeared about two minutes faster than the wildtype signal (2.50 min/4.20min). Re-screening filter of the $MnCl_2$ and Mutazyme II fragment 2 and 3 libraries are shown in Figure 23 and Figure 24.
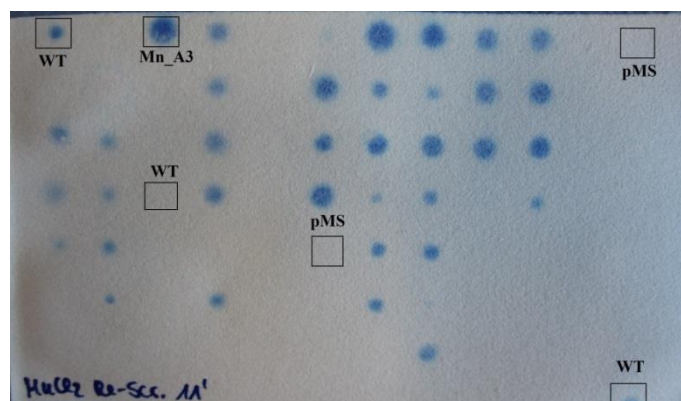


**Figure 21: Re – screening filter of the $MnCl_2$ library of fragment 1 with hit Mn_A3, which appeared after 1.01 min. Wildtype (WT) appeared after 2.50 min. It was screened towards 20 mM (R) – mandelonitrile and the reaction was stopped after eleven minutes.**
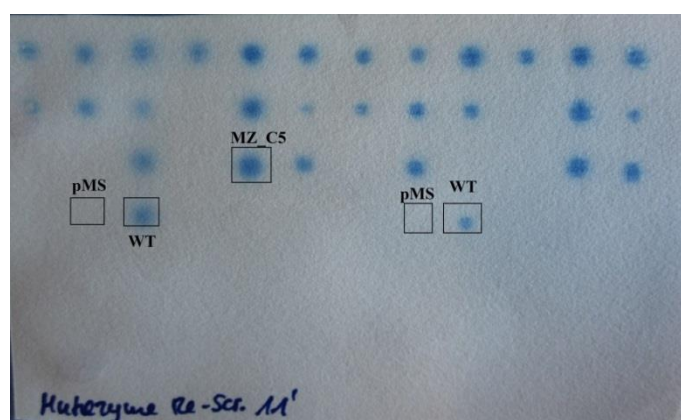


**Figure 22: Re-screening filter of the Mutazyme library of fragment 1 with hit MZ-C5, which appeared after 2.50 min, WT appeared after 4.20 min. The whole reaction was stopped after eleven minutes, 20 mM (R) – mandelonitrile were used for screening.**
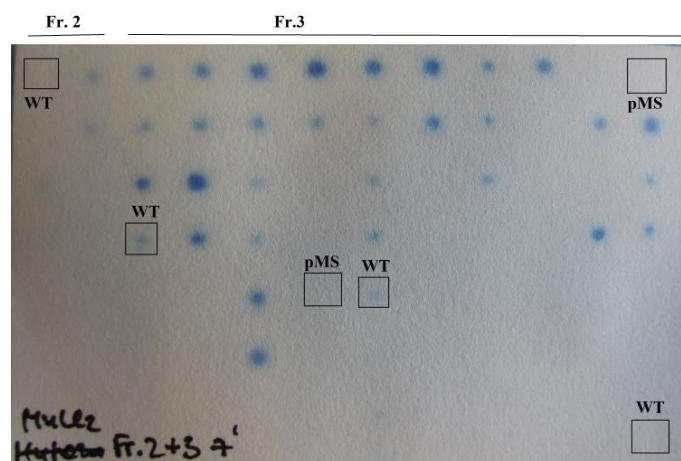
**Figure 23: Re-screening filter of the MnCl₂ library of fragment 2 and 3. It was screened towards 20 mM (*R*)-mandelonitrile. The reaction was stopped after seven minutes.**
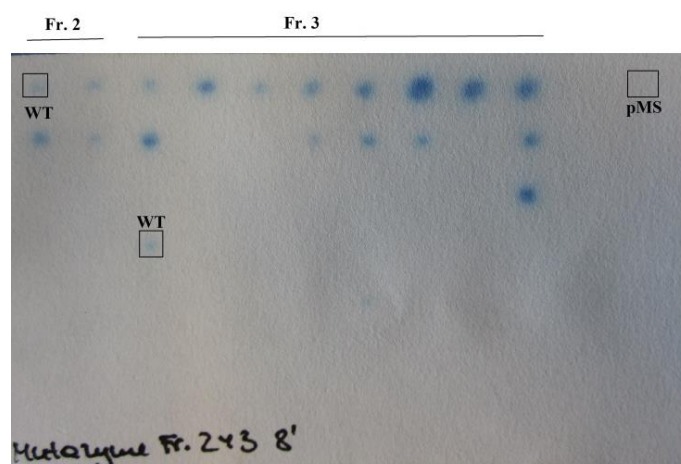


**Figure 24: Re-screening filter of the Mutazyme library of fragment 2 and 3. It was screened towards 20 mM (*R*)-mandelonitrile. The reaction was stopped after eight minutes.**

Hits of the re-screenings were collected, sub-cloned into pET26b(+), transformed in *E. coli* BL21(DE3) Gold and screened once again towards 20 mM (*R*)-mandelonitrile. The plates were screened twice. One filter was tested under standard conditions, without cell disruption (Figure 25), another one was treated with freezing and thawing cycles (Figure 26). After final re-screening in pET26b(+), nine variants of all libraries seemed to have higher cyanogenesis activity or seemed to be more stable at low pH than the wildtype. Eight of these variants were mutants from fragment 3 libraries (two from Mutazyme and five from MnCl₂ libraries). One improved variant had mutations in fragment 1 and originated from MnCl₂ library. No improved variants could be found in fragment 2 libraries after re-screening in pET26b(+). The highest number of improved variants originated from libraries of fragment 3.
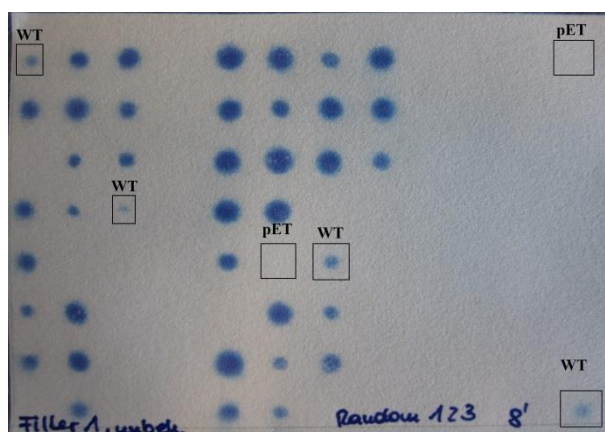
**Figure 25: Filter of re-screening of random libraries (fragment 1, 2 and 3) in *E. coli* BL21 (DE3) Gold under standard conditions. The reaction was stopped after eight minutes. WT is the wildtype, pET is pET26b(+).**
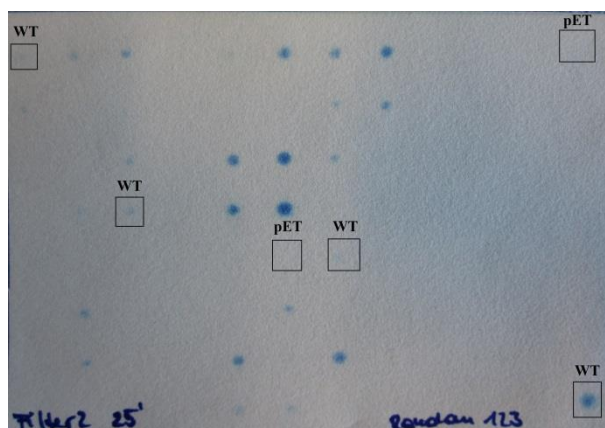


**Figure 26: Filter of re-screening of random libraries (fragment 1, 2 and 3) in *E. coli* BL21 (DE3) Gold after freezing and thawing. The reaction was stopped after 25 minutes. WT is the wildtype, pET is pET26b(+).**

### 5.2.2.1 *Sequencing of Hits*

Plasmids of hits of fragment 1 libraries from the re-screening in pMS470Δ8 in *E. coli* Top10F' were isolated and sent to sequencing before they were sub-cloned and re-screened in pET26b(+). Sequencing results are shown in Table 29. Fragment 2 and 3 mutants were first sub-cloned and re-screened in pET26b(+) in *E. coli* BL21(DE3) Gold prior sequencing. Sequencing results are shown inTable 30.

**Table 29: Nucleotide and amino acid exchanges of hits of fragment 1 libraries.**

| sample | nucleotide exchange | aa exchange | sample | nucleotide exchange | aa exchange |
|--------|--------------------|-------------|--------|--------------------|-------------|
| Mn_A7 | G4A | E2K | Mn_A3 | T75G | I25M |

| sample | nucleotide exchange | amino acid exchange | sample | nucleotide exchange | amino acid exchange |
|---|---|---|---|---|---|
| | A26G | Q9R | | T87C | |
| | A39G | | | T107A | L36Q |
| | G46A | A16T | **Mn_C9** | G4A | E2K |
| | T110C | V37A | | A37G | K13E |
| | A144T | | | T51C | |
| Mn_A8 | T69A | | | T75A | |
| | T85C | F29L | | A105T | |
| | T107G | L36R | Mn_D6 | T8A | |
| | T125C | V42A | | T9A | |
| | A144G | | | A48T | |
| | T147A | | | T75G | I25M |
| Mn_B6 | A12G | | Mn_C8 | T21A | |
| | G19A | G7S | | C24T | |
| | T51A | F19Y | | A38T | K13I |
| | A77T | D26V | | C95G | P32R |
| | C92T | A31V | MZ_A5 | A5C | E2A |
| | C129A | | | C129A | |
| | G138A | | MZ_A9 | T18A | |
| Mn_B9 | T12A | V6D | | T69A | |
| | G116C | G39A | | T74C | I25T |
| | A135G | | MZ_A12 | C79T | P27S |
| | C150T | | | G103A | A35T |
| Mn_B10 | A31T | S11C | MZ_B5 | T57C | |
| | T56A | F19Y | | C101T | P34L |
| | T132C | | | C123T | |
| Mn_C6 | T15C | | MZ_C5 | G71A | R24H |
| | T56A | F19Y | | | |
| | T75C | | | | |
| Mn_C7 | T15A | | | | |
| | T51C | | | | |
| | T75G | I25M | | | |
| | A135T | E45D | | | |

**Table 30: Nucleotide and amino acid exchanges found in hits of fragment 3 libraries of *Gt*HNL.**

| sample | nucleotide exchange | amino acid exchange |
|---|---|---|
| Mn_A3 | G359T | W120L |
| **Mn_A5** | G330T | Q110H |
| | A347T | K116I |
| **Mn_A6** | G330T | Q110H |
| | A332G | E111G |
| Mn_A10 | A329T | Q110L |
| | A365G | E122G |
| | T369C | |
| **Mn_C4** | A294T | |

| | | |
|---|---|---|
| | C306T | |
| | G330C | Q110H |
| | T354G | |
| Mn_D4 | G300T | |
| | A325C | I109L |
| | G330C | Q110H |
| MZ_B3 | G322T | A108S |
| | T327A | |
| | A361T | M121L |
| MZ_C10 | C315A | |
| | G330T | Q110H |

## 5.3 First cultivation and protein expression of selected hits

Best variants from site-directed and random libraries were fermented in shake flasks. Total protein concentration of the lysates was estimated using the Bradford assay (Table 31). Samples included 10 to 18 mg/mL protein.

Table 31: Protein concentration of lysates after sonication, determined with the Bradford assay.

| Sample | concentration [mg/mL] |
|---|---|
| A40R 8.2 (CGG) | 17.67 |
| A40R 6.2 (AGG) | 12.40 |
| A40H | 11.70 |
| V42T | 9.89 |
| H106Y | 10.80 |
| H106N | 11.97 |
| Q110H | 12.66 |
| Mn_A3 | 11.33 |
| MZ_C5 | 12.38 |

The localisation of proteins after sonication was analysed by SDS-PAGE. Lysates as well as pellets of A40R 8.2, A40R 6.2, A40H, V42T, H106Y, H106N, Q110H, Mn_A3 and MZ_C5 were loaded on NuPage gels (Figure 27 and Figure 28). Bands at about 15 kDa belong to the *Gt*HNL variants (monomers). Bands at about 33 kDa belong to the dimers of *Gt*HNL. Expression and sonication seemed to have worked out quite well because the respective thick bands in the lysate fractions reveal a high level expression of the desired proteins in soluble form.
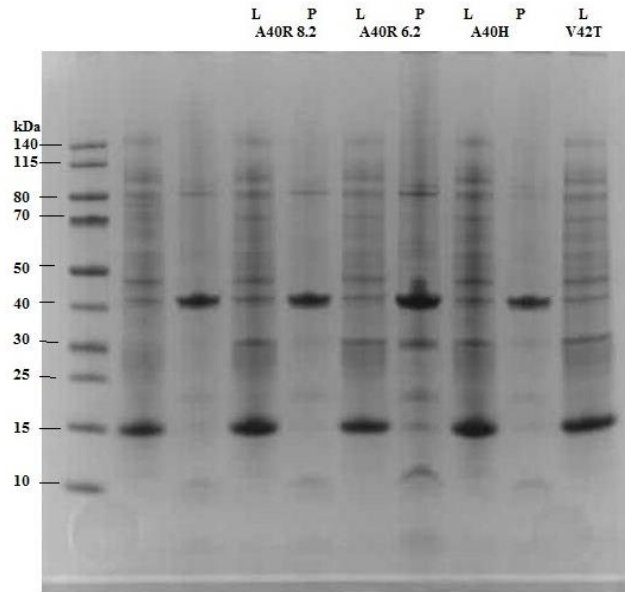
**Figure 27: SDS-gel including lysates (L) and pellets (P) of A40R 8.2, A40R 6.2, A40H and V42T. Slot 1 includes the Page Ruler Prestained protein ladder (Fermentas). The GtHNL monomer has about 15 kDa. Slot 2 and 3 include some other samples, belonging to another experiment.**
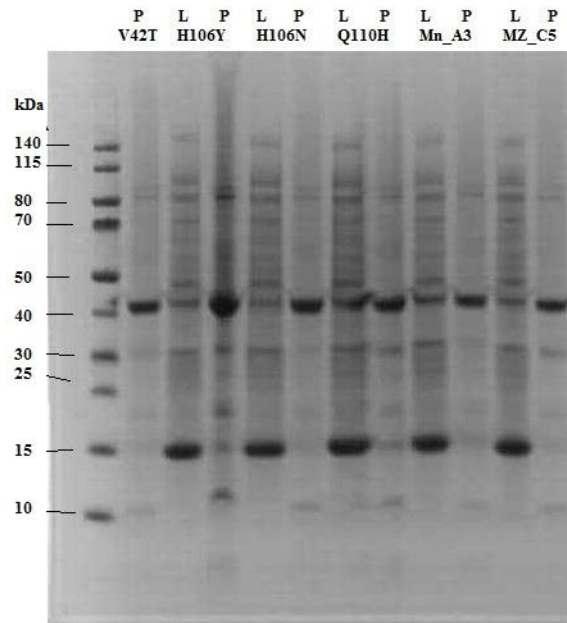


**Figure 28: SDS-gel including lysates (L) and pellets (P) of V42T, H106Y, H106N, Q110H, Mn_A3 and MZ-C5. Slot 1 contains the Page Ruler Prestained protein ladder (Fermentas). Band at about 15 kDa belongs to *Gt*HNL variants (monomer).**

## 5.4 HNL – activity assay in microtiterplates with cell lysates

Strongest signals arose in 0.1 M MES oxalate buffer, pH 5.6 (Figure 29) and 0.1 M citrate phosphate buffer, pH 6.5 (Figure 30). CH2 was used as positive control and showed a signal after 1.44 min in MES oxalate buffer. The wildtype *Gt*HNL signal appeared after four minutes and the signal of mutant *Gt*HNL_A40H arose after 40 seconds.
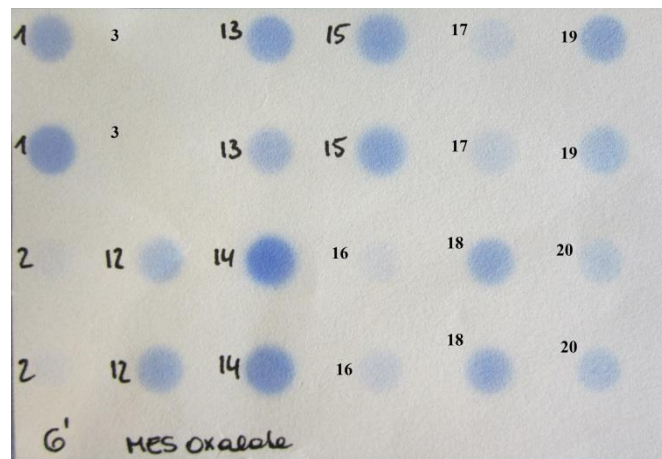


**Figure 29: Filter of lysate screening using 0.1 M MES oxalate, pH 5.6 and 20 mM (*R*)-mandelonitrile. 1 = CH2 as positive control (1.44 min), 2 = *Gt*HNL (4 min), 3 = empty pET26b(+) vector as negative control, 12 = A40R 8.2 (1.23 min), 13 = A40R 6.2 (1.39 min), 14 = A40H (40 sec), 15 = V42T (1.06 min), 16 = H106Y, 17 = H106N, 18 = Q110H, 19 = Mn_A3, 20 = MZ_C5. The reaction was stopped after six minutes.**

Figure 30 shows signals of variants in citrate phosphate buffer, pH 6.5. The signal of variant V42T came up first after 1.25 minutes, whereas the wildtype signal appeared after 7.08 minutes and CH2 needed 3.16 minutes until blue spots appeared.
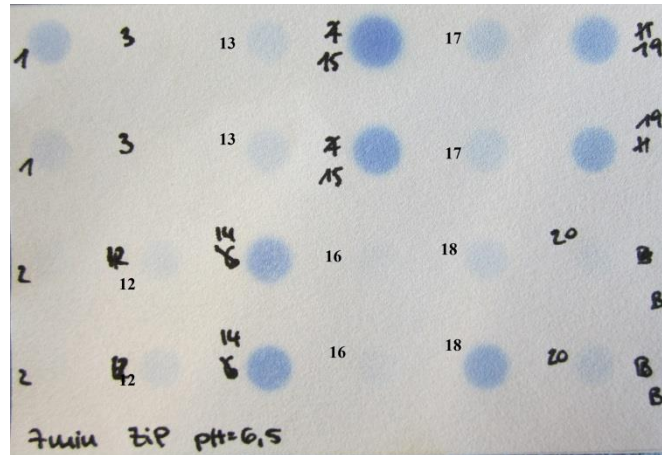
**Figure 30: Filter of lysate screening using 0.1 M citrate phosphate buffer, pH 6.5 and 20 mM (*R*)-mandelonitrile. 1 = CH2 as positive control (3.16 min), 2 = *Gt*HNL (7.08 min), 3 = empty pET26b(+) vector as negative control, 12 = A40R 8.2 (5.00 min), 13 = A40R 6.2 (5.00 min), 14 = A40H (1.25 min), 15 = V42T (1.09 min), 16 = H106Y, 17 = H106N, 18 = Q110H, 19 = Mn_A3 (1.55 min), 20 = MZ_C5, B = Blank (buffer without lysate). The reaction was stopped after seven minutes.**

The cyanogenesis activity in citrate phosphate buffer at pH 3.5 was very low. No variant seemed to be active at this pH, except variant *Gt*HNL_V42T which showed a faint signal after eleven minutes (Figure 31).
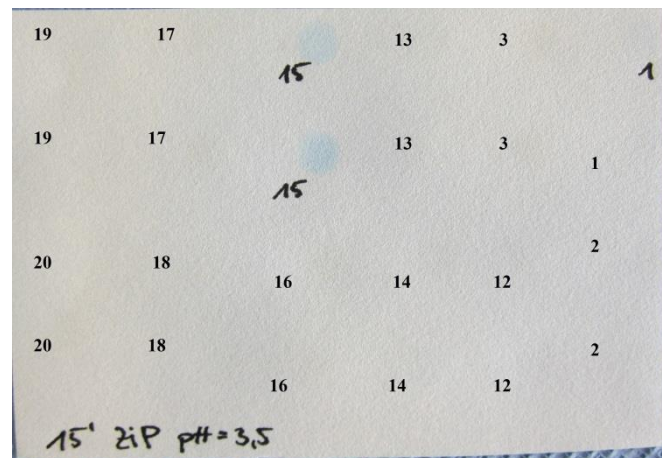


**Figure 31: Filter of lysate screening using 0.1 M citrate phosphate buffer, pH 3.5 and 20 mM (*R*)-mandelonitrile. No variant was active at this pH, except V42T (=15) showed a faint signal after eleven minutes. The reaction was stopped after 15 minutes.**

## 5.5  pH stability test with crude lysate of V42T

Due to the results gained in the HNL-activity assay in microtiter plates, where mutant V42T was the only variant that showed cyanogenesis activity at pH 3.5, pH stability of V42T lysate was analysed (Figure 32 and Figure 33). In comparison to wildtype *Gt*HNL, protein seems to be present in the same

amounts in both supernatants, as the bands on the gel look quite similar; so V42T doesn't seem to be more stable at lower pH than wildtype *Gt*HNL.
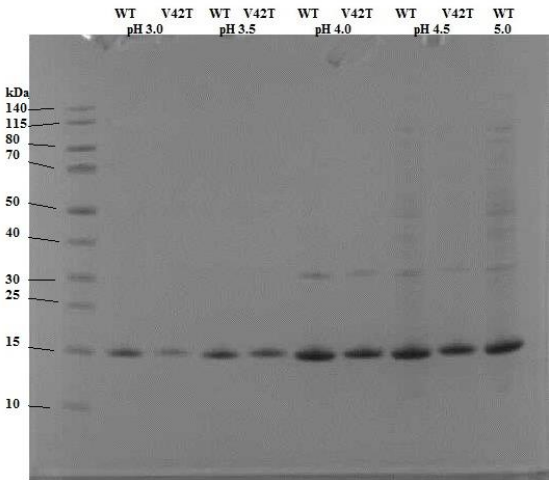


**Figure 32: SDS-gel showing the amount of proteins in supernatants of *Gt*HNL and variant V42T after incubation of lysates in citrate phosphate buffer pH 3.0, 3.5, 4.0, 4.5 and 5.0. The size of the monomer is about 15 kDa, the dimer has about 33 kDa.**
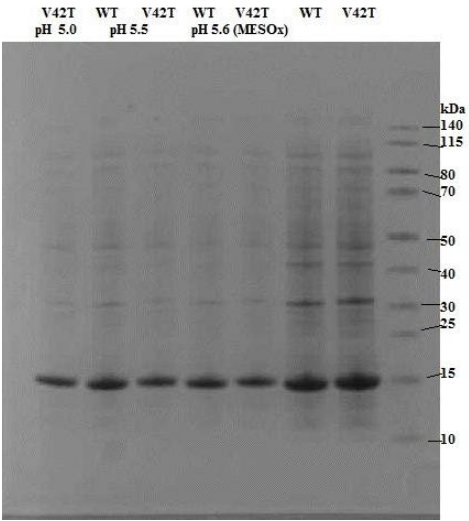


**Figure 33: SDS-gel showing the amount of proteins in supernatants of *Gt*HNL and variant V42T after incubation of lysates in citrate phosphate buffer pH 5.0, 5.5 and MES oxalate buffer pH 5.6 as well as untreated lysates in slots 6 and 7. The size of the monomer is about 15 kDa, the dimer has about 33 kDa.**

## 5.6 Cyanohydrin synthesis

Enzyme activities in the synthesis direction were tested for wildtype *Gt*HNL as well as for variants harbouring the mutations A40H, A40R (CGG), A40R (AGG), H106N, H106Y, Q110H, V42T and the variants Mn_A3 and MZ_C5. Compared to wildtype *Gt*HNL, with about 85% of benzaldehyde conversion after 24 hours, variant A40H had already consumed 99% of the substrate at the same time. Due to the exchange of glutamine to histidine at position 110, 95% of substrate was converted after 24 hours and the enantiomeric excess (*R*) was improved from 89% to 95%. The conversions of benzaldehyde as well as the enantiomeric excess are summarized in Table 32.

**Table 32: Benzaldehyde conversion [% ] and enantiomeric excess (*R*) [%] after 1 hour, 2 hours, 4 hours, 8 hours and 24 hours of reaction.**

| Sample | 1h | 2h | 4h | 8h | 24h | |
|---|---|---|---|---|---|---|
| *Gt*HNL | 26.5 | -43.9 | n. a. | 55.2 | 84.6 | conversion (%) |
| | 90.4 | 89.6 | n.a. | 89.4 | 88.7 | *ee* (%) |
| **A40H** | 35.1 | 58.5 | 79.6 | 94.8 | 99 | conversion (%) |
| | 88.7 | 89.5 | 88.7 | 88.5 | 87.9 | *ee* (%) |
| A40R (CGG) | 20.5 | -4.7 | 33.4 | 65.1 | 87.4 | conversion (%) |
| | 93.9 | 93.9 | 93.6 | 93.7 | 93.7 | *ee* (%) |
| **A40R 6.2 (AGG)** | 24.6 | 41.5 | 60.3 | 82.4 | 97.6 | conversion (%) |
| | 94.7 | 95 | 94.8 | 94.6 | 94.5 | *ee* (%) |
| H106N | 15.3 | 23.3 | 34.1 | 51.4 | 38.4 | conversion (%) |
| | 73.9 | 73.8 | 73.9 | 73.7 | 73.7 | *ee* (%) |
| H106Y | 38.6 | 57.8 | 77.2 | 92.7 | 97.9 | conversion (%) |
| | -1.2 | -0.9 | -0.8 | -0.8 | -0.8 | *ee* (%) |
| **Q110H** | 35.1 | -8.3 | 58.4 | 89.1 | 95.4 | conversion (%) |
| | 96.2 | 95.7 | 95.8 | 95.8 | 95.4 | *ee* (%) |
| **V42T** | 36.6 | 57.5 | 78.3 | 93.5 | 98.8 | conversion (%) |
| | 94 | 96.6 | 96.6 | 96.5 | 96.3 | *ee* (%) |
| **Mn_A3** | -2.5 | -1 | 47.4 | 82.4 | 92.4 | conversion (%) |
| | 94.6 | 94.2 | 93.9 | 93.9 | 93.6 | *ee* (%) |
| MZ_C5 | 21.1 | -33.9 | 36.4 | 58.6 | 77.4 | conversion (%) |
| | 86 | 85.5 | 85.1 | 84.6 | 83.7 | *ee* (%) |
| pET26b(+) | 8.7 | -146.6 | -144.1 | -21.8 | -13.1 | conversion (%) |
| | 5.7 | 0.5 | -0.4 | 0.9 | 1.2 | *ee* (%) |

After 24 hours, mutant Mn_A3 had converted 92.4% of the substrate with an (*R*)-*ee* of 93.6%. In comparison to wildtype *Gt*HNL, the variant shows an improved conversion as well as a better enantiomeric excess (*R*) (Figure 34). The chemical background is not shown because the conversion was too low for detection. Conversion and *ee* (*R*) of A40H, V42T and Q110H are visualized in Figure 35.
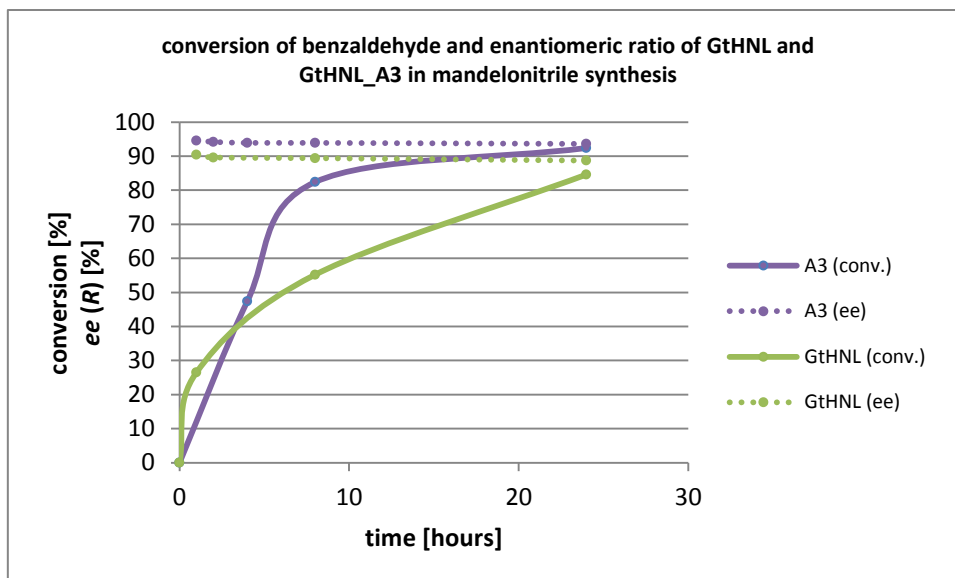
**Figure 34: Conversion [%] of benzaldehyde and enantiomeric excess (*ee*) [%] of Mn_A3 compared to wildtype *Gt*HNL. Mn_A3 is shown in purple, *Gt*HNL is shown in green. The dashed lines refer to the *ee* and the solid lines refer to the conversion.**
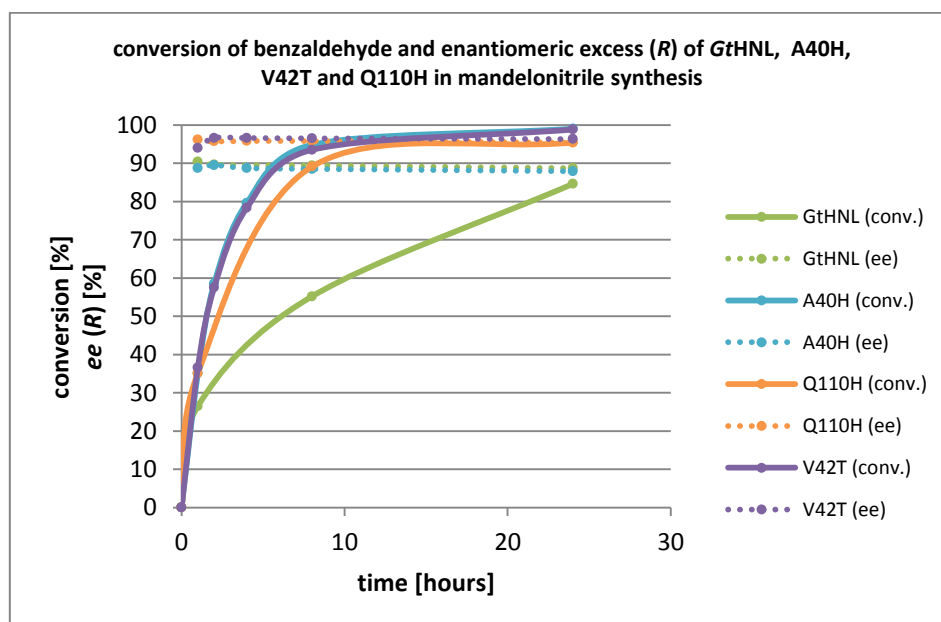


**Figure 35: Conversion [%] of benzaldehyde and enantiomeric excess (*ee*) [%]. A40H (blue), Q110H (orange) and V42T (purple) compared to wildtype *Gt*HNL. *Gt*HNL is shown in green. The dashed lines refer to the *ee* and the solid lines refer to the conversion.**

## 5.7   Combination of beneficial mutations

Mutations, which were beneficial regarding the conversion of benzaldehyde to (*R*)-mandelonitrile and/or lead to improved *ee* -values of *Gt*HNL, were combined. Some random mutations of fragment

1 (Mn_C9, compare Table 29) were combined with mutations in fragment 3 (Mn_A5, Mn_A6, Mn_C4, compare Table 30) and one mutant was generated, which harboured mutations of fragment 1 (Mn_C9), fragment 3 (clone Mn_A6) in addition to A40H and V42T mutations. This means, that this mutant included the mutations E2K, K13E, Q110H, E111G, A40H and V42T (compare Table 29 and Table 30). Plasmids of the combinatorials were sent to sequencing. Combined variants were not tested in cyanogenesis activity using the colony-based filter assay. They were tested directly in the synthesis reaction.

## 5.8 Cultivation and protein expression of combined mutants

Combinatorials were cultivated and expressed in shake flasks and disrupted by sonication. Total protein concentration of the lysates was estimated using the Bradford assay (Table 33). Samples included appr. 8 to 14 mg/mL protein.

Table 33: Protein concentration of lysates after sonication, determined by the Bradford assay.

| Sample | concentration [mg/mL] |
|---|---|
| Mn_C9_Mn_A5 | 8.3 |
| Mn_C9_Mn_A6 | 8.2 |
| Mn_C9_Mn_C4 | 12 |
| V42TQ110H | 10.3 |
| A40R(CGG)Q110H | 8.3 |
| H106NQ110H | 14.4 |
| A40HV42TQ110H | 9.0 |
| A40R(AGG)Q110H | 10.0 |
| A40H_V42T_Mn_C9_Mn_A6 | 8.4 |

The localisation of proteins after sonication was analysed by SDS-PAGE. Lysates as well as pellets of Mn_C9_Mn_A5, Mn_C9_Mn_A6, Mn_C9_Mn_C4, V42T_Q110H, A40R(CGG)_Q110H, H106N_Q110H, A40H_V42T_Q110H, A40R(AGG)_Q110H and A40H_V42T_Mn_C9_Mn_A6 were loaded on NuPage gels (Figure 36 Figure 37). In most cases expression and sonication seemed to have worked out quite well because the bands are thick and most of the protein can be found in the lysates.
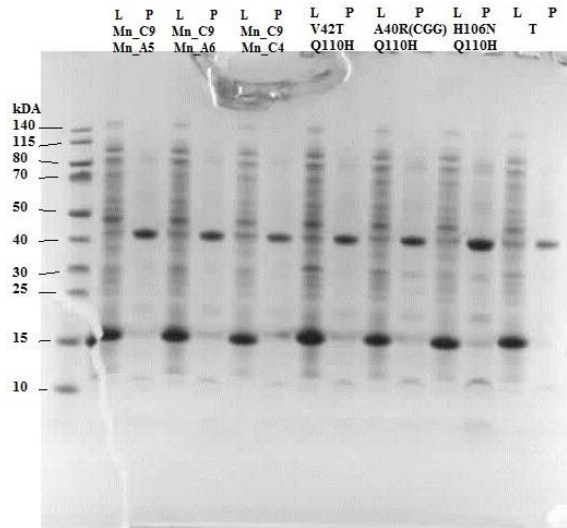
**Figure 36: SDS gel including lysates (L) and pellets (P) of combinatorial mutants Mn_C9_Mn_A5, Mn_C9_Mn_A6, Mn_C9_Mn_C4, V42TQ110H, A40R(CGG)Q110H, H106NQ110H and A40HV42TQ110H (T). Page Ruler Prestained protein ladder (Fermentas) was used. *Gt*HNL monomer has about 15 kDa.**
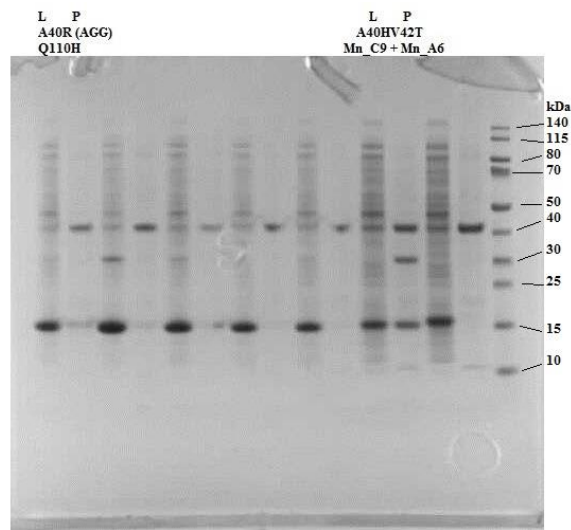


**Figure 37: SDS gel including lysates (L) and pellets (P) of combinatorial mutants A40R(AGG)_Q110H and Mn_C9_Mn_A6_A40HV42T. Page Ruler Prestained protein ladder (Fermentas) was used. *Gt*HNL monomer has about 15 kDa. Unlabelled slots include samples of another experiment.**

## 5.9   Synthesis reaction with combined mutants

Combinatorial mutants were tested again for their activities in the synthesis reaction. Triple mutant A40HV42TQ110H (T) had converted the substrate completely after two hours with an *ee* of 100%. *Gt*HNL showed a conversion of 63% after two hours and an *ee* of about 92%. To estimate the chemical background reaction, the lysate of the empty vector (pET26b(+)) was used as control. The double mutant V42TQ110H had also an *ee* (*R*) of almost 100% but was not as efficient in converting benzaldehyde as the triple mutant. All the other combinatorials didn't show any or just a slight improvement in synthesizing (*R*)-mandelonitrile. The conversions of benzaldehyde as well as the enantiomeric excess (*R*) are summarized in Table 34 and visualised in Figure 38.

**Table 34: Benzaldehyde conversion [% ] and enantiomeric excess (*R*) [%] after 1 hour, 2 hours, 4 hours, 8 hours and 24 hours of reaction.**

| Sample | 1 h | 2 h | 4 h | 8 h | 24 h | |
|---|---|---|---|---|---|---|
| *Gt*HNL | 36.2 | 62.8 | 84.8 | 95.3 | 98.6 | conversion (%) |
| | 92.4 | 92 | 91.7 | 91.5 | 90.7 | *ee* (%) |
| **A40HV42TQ110H** | **89.2** | **98** | **98.4** | **98.5** | **98.6** | **conversion (%)** |
| | **100** | **99.9** | **99.9** | **99.8** | **99.5** | ***ee* (%)** |
| Mn_C9+Mn_C4 | 27.9 | 59.2 | 85.1 | 96.6 | 98.7 | conversion (%) |
| | 95.7 | 96.5 | 96.5 | 96.3 | 95.9 | *ee* (%) |
| Mn_C9+Mn_A5 | 17.7 | 44.6 | 72.3 | 92.4 | 98.7 | conversion (%) |
| | 88.4 | 96.3 | 96.1 | 95.7 | 95.4 | *ee* (%) |
| Mn_C9+Mn_A6 | -1.1 | 13.9 | 21.2 | 27.7 | 39 | conversion (%) |
| | 88 | 83.9 | 78.8 | 68.2 | 49.4 | *ee* (%) |
| A40HV42T+d+10 | 13.7 | 17.1 | 27.1 | 32.5 | 45.7 | conversion (%) |
| | 94 | 90.7 | 86.4 | 80.1 | 68.2 | *ee* (%) |
| A40R_A2Q110H | 4.3 | 27.8 | 58.6 | 85 | 98.2 | conversion (%) |
| | 95 | 95.4 | 95.5 | 95.4 | 95.2 | *ee* (%) |
| A40R_C5Q110H | 12.6 | 36.4 | 60 | 83.9 | 98.2 | conversion (%) |
| | 94.1 | 95 | 95.1 | 94.8 | 94.7 | *ee* (%) |
| H106NQ110H | 0.6 | 14.6 | 27 | 39.2 | 65.9 | conversion (%) |
| | 74.9 | 74.1 | 70.5 | 66.7 | 61.2 | *ee* (%) |
| **V42TQ110H** | **47.4** | **80.6** | **97.1** | **98.5** | **98.7** | **conversion (%)** |
| | **99.1** | **99** | **99.1** | **99** | **98.7** | ***ee* (%)** |
| pET26b(+) | -6.3 | 2.5 | 5.9 | 14.7 | 26 | conversion (%) |
| | -0.2 | -0.8 | -0.2 | 0.1 | 0.1 | *ee* (%) |
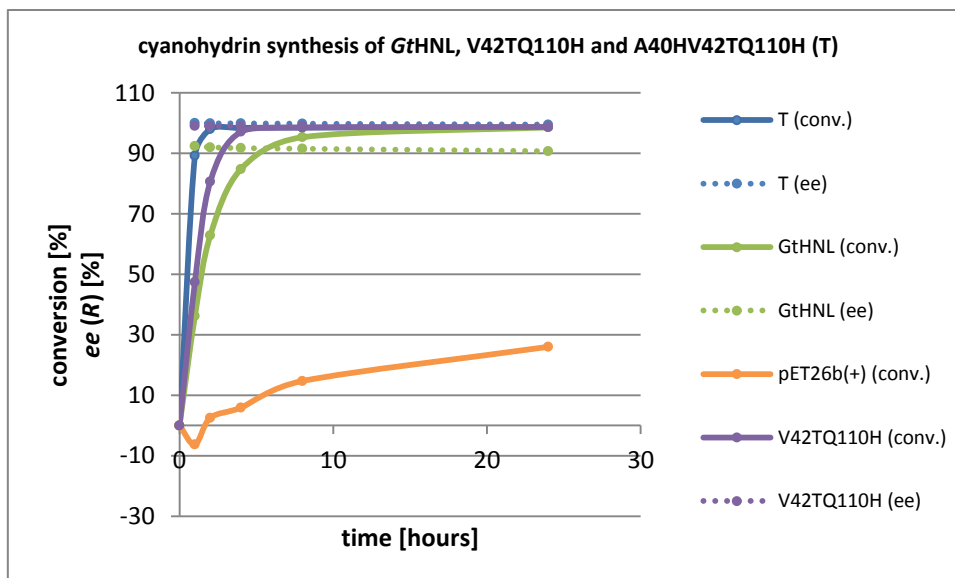
**Figure 38: Conversion [%] of benzaldehyde and enantiomeric excess (*ee*) (*R*) [%] of V42TQ110H (purple) and triple mutant T (A40HV42TQ110H, blue) compared to wildtype *Gt*HNL (green). Chemical background (pET26b(+)) is shown in orange. The dashed lines refer to the *ee* and the solid lines refer to the conversion. The product obtained with the pET26b(+) vector control is racemic.**

## 5.10 Protein purification

For protein purification, mutants Mn_A3 and T were cultivated and expressed in shake flasks and disrupted by sonication. Protein concentration of the lysates was estimated using the Bradford assay (Table 35). Samples included approximately 20 mg/mL protein.

**Table 35: Protein concentration of lysates after sonication, determined using the Bradford assay.**

| Sample | concentration [mg/mL] |
|--------|----------------------|
| T | 22.1 |
| Mn_A3 | 19.1 |

Lysates of triple mutant T including the mutations A40HV42TQ110H and Mn_A3 were purified by anion exchange and size exclusion chromatography. After anion exchange chromatography, fractions were selected and analysed on SDS-gels. T was present in fractions 23 – 66 and Mn_A3 was present in fractions B4 – G3 (compare Figure 39 and Figure 40). The chromatograms are shown in Figure 41 and Figure 42.
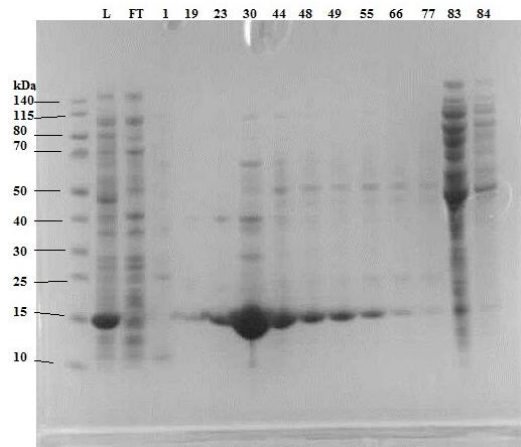
Figure 39: SDS-gel of T after purification with anion exchange chromatography. First slot includes Page Ruler Prestained protein ladder. L = cleared lysate (11 µg), FT = flowthrough. 1 – 84 are selected fractions.
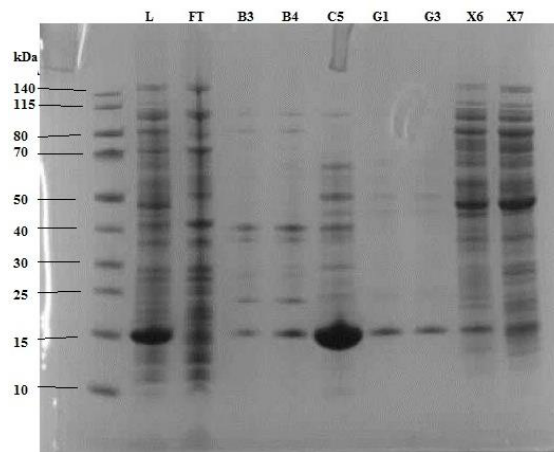


Figure 40: SDS – gel of Mn_A3 after purification with anion exchange chromatography. First slot includes Page Ruler Prestained protein ladder. L = cleared lysate (10 µg), FT = flowthrough. B3, B4, C5, G1, G3, X6 and X7 are selected fractions.
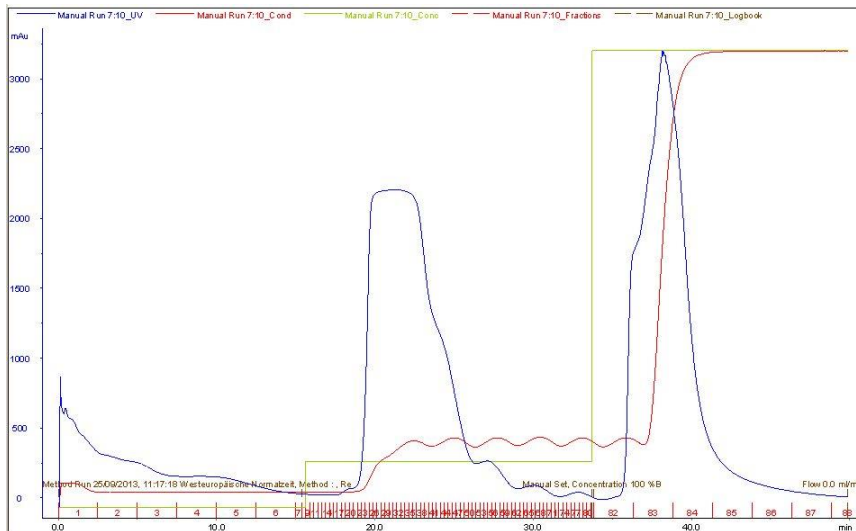
**Figure 41: Chromatogram of anion exchange chromatography of the triplemutant. Blue line shows the absorption (mAU), purple line shows the conductivity and green line shows the gradient (percent buffer B).**
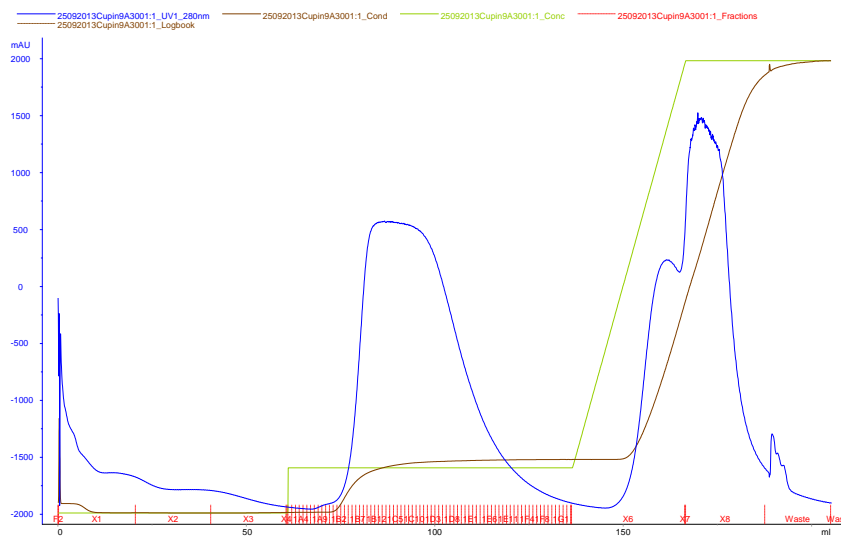


**Figure 42: Chromatogram of anion exchange chromatography of Mn_A3. Blue line shows the absorption (mAU), purple line shows the conductivity and green line shows the gradient (percent buffer B).**

Fractions including the *Gt*HNL variants were pooled and further purified by size exclusion chromatography. The combined fractions (appr. 60 mL) were concentrated with Vivaspin (20 mL, 10,000 Da cut off) and about five mL with about 30 mg/mL protein concentration (estimated by measurement with Nanodrop) were loaded on SEC column. Selected fractions were analysed by SDS PAGE (Figure 43). The chromatograms are shown in Figure 44 and Figure 45 Fractions E4 – F4 of T as well as of Mn_A3 were combined and concentrated (finally approximately 5 mL of 16 mg/mL protein).
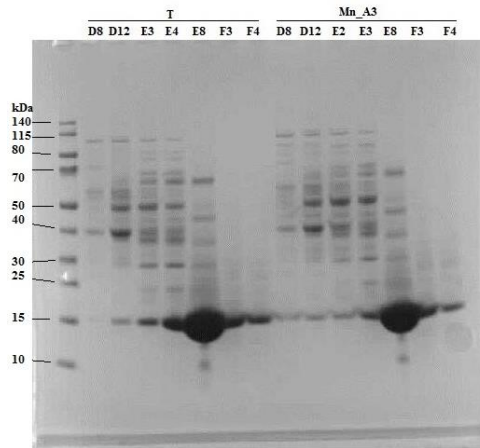
**Figure 43: SDS-gel of different fractions of size exclusion chromatography of the triple mutant (T) and Mn_A3. First slot includes Page Ruler Prestained protein ladder.**
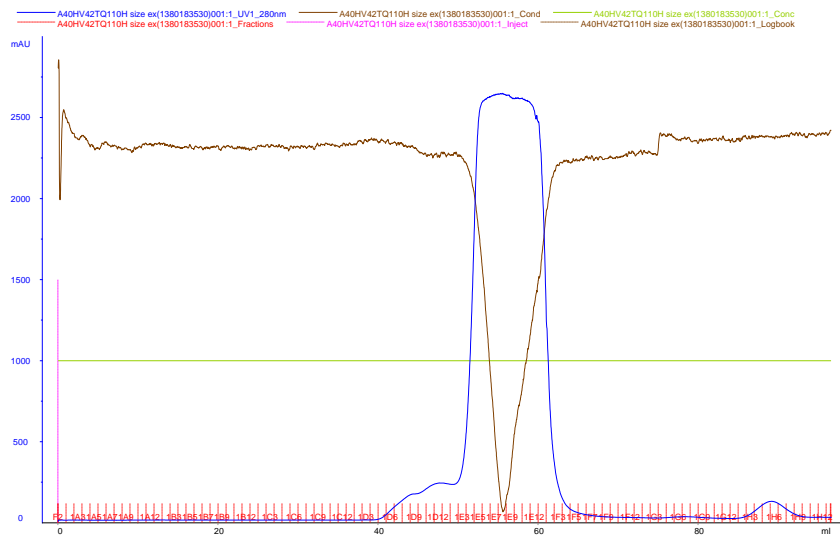


**Figure 44: Chromatogram of the triple mutant after size exclusion chromatography. Blue line shows the absorption (mAU), purple line shows the conductivity and green line shows the gradient of buffer.**
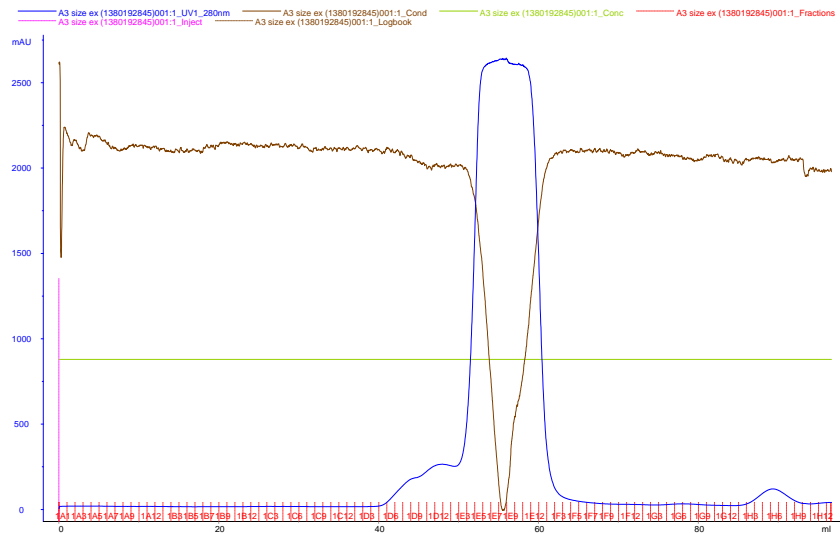
**Figure 45: Chromatogram of Mn_A3 after size exclusion chromatography. Blue line shows the absorption (mAU), purple line shows the conductivity and green line shows the gradient of buffer.**

## 5.11 pH – stability test with purified protein

The pH stability of purified *Gt*HNL wildtype (WT), variant Mn_A3 and the triple mutant (T) was analysed. Protein contents in the supernatants were estimated with SDS-PAGE. SDS gels are shown in Figure 46 and Figure 47. At all pH values investigated, monomers of *Gt*HNL wildtype and mutants are present in equal amounts as the bands look quite similar but the bands of the dimers are visible only in the Mn_A3 and T samples.
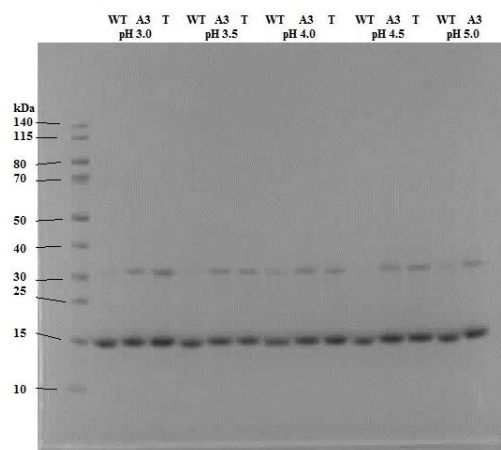


**Figure 46: Stability test with purified proteins of *Gt*HNL (WT), variant Mn_A3 (A3) and triple mutant (T) in 0.1 M citrate phosphate buffer, pH 3.0, pH 3.5, 4.0, 4.5 and 5.0.**
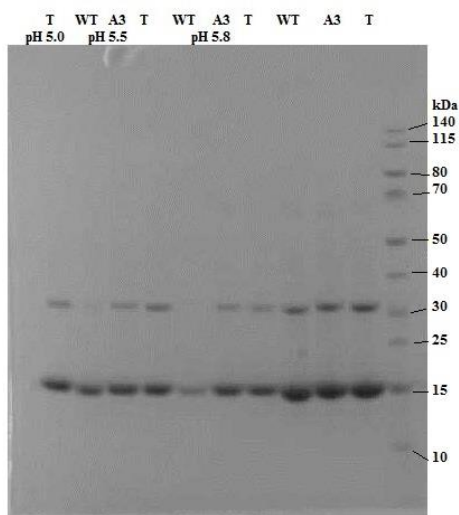
**Figure 47: Stability test with purified proteins of *Gt*HNL (WT), variant Mn_A3 (A3) and triple mutant (T) in 0.1 M citrate phosphate buffer, pH 5.0, pH 5.5 and 0.1 M MES oxalate buffer, pH 5.8. Slots 8 -10 contain proteins that were not incubated in buffers.**

## 5.12 HNL-activity assay in microtiter plates with purified proteins

The cyanogenesis activity of the purified triple mutant and clone Mn_A3 was tested in microtiter plates using 20 mM (*R*)-mandelonitrile and different reaction buffers (citrate phosphate buffer, pH 3.5 and pH 5.5 and MES oxalate buffer, pH 5.6). Activities of both mutants were quite similar, except in citrate phosphate buffer, pH 3.5, the triple mutant T seemed to be more active than variant Mn_A3. The screening filter of the assay is shown in Figure 48.
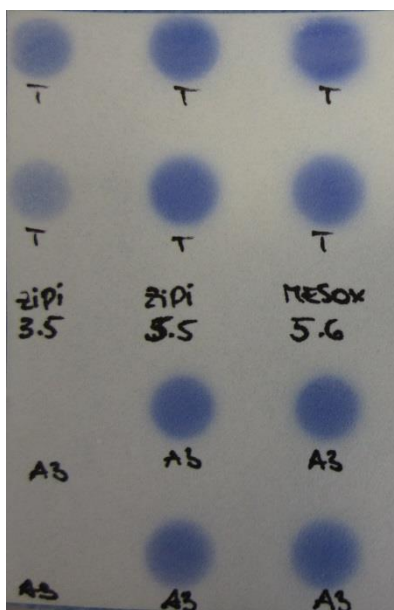
**Figure 48: Filter of HNL-activity assay in microtiter plates of the purified triple mutant T and Mn_A3 in citrate phosphate buffer (ZiPi), pH 3.5, citrate phosphate buffer (ZiPi), pH 5.5 and MES oxalate buffer (MESOx), pH 5.6. The reaction was stopped after five minutes.**

## 5.13 Cyanogenesis activity assay in quartz cuvettes with purified proteins

The cyanogenesis activity of purified proteins T and Mn_A3 was tested in quartz cuvettes following the formation of benzaldehyde from 2.5, 5, 10 or 18 mM (*R*)-mandelonitrile at 280 nm over ten minutes. The chemical background reaction was considered in calculating enzyme activities and was subtracted.

The release of benzaldehyde from 18 mM (*R*)-mandelonitrile in using 50 µg of Mn_A3 and 0.1 M MES oxalate buffer is shown in Figure 49. The chemical background reaction (shown in blue) was quite high. A specific activity of 2.1 U/mg was calculated.
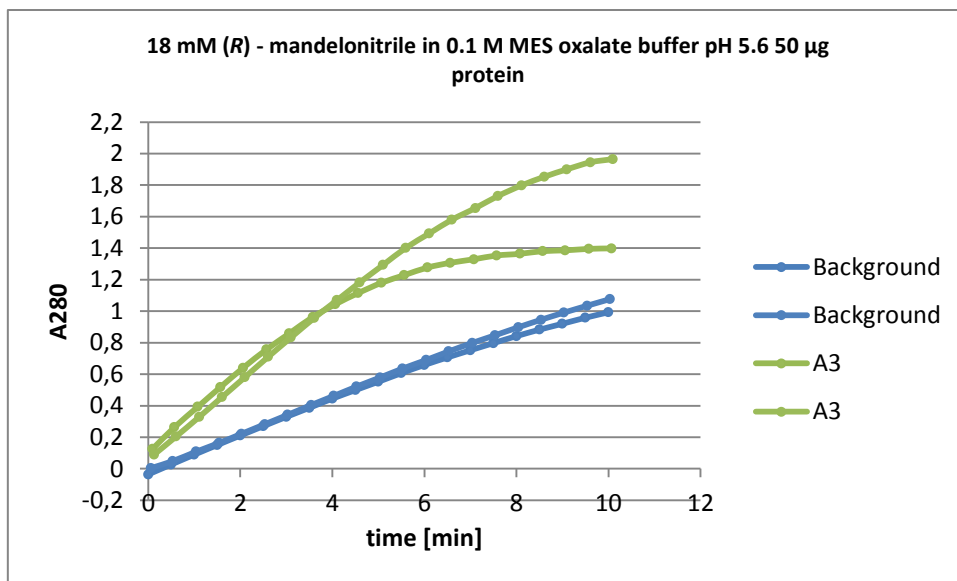
**Figure 49: Release of benzaldehyde in 0.1 M MES oxalate buffer, pH 5.6, using 18 mM (*R*)-mandelonitrile and 50 µg of Mn_A3 (green) in comparison to the chemical background reaction (blue). The overall activity was 32.9 U/mL, specific activity was 2.1 U/mg.**

Figure 50 shows that Mn_A3 was more active in 0.1 M MES oxalate buffer, pH 5.6 than in citrate phosphate buffer, pH 5.5 as a specific activity of 1.2 U/mg could be calculated. The chemical background reaction seemed to be lower than in MES oxalate buffer.
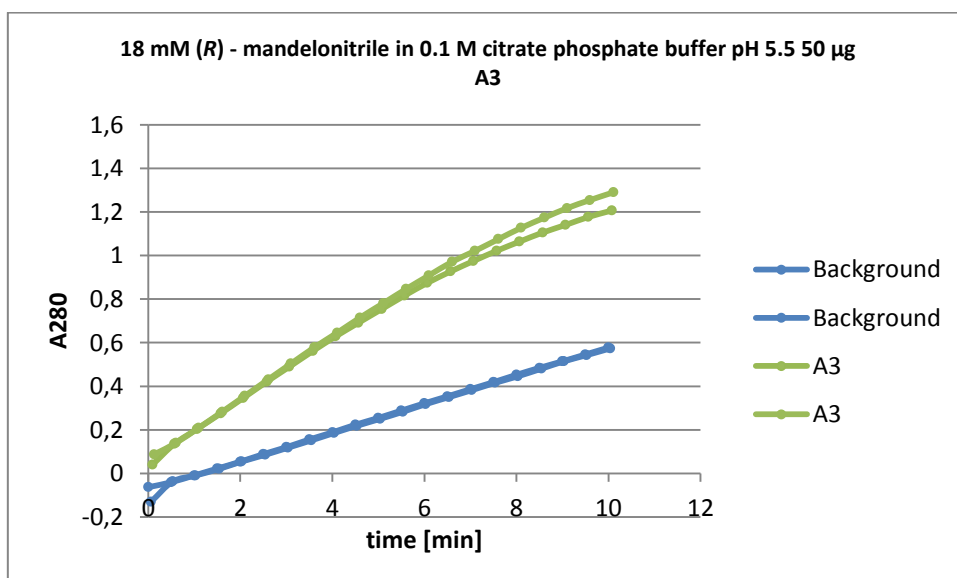


**Figure 50: Release of benzaldehyde in 0.1 M citrate phosphate buffer, pH 5.5 using 18 mM (*R*)-mandelonitrile and 50 µg of Mn_A3 (green) in comparison to the chemical background reaction (blue). Overall activity: 19.8 U/mL, specific activity: 1.2 U/mg.**

The release of benzaldehyde from 18 mM (*R*)-mandelonitrile using 6.4 µg of triple mutant and 0.1 M MES oxalate buffer, pH 5.6 is visualised in Figure 51. The chemical background reaction was quite high. A specific activity of 20.6 U/mg was estimated.
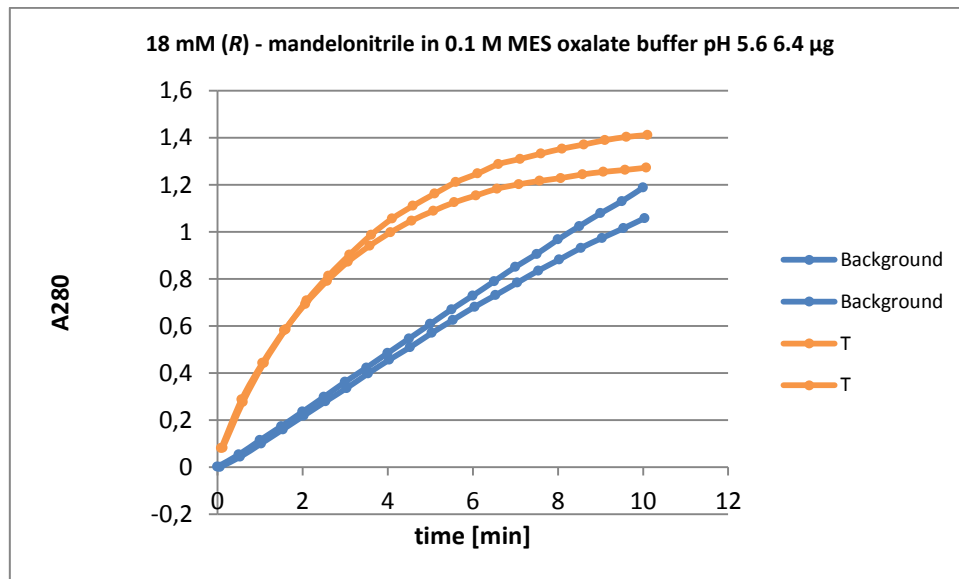


**Figure 51: Release of benzaldehyde in 0.1 M MES oxalate buffer, pH 5.6 using 18 mM (*R*)-mandelonitrile and 6.4 µg of triple mutant (T) (orange) in comparison to the chemical background reaction (blue). Overal activity: 330 U/mL, specific activity: 20.6 U/mg.**

A specific activity of 112 U/mg was determined using 3.2 µg of the triple mutant protein in 0.1 M MES oxalate buffer, pH 5.6. This is shown in Figure 52.
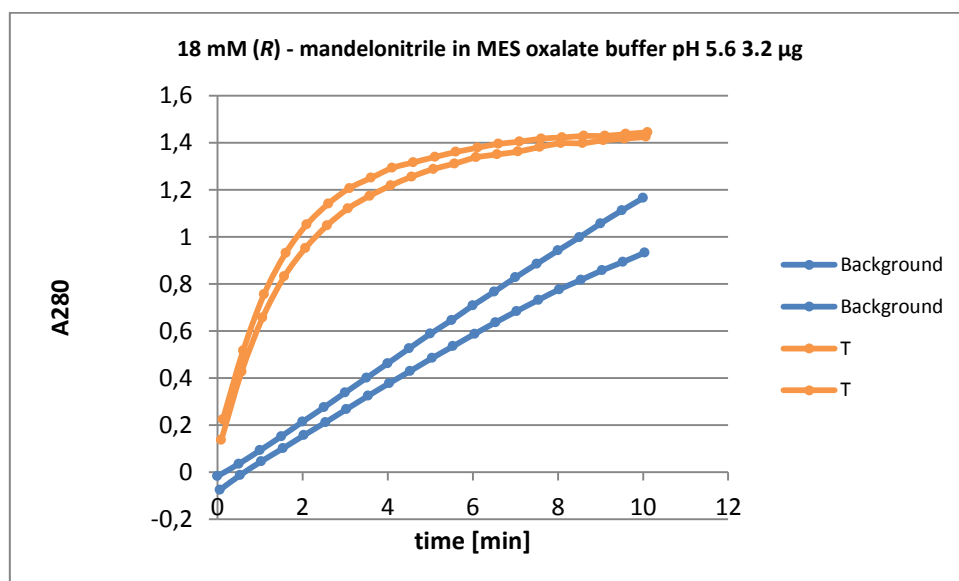


**Figure 52: Release of benzaldehyde in 0.1 M MES oxalate buffer, pH 5.6 using 18 mM (*R*)-mandelonitrile and 3.2 µg of triple mutant (T) (orange) in comparison to the chemical background reaction (blue). Overall activity: 1789 U/mL, specific activity: 112 U/mg.**

Figure 53 shows the release of benzaldehyde using 1.6 µg of the triple mutant in the reaction mixture. A specific activity of 65 U/mg was determined.
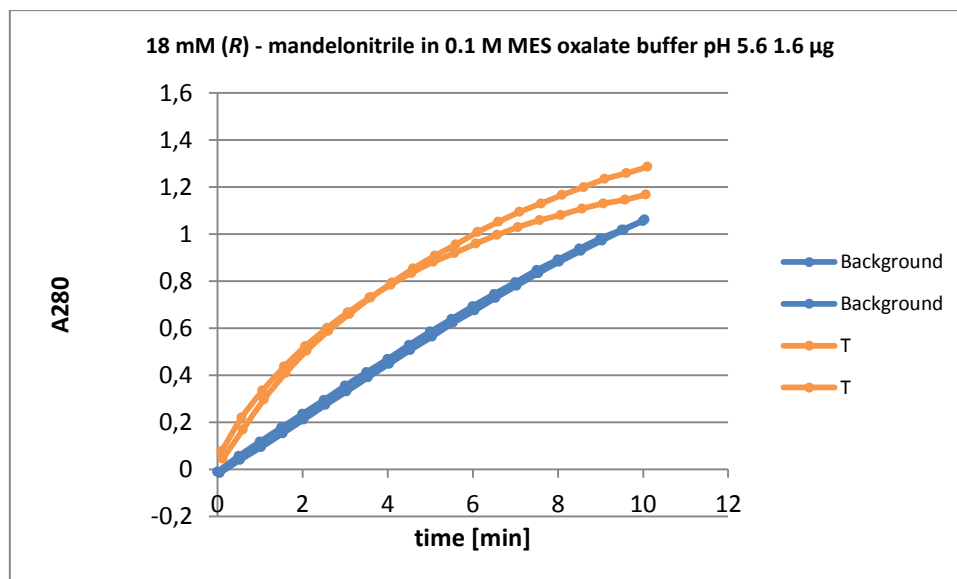


**Figure 53: Release of benzaldehyde in 0.1 M MES oxalate buffer, pH 5.6 using 18 mM (*R*)-mandelonitrile and 1.6 µg of the triple mutant (T) (orange) in comparison to the chemical background reaction (blue). Overall activity: 1036 U/mL, specific activity: 65 U/mg.**

A specific activity of 263 U/mg was determined using 3.2 µg protein of the triple mutant and 0.1 M citrate phosphate buffer, pH 5.5 in the reaction mixture. The chemical background reaction is much lower than with 0.1 M MES oxalate buffer, pH 5.6. This is visualised in Figure 54.
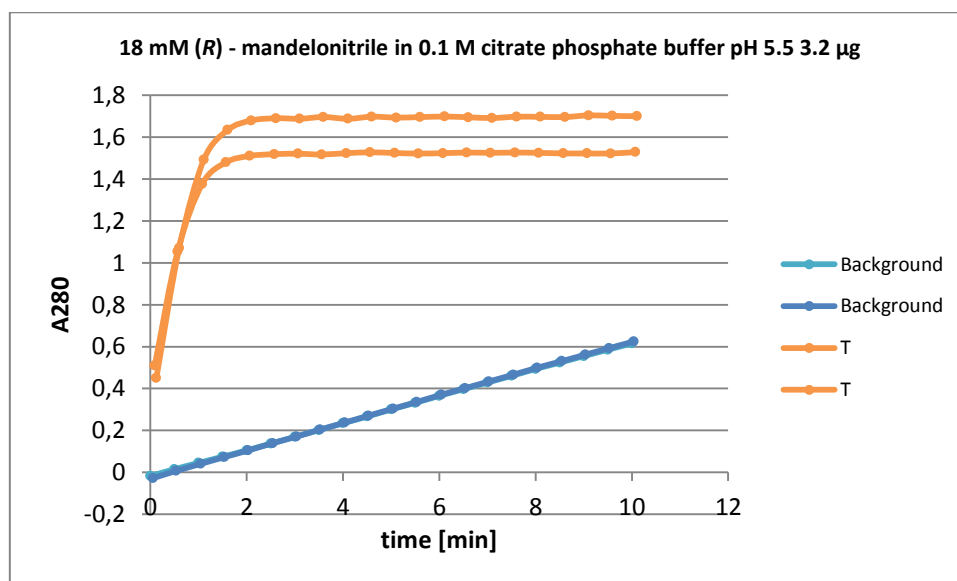


**Figure 54: Release of benzaldehyde in 0.1 M citrate phosphate buffer, pH 5.5 using 18 mM (*R*)-mandelonitrile and 3.2 µg of the triple mutant (T) (orange) in comparison to the chemical background reaction (blue). Overall activity: 4208 U/mL, specific activity. 263 U/mg.**

Release of benzaldehyde from 18 mM (R)-mandelonitrile catalysed by 1.6 µg of triple mutant *Gt*HNL is shown in Figure 55. A specific activity of 281 U/mg was estimated.
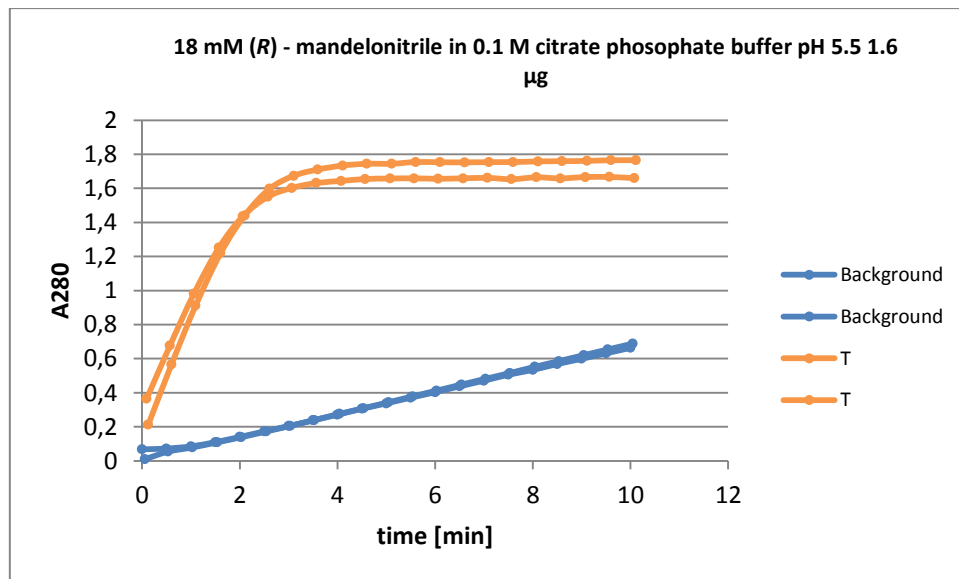


**Figure 55: Release of benzaldehyde in 0.1 M citrate phosphate buffer, pH 5.5 using 18 mM (*R*)-mandelonitrile and 1.6 µg of the triple mutant (T) (orange) in comparison to the chemical background reaction (blue). Overall activity: 4502 U/mL, specific activity: 281 U/mg.**

Using 0.4 µg of protein in 0.1 M citrate phosphate buffer revealed a specifc activity of 287 U/mg. The release of benzaldehyde under these conditions is shown in Figure 56.
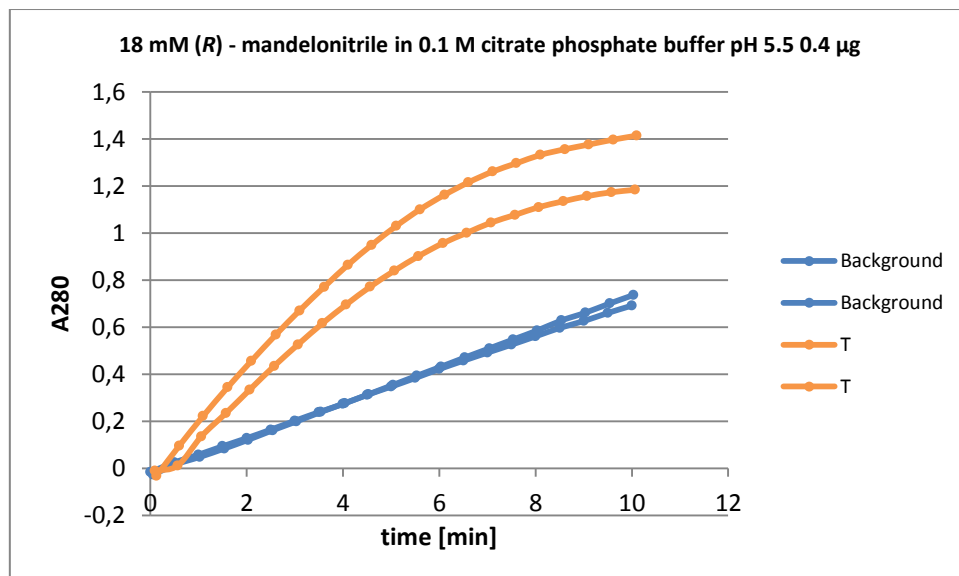


**Figure 56: Release of benzaldehyde in 0.1 M citrate phosphate buffer, pH 5.5 using 18 mM (*R*)-mandelonitrile and 0.4 µg of the triple mutant (T) (orange) in comparison to the chemical background reaction (blue). Overall activity: 4589 U/mL, specific activity: 287 U/mg.**

Overall and specific activities of Mn_A3 and T under different substrate conditions (2.5 mM, 5 mM, 10 mM, 18 mM) using either 0.1 M citrate phosphate buffer, pH 5.5 and pH 4.5 or 0.1 M MES oxalate buffer, pH 5.6 are summarized in Table 36, Table 37 and Table 38. Highest specific activity that could be calculated was in 0.1 M citrate phosphate buffer, pH 5.5. using 0.4 µg of T (287 U/mg). Mn_A3 was not active at pH 4.5, whereas T still showed a specific activity of 1.75 U/mg.

**Table 36: Activities and specific activities of Mn_A3 and T in citrate phosphate buffer, pH 5.5, using different substrate concentrations.**

| Sample | substrate conc. [mM]] | amount of protein[µg] | activity [U/mL] | specific activity [U/mg] |
|--------|------|------|------|------|
| Mn_A3 | 18 | 50 | 19.8 | 1.24 |
| Mn_A3 | 18 | 16 | - | - |
| Mn_A3 | 2.5 | 320 | 2.9 | 0.18 |
| Mn_A3 | 2.5 | 160 | 3.5 | 0.2 |
| | | | | |
| T | 18 | 3.2 | 4208 | 263 |
| T | 18 | 1.6 | 4502 | 281 |
| T | 18 | 0.8 | 4419 | 276 |
| T | 18 | 0.4 | 4589 | 287 |
| T | 2.5 | 8 | 713 | 44,6 |
| T | 2.5 | 4 | 837 | 52 |
| T | 2.5 | 2 | 795 | 48 |

**Table 37: Activities and specific activities of Mn_A3 and T in citrate phosphate buffer, pH 4.5, using different substrate concentrations.**

| Sample | substrate conc. [mM] | amount [µg] | activity [U/mL] | specific activity [U/mg] |
|--------|------|------|------|------|
| Mn_A3 | 18 | 50 | 1.39 | 0.09 |
| Mn_A3 | 5 | 160 | - | - |
| Mn_A3 | 2.5 | 800 | - | - |
| Mn_A3 | 2.5 | 32 | - | - |
| | | | | |
| T | 2.5 | 16 | 23.6 | 1.5 |
| T | 2.5 | 32 | 28 | 1.75 |
| T | 2.5 | 160 | 25 | 1.6 |

**Table 38: Activities and specific activities of Mn_A3 and T in MES oxalate buffer, pH 5.6 using different substrate conditions. Using 0.6 µg of protein in the reaction seemed to be the optimum as a specific activity of about 130 U/mg could be calculated.**

| Sample | substrate conc. [mM] | amount [µg] | activity [U/mL] | specific activity [U/mg] |
|--------|------|------|------|------|
| Mn_A3 | 18 | 50 | 32.9 | 2.1 |
| Mn_A3 | 10 | 160 | 32 | 2 |

| | | | | |
|---|---|---|---|---|
| Mn_A3 | 5 | 160 | 21 | 1.3 |
| Mn_A3 | 5 | 80 | 26 | 1.6 |
| | | | | |
| T | 18 | 6.4 | 330 | 20.6 |
| T | 18 | 3.2 | 1789 | 112 |
| T | 18 | 1.6 | 1036 | 65 |
| T | 18 | 0.6 | 2057 | 129 |

# 6   Discussion

## 6.1   Mutagenesis

Site-directed mutagenesis of V42, T50, L61, H96, H106 and Q110 worked out quite well as the sequencing results of randomly picked clones showed a great variety of different mutations at putative active site positions. Four out of five clones originating from the A40 library were identified as wildtype and all clones from the F44 library that were sent to sequencing still carried the wildtype *Gt*HNL sequence. In consequence, it had to be assumed that mutagenesis rates within these two libraries seemed to be very low. Nevertheless, they were investigated further and promising hits were found within the A40 library, actually.

The MnCl$_2$ library of fragment 1 showed an average mutation rate of 2.4%, while the mutation rate of the fragment 2 library was 2.9%. The highest mutation rates were gained in the MnCl$_2$ library of fragment 3 (3.2%). The mutation rates within the Mutazyme library were much lower (0.8%), although only clones from the fragment 1 library were sent to sequencing. It was assumed that mutation rates within the fragment 2 and 3 libraries were comparable. Although the mutation rates were much higher in the MnCl$_2$ libraries, the Mutazyme libraries showed similar numbers of clones that had lost its cyanogenesis activity. It is a crucial step to generate libraries with proper mutation rates. Too many mutations result in a high number of inactive variants whereas low mutation rates lead to a high background of wildtype enzyme within the library. Ideally, mutational diversity should be achieved, that has no negative effects on enzyme activity but might reveal mutants with improved properties.

## 6.2   Colony-based filter assay

Hits could be isolated from A40, V42, H106 and Q110 libraries although the number of inactive clones in the Q110 and H106 libraries was quite high. That gives a hint that these two putative active site positions might play an important role in the cyanogenesis of *Gt*HNL. Within the A40 and V42 libraries most of the clones were still active and some hits that showed improved cyanogenesis activity were isolated. The exchange of alanine at position 40 and the exchange of valine at position 42 don't seem to have negative effects concerning enzyme activity in the cleavage reaction of mandelonitrile. No hits were found in the F44 library, although most of the clones within this library showed still activity that was similar to that of the wildtype. It could be that phenylalanine doesn't

play an essential role in the activity of HNL. According to Hajnal et al. mutation F44A didn't show any effect on cyanogenesis in the colony based filter assay. Another reason could be that mutagenesis didn't work out well and that most of the clones harbour still the wildtype *Gt*HNL. This theory is affirmed by the fact that all randomly picked clones from the F44 library that were sent for sequencing, included still the wildtype *Gt*HNL sequence.

Histidines are known to play an important role in the catalytic mechanism of HNLS from *Hevea brasiliensis* and *Prunus amygdalus* (57) (58) (20). The site-directed mutagenesis of H96 in *Gt*HNL led to a library with 46% inactive clones.

## 6.3 pH stability

Random mutagenesis was applied to generate variants that show higher pH stability as it is of great advantage to perform the synthesis reaction at low pH in order to keep the base catalysed chemical background reaction at a minimum. One mutant originating from a random library, which was further investigated, was Mn_A3. After incubation in buffers of different pH, the solubility of the protein was analysed by SDS − PAGE. The gel showed that the monomers were present in the supernatants in quite similar amounts to the wildtype while the dimer could only be detected in the Mn_A3 samples. Improved pH stability might be the reason. However it is not clear why the dimer is neither present in higher pH, although it could be detected in the untreated lysate. Actually, the triple mutant was meant to be an improved variant in enzyme activity but it showed the same characteristics in the pH stability test as mutant Mn_A3 and might also exhibit improved properties at low pH.

Crude lysate of V42T was analysed towards its stability at low pH as it still showed cyanogenesis activity at pH 3.5 in the HNL − activity assay in microtiter plates. Compared to the wildtype, V42T doesn't seem to be more stable as less protein could be detected in the supernatant on the SDS gel but it would be interesting to test the purified mutant V42T in the quartz cuvettes assay using buffers of different pH.

## 6.4 (*R*) – mandelonitrile synthesis

In the first synthesis reaction wildtype *Gt*HNL showed a conversion of benzaldehyde of about 85% with an *ee* (*R*) of 89% after 24 hours. Most of the variants that were generated using site - directed

and random mutagenesis showed either an improvement in converting benzaldehyde or higher enantioselectivity. The most promising mutants were A40H (conv. 99%), A40R(AGG) (conv. 98%, *ee* 95%), Q110H (conv. 95%, *ee* 95%), V42T (conv.99%) and Mn_A3 (conv. 92%, *ee* 94%). Two different codons in exchanging alanine to arginine at position 40 were tested. Mutant A40R harbouring AGG showed improved conversion (98%) and *ee* (95%) while A40R using codon CGG showed improved *ee* (94%) but only a slightly improved conversion (87%). This is interesting because codon AGG is usually rarely used by *E. coli* and it is known to cause problems in expression and to have negative effects on the quantity or quality on the protein that is synthesized (59). Additionally, expression of CGG and AGG arginine variants seemed to have worked out similarly, as the bands on the SDS gels look the same and are in the soluble fraction.

It has to be mentioned that the exchange of histidine in the active site doesn't seem to be advantageous as conversion (38%) and *ee* (74%) of H106N changed for the worse and H106Y had lost its enantioselectively completely. The clone originating from the mutazyme library MZ_C5 didn't show any improvements. Histidine residues seem to play an important role in the active site as the insertion of histidine lead to improved activities and enantioselectivity as well. Any exchange to another amino acid lead to incomplete conversion or racemic products. Histidine is assumed to play also an essential role in the HNL of *Hevea brasiliensis* and *Prunus amygdalus* where the histidine might act as a base and attracts the proton from the hydroxyl group of mandelonitrile. In *Hevea brasiliensis* histidine belongs to the catalytic triad formed by Asp, His and Ser which deprotonates the cyanohydrin (58) (57). The exchange from nonpolar to (basic) polar amino acids (e.g. valin to threonine, alanine to histidine, alanine to arginine) was beneficial. It seems that *Gt*HNL prefers amino acids in the active site that are (basic) polar and positively charged in synthesizing (*R*) – mandelonitrile. It would be interesting to exchange amino acids in the active site to lysine, which is also a basic polar, positively charged amino acid. Hajnal et al. exchanged histidine at position 106 to lysine and reported that that the variant was inactive in cleaving mandelonitrile but it was not tested in synthesis reaction. H106A and H106D were not very efficient in synthesizing mandelonitrile (5-26% conversion, ee 54%; WT: 64% conversion, ee 86% after six hours) (20).

In the second synthesis, A40H V42T and Q110H mutations were combined which led to a variant that showed an *ee* of 100% and was very efficient in converting benzaldehyde as 98% were already consumed after two hours. At the same time, wildtype *Gt*HNL had only converted 63% of the substrate with an *ee* of 92%. This is another fact that would suggest that *Gt*HNL prefers (basic) polar and neutral or positively charged amino acids in the active site. None of the other combinatorials showed a better performance than the triple mutant, although the double mutant V42TQ110H showed also a good *ee* of almost 100% and had consumed all of the substrate after eight hours. Most

of the other variants showed similar conversions or *ee* to the wildtype or were actually worse in synthesizing (*R*) – mandelonitrile.

## 6.5   Cyanogenesis in quartz cuvettes

The purified triple mutant and mutant Mn_A3 were tested in cleaving (*R*) – mandelonitrile in quartz cuvettes. Highest specific activity of Mn_A3 could be detected using MES oxalate buffer, pH 5.6 (2.1 U/mg). Compared to the wildtype with a specific activity of 1.74 U/mg (measured by Hajnal et al) that is an improvement of 1.2. It has to be mentioned that specific activity of wildtype *Gt*HNL was determined in sodium oxalate buffer, pH 5.5. Despite of this fact, the results obtained in this thesis are compared to this value. The triple mutant showed the highest activity in citrate phosphate buffer, pH 5.5 (287 U/mg). This means that this variant seems to be 137 fold more efficient in cleaving (*R*) – mandelonitrile than the wildtype. The enzymes were also tested in citrate phosphate buffer, pH 4.5 but the enzyme activities were comparable low in this buffer. Mn_A3 was not active at all whereas the triple mutant showed a specific activity of 1.75 U/mg. Although the activity of the triple mutant decreased drastically in pH 4.5, it showed still comparable activity to the wildtype *Gt*HNL at pH 5.5. As the crude lysate of V42T showed still cyanogenesis activity in the HNL – assay in microtiter plates and because of the fact that this mutation is also present in the triple mutant, this mutation resulted in improved pH stability.

Generally, the assay worked out better using citrate phosphate buffer, pH 5.5, as the chemical background reaction was much lower than using MES oxalate buffer, pH 5.6. Using 2.5 mM substrate concentration leads to even lower chemical background reaction but the results show that the substrate is completed too fast. For determining enzyme activities it is essential that the substrate concentration is not limiting, thus a concentration of 18 mM (*R*)-mandelonitrile was used for activity determination.

## 6.6   Conclusion

A variant of *Gt*HNL was generated that exhibits improved properties in synthesising (*R*) – mandelonitrile and additionally is more efficient in cleaving (*R*) – mandelonitrile. This mutant includes three mutations in the active site (A40H V42T and Q110H). Furthermore, the triple mutant was still active at pH 4.5 in the cleavage assay and the dimeric form of the mutant could be detected in the soluble fractions after incubation in buffers of different pH, which might indicate improved pH stability.

Variant Mn_A3, originating from a random library showed slightly improved enzyme activity in cleavage and synthesis reaction. This mutant might exhibit slightly improved pH stability, too, because it showed similar amounts of the dimeric form of the protein in the soluble fractions after incubation in buffers of different pH as the triple mutant.

# 7 Literature

1. **Nahrstedt, A.** Cyanogenesis and the role of cyanogenic compounds in insects. *Plant Systematic and Evolution.* 1985, 150, S. 35-47.

2. **Yemm, R und Poulton, J.** Isolation and Characterization of Multiple Forms of Mandelonitrile Lyase from Mature Black Cherry (*Prunus serotina*) Seeds. *Archives of Biochemistry and Biophysics.* 1986, 247, S. 440-445.

3. **Gruber-Khadjawi, M, Fecher, MH und Griengl, H.** Cleavage and formation of cyanohydrins. *Enzyme Catalysis in Organic Synthesis (Drauz K., Gröger H, May O).* 2012, S. 947-990.

4. **Fechter, MH und Griengl, H.** Hydroxynitrile Lyases: Biological Sources and Application as Biocatalysts. *Food Technol. Biotechnol.* 2004, 42, S. 287-294.

5. **LP, Solomonson.** Cyanide as a metabolic inhibitor. [editor] B Vennesland, EE Conn und CJ Knowls. *Cyanide in biology.* s.l. : Academic Press, 1981, S. 11-28.

6. **Blumer, C und Haas, D.** Mechanism, regulation, and ecological role of bacterial cyanide biosynthesis. *Arch. Microbiol.* 2000, 173, S. 170-177.

7. **Vetter, J.** Plant cyanogenic glycosides. *Toxicon.* 2000, 38, S. 11-36.

8. **Zagrobelny, M, Bak, S und Rasmussen, AV.** Cyanogenic glucosides and plant-insect interactions. *Phytochemistry.* 2004, 65, S. 293-306.

9. **Griengl, H, et al., et al.** Enzymatic cleavage and formation of cyanohydrins: a reaction of biologocal and synthetic relevance. *ChemComm.* 1997, S. 1933-1940.

10. **Goldfarb, W und Margraf, H.** Cyanide Production by *Pseudomonas Aeruginosa*. *Ann Surg.* 1967, 165, S. 104-110.

11. **Sanderson, K, et al., et al.** Bacterial cyanogenesis in the cystic fibrosis lung. *Eur Respir J.* 2008, 32, S. 329-333.

12. **Clawson, BJ und Young, CC.** Preliminary Report on the Production of Hydrocyanic Acid By Bacteria. *Journal of Biological Chemistry.* 1913, 15, S. 419-422.

13. **Antoun, H, et al., et al.** Potential of *Rhizobium* and *Bradyrhizobium* species as plant growth promoting rhizobacteria on non-legumes: Effect on radishes (*Raphanus sativus L.*). *Plant and Soil.* 1998, 204, S. 57-67.

14. **Knowles, CJ.** Cyanide utilization and degradation by microorganisms. [editor] J Wiley. *Cyanide Compounds in Biology.* 1988, S. 3-15.

15. **Knowles, CJ und Bunch, AW.** Microbial Cyanide Metabolism. [editor] Academic Press London. *Advances in Microbial Physiology.* 1986, Bd. 27, S. 73-86.

16. **Castric, PA.** Glycine metabolism by *Pseudomonas aeruginosa*: hydrogen cyanide biosynthesis. *Journal of Bacteriology.* 1977, 130, S. 826-831.

17. **Holt, J und Hanefeld, U.** Enantioselective enzyme-catalysed synthesis of cyanohydrins. *Curr. Org. Synth.* 2010, 6, S. 15-37.

18. **Sulzbacher Caruso, C.** alpha-Hydroxynitrile lyase protein from *Xylella fastidiosa*: cloning, expression, and characterization. *Microb. Pathog.* 2009, 47, S. 118-127.

19. **Hussain, Zahid, et al., et al.** Characterization of Two Bacterial Hydroxynitrile Lyases with High Similarity to Cupin Superfamily Proteins. *AEM.* 2012, S. 2053-2055.

20. **Hajnal, Ivan, et al., et al.** Biochemical and structural characterisation of a novel bacterial manganese-dependent hydroxynitrile lyase. *The FEBS Journal.* 2013.

21. **Bornscheuer, UT, et al., et al.** Engineering the third wace of biocatalysis. *Nature.* 2012, 485, S. 185-194.

22. **Purkarthofer, T, et al., et al.** Potential and capabilities of hydroxynitrile lyases as biocatalysts in the chemical industry. *Appl Microbiol Biotechnol.* 2007, 76, S. 309-320.

23. **Rosenthaler, L.** Durch Enzyme bewirkte assymmetrische Synthesen. *Biochem Z.* 14, 1908, S. 238-253.

24. **Kragl, U, et al., et al.** Engineering Aspects of Enzyme Engineering. *Ann. N.Y. Acad. Sci.* 1990, 613, S. 167-175.

25. **Costes, D, Wehtje, E und Adlercreutz, P.** Hydroxynitrile lyase-catalyzed synthesis of cyanohydrins in organic solvents. Parameters influencing activity and enantiospecificity. *Enzyme and Microbial Technology.* 1999, 25, S. 384-391.

26. **Effenberger, F.** Hydroxynitrile Lyases, Interesting Biocatalysts in Stereoselective Organic Syntheses. 1999.

27. **Sukumaran, J und Hanefeld, U.** Enantioselective C-C bond synthesis catalysed by enzymes. *Chem. Soc. Rev.* 200, 34, S. 530-542.

28. **Sharma, M, Sharma, NN und Bhalla, TC.** Hydroxynitrile lyases: At the interface of biology and chemistry. *Enzyme and Microbial Technology.* 2005, 37, S. 279-294.

29. **Yamamoto, K, et al., et al.** Production of (*R*)-mandelic acid from mandelonitrile by *Alcaligenes faecalis* ATCC 8750. *Appl. Environ. Microbiol.* 1991, 57, S. 3028-3032.

30. **Dadashipour, Mohammad und Asano, Yasuhisa.** Hydroxynitrile Lyases: Insights into Biochemistry, Discovery and Engineering. *ACS Catalysis.* 2011, 1, S. 1121-1149.

31. **Trummler, K und Wajant, H.** *J. Biol. Chem.* 1997, 272, S. 4770-4774.

32. **Andexer, JN, et al., et al.** Hydroxynitrile Lyases with alpha/beta-hydrolase fold: Two Enzymes with Almost Identical 3D Structures but Opposite Enantioselectivities and Different Reaction Mechanisms. *ChemBioChem.* 2012, 13, S. 1932-1939.

33. **Khuri, S, Bakker, FT und Dunwell, JM.** Phylogeny, Function, and Evolution of the Cupins, a Strucuturally Conserved, Functionally Diverse Superfamily of Proteins. *Mol. Biol. Evol. .* 2001, 18, S. 593-605.

34. **Agarwal, G, et al., et al.** Structure-Based Phylogeny as a Diagnostic for Functional Characterization of Proteins with a Cupin Fold. *PLoS ONE.* 2009, 4.

35. **Dunwell, JM, et al., et al.** Evolution of functional diversity in the cupin superfamily. *Trends in Biochemical Sciences.* 2001, 26, S. 740-746.

36. **Dunwell, JM, Purvis, Alan und Khuri, Sawsan.** Cupins: The most functionally diverse protein superfamily? *Phytochemistry.* 2004, 65, S. 7-17.

37. **Arnold, FH, et al., et al.** How enzymes adapt: lessons from directed evolution. *TRENDS in Biochemical Sciences.* 2001, 26, S. 100-106.

38. **Powell, KA, et al., et al.** Directed Evolution and Biocatalysis. *Angewandte Chemie.* 2001, 40, S. 3948-3959.

39. **Reetz, MT, et al., et al.** Expanding the Range of Substrate Acceptance of Enzymes: Combinatorial Acite-Site Saturation Test. *Angewandte Chemie.* 2005, 44, S. 4192-4196.

40. **Bornscheuer, UT und Pohl, M.** Improved biocatalysts by directed evolution and rational protein design. *Current Opinion in Chemical Biology.* 5, 2001, S. 137-143.

41. **Kuchner, O und Arnold, FH.** Directed evolution of enzyme catalysts. *TIBTECH.* 1997, 15, S. 523-530.

42. **Steiner, K und Schwab, H.** Recent advances in rational approaches for enzyme engineering. *Computational and Structural Biotechnology Journal.* 2012, 2.

43. **Shivange, AV, et al.** Advances in generating functional diversity for directed protein evolution. *Current Opinion in Chemical Biology.* 2009, 13, S. 19-25.

44. **Eggert, T, Reetz, MT und Jaeger, KE.** [editor] A Svendsen. *Enzyme Functionality - Designe, Engineering and Screening.* 2004, S. 375-390.

45. **Seng Wong, T, et al., et al.** Sequence saturation mutagenesis (SeSaM): a novel method for directed evolution. *Nucleic Acid Reasearch.* 2004, 32.

46. **Bommarius, AS, Blum, JK und Abrahamson, MJ.** Status of protein engineering for biocatalysts: how to design an industrially useful biocatalyst. *Current Opinion in Chemical Biology.* 2011, 15, S. 194-200.

47. **Hickel, A, Radke, CJ und Blanch, HW.** Hydroxynitrile lyases at the diisopropyl ether/water interface: evidence for interfacial enzyme activity. *Biotechnol. Bioeng.* 1999, 65, S. 425-436.

48. **Krammer, B, et al., et al.** A novel screening assay for hydroxynitrile lyases suitable for high-throughput screening. *Journal of Biotechnology.* 2007, 129, S. 151-161.

49. **Reetz, MT, Kahakeaw, D und Lohmer, R.** Addressing the Numbers Problem in Directed Evolution. *ChemBioChem.* 2008, 9, S. 1797-1804.

50. **Clouthier, CM, Kayser, MM und Reetz, MT.** Designing New Bayer-Villinger Monooxygenases Using Restricted CASTing. *J. Org. Chem.* 2006, 71, S. 8431-8437.

51. **Cadwell, RC und Joyce, GF.** Radomization of genes by PCR mutagenesis. *Genome Res.* 1992, 2, S. 28-33.

52. **Balzer, D, et al., et al.** KorB protein of promiscuous plasmid RP4 recognizes inverted sequence repetitions in regions essential for conugative plasmid transfer. *Nucleic Acid Research.* 1992, 8, S. 1851-1858.

53. **Bradford, Marion M.** A Rapid and Sensitive Method for the Quantitation of Microgram Quantities of Protein Utilizing the Principle of Protein - Dye Binding. *Analytical Biochemistry 72.* 1976, S. 248 - 254.

54. **Hajnal, I, Steiner, K und Schwab, H.** Cyanohydrin Synthesis with HCN in organic solvent. *ACIB Protocol.* 2012.

55. **Choudhary, G und Horvath, C.** Ion-exchange chromatography. [editor] H Rehm und T Letzel. *Der Experimentator Proteinbiochemie/Proteomics.* 2010, S. 155-156.

56. **Stellwagen, E.** Gel filtration. [editor] H Rehm und T Letzel. *Der Experimentator Proteinbiochemie/Proteomics.* 2010, S. 152.

57. **Gruber, K, et al., et al.** Reaction mechanism of hydroxynitrile lyases of the alpha/beta-hydrolase superfamily: the three-dimensional structure of the transient enzyme-substrate complex certifies the crucial role of LYS236. *J Biol Chem.* 2004, 279, S. 20501-20510.

58. **Dreveny, I, et al., et al.** Substrate binding in the FAD-dependent hydroxynitrile lyase from almond provides insight into the mechanism of cyanohydrin formation and explains the absence of dehydrogenation activity. *Biochemistry.* 2009, 48, S. 3370-3377.

59. **Kane, JF.** Effects of rare codon clusters on high-level expression of heterologous proteins in Escherichia coli. *Current Opinion in Biotechnology.* 1995, 6, S. 494-500.

60. **Technologies, Agilent.** GeneMorph II Random Mutagenesis Kit - Instruction Manual.

61. **Edelheit, O, Hanukoglu, A und Hanukoglu, I.** Simple and efficient site-directed mutagenesis using two single-primer reactions in parallel to generate mutants for protein structure-function studies. *BMC Biotechnology.* 2009, 9, S. 61.

# 8 Appendices

## 8.1 List of Figures

## 8.2 List of Tables